Total OH Reactivity Measurements at the Biosphere-Atmosphere Interface

DISSERTATION

zur Erlangung des Grades eines 'Doktor rerum naturalium (Dr.rer.nat)'
der Fachbereiche:
08 - Physik, Mathematik und Informatik,
09 - Chemie, Pharmazie und Geowissenschaften,
10 - Biologie,
Universitätsmedizin
der Johannes Gutenberg-Universität

Anke Christine Nölscher

Max Planck Graduate Center
mit der Johannes Gutenberg-Universität Mainz

September 2012

Tag der mündlichen Prüfung: 21. Dezember 2012

I hereby declare that I wrote the dissertation submitted without any unauthorized external assistance and used only sources acknowledged in the work. All textual passages which are appropriated verbatim or paraphrased from published and unpublished texts as well as all information obtained from oral sources are duly indicated and listed in accordance with bibliographical rules. In carrying out this research, I complied with the rules of standard scientific practice as formulated in the statutes of Johannes Gutenberg-University Mainz to insure standard scientific practice.

Zusammenfassung Die Biosphäre emittiert eine Vielzahl an flüchtigen Kohlenwasserstoffen in die Atmosphäre, welche durch chemische Oxidationsreaktionen, sowie Transport oder Deposition wieder aus der Atmosphäre entfernt werden. Durch die Reaktion zwischen biogenen Emissionen und dem Hydroxyl-Radikal (OH), dem wichtigsten Oxidationsmittel in der Atmosphäre, können troposphärisches Ozon und Aerosole entstehen, welche regional Klima und Luftqualität beeinflussen. Die gesamte OH Senke, abhängig von Konzentration und Reaktionsgeschwindigkeit aller reaktiver Substanzen in der Atmosphäre, kann direkt als totale OH Reaktivität gemessen werden. Ein Verfahren zur Messung der OH Reaktivität ist die "Comparative Reactivity Method - CRM". Diese Methode vergleicht die Reaktion eines bestimmten Moleküls (hier Pyrrol) mit OH in sauberer und atmosphärischer, reaktiver Luft. In dieser Arbeit wurden Messungen der OH Reaktivität zwischen Biosphäre und Atmosphäre durchgeführt, um verschiedenste Einflüsse und Schlüsselfaktoren zu charakterisieren.
Für Messungen in natürlicher Umgebung wurde die bereits vorhandene Methode automatisiert, eine direkte, kontaminationsfreie Probennahme ermöglicht und neben dem ursprünglichen Detektor (Protonen-Transfer-Reaktions-Massenspektrometrie, PTR-MS) wurde eine kompakte und günstige Alternative getestet. Der GC-PID (Gaschromatograph-Photoionisationdetektor) ist für zukünftige Projekte eine zuverlässige und einfach anwendbare Technik zur Messung der OH Reaktivität.
Die Feldmesskampagne HUMPPA-COPEC 2010 im finnischen Wald war neben typischen borealen Einflüssen von langanhaltender Hitze und Waldbränden geprägt. Der Vergleich von Messungen der atmosphärischen Mischungsverhältnisse einzelner biogener Emissionen, einiger ihrer Oxidationsprodukte und weiteren Spurengasen mit der Messung der OH Reaktivität zeigte signifikante Diskrepanzen. Diese unerklärte OH Senke konnte im Detail untersucht werden, da die OH Reaktivität in und über der Baumkrone gemessen wurde.
Der direkte Einfluss von biogenen Emissionen auf die atmosphärische OH Reaktivität wurde in einer Studie am Kleinen Feldberg (Taunus, Deutschland) von Frühling bis Herbst 2011 untersucht. Der Ast einer Fichte wurde mit einer Küvette umschlossen, und die emittierte OH Reaktivität mit den Emissionsraten bekannter biogener flüchtiger Kohlenwasserstoffe verglichen. Vor allem im Sommer konnten diese die gemessene OH Reaktivität nicht vollständig erklären.
Während der kontrollierten Oxidation von Isopren mit OH in der EUPHORE Reaktionskammer (CHEERS, Spanien 2011) wurde neben Isopren und seinen Produkten auch die OH Reaktivität gemessen. Außerdem wurden die Messwerte mit den Ergebnissen von zwei unterschiedlichen Model-Simulationen verglichen. Gute Übereinstimmung zwischen der OH Reaktivität, den Einzelkomponenten und dem traditionellen Isopren-Mechanismus im Model (MCM 3.2) konnte beobachtet werden. Frühere Feldmessungen in den Tropen fanden erhöhte OH Konzentrationen in Isopren-dominierter Umgebung. Dies wurde in einem neuen Isopren-Mechanismus umgesetzt, indem während der Isopren-Oxidation zusätzlich OH generiert wird. Dieser Mechanismus (MIME v4) konnte in den getesteten Bedingungen, während des CHEERS Experiments, nicht bestätigt werden.

Summary. The biosphere emits copiously volatile organic compounds (VOCs) into the atmosphere, which are removed again depending on the oxidative capacity of the atmosphere and physical processes such as mixing, transport and deposition. Biogenic VOCs react with the primary oxidant of the atmosphere, the hydroxyl radical (OH), and potentially lead to the formation tropospheric ozone and aerosol, which impact regional climate and air quality. The rate of OH decay in the atmosphere, the total OH reactivity is a function of the atmospheric, reactive compound's concentration and reaction velocity with OH. One way to measure the total OH reactivity, the total OH sink, is with the "Comparative Reactivity Method - CRM". Basically, the reaction of OH with a reagent (here pyrrole) in clean air and in the presence of atmospheric, reactive molecules is compared. This thesis presents measurements of the total OH reactivity at the biosphere-atmosphere interface to analyze various influences and driving forces.

For measurements in natural environment the instrument was automated and a direct, undisturbed sampling method developed. Additionally, an alternative detection system was tested and compared to the originally used detector (Proton Transfer Reaction-Mass Spectrometer, PTR-MS). The GC-PID (Gas Chromatographic Photo-Ionization Detector) was found as a smaller, less expensive, and robust alternative for total OH reactivity measurements.

The HUMPPA-COPEC 2010 measurement campaign in the Finish forest was impacted by normal boreal forest emissions as well as prolonged heat and biomass burning emissions. The measurement of total OH reactivity was compared with a comprehensive set of monitored individual species' ambient concentration levels. A significant discrepancy between those individually measured OH sinks and the total OH reactivity was observed, which was characterized in detail by the comparison of within and above the forest canopy detected OH reactivity.

Direct impact of biogenic emissions on total OH reactivity was examined on Kleiner Feldberg, Germany, 2011. Trans-seasonal measurements of an enclosed Norway spruce branch were conducted via PTR-MS, for individual compound's emission rates, and CRM, for total OH reactivity emission fluxes. Especially during summertime, the individually monitored OH sink terms could not account for the measured total OH reactivity.

A controlled oxidation experiment in a low NO_x environment was conducted in the EUPHORE reaction chamber (CHEERS, Spain 2011). The concentration levels of the reactant isoprene and its major products were monitored and compared to total OH reactivity measurements as well as to the results of two models. The individually measured compounds could account for the total OH reactivity during this experiment as well as the traditional model-degradation scheme for isoprene (MCM 3.2). Due to previous observations of high OH levels in the isoprene-rich environment of the tropics, a novel isoprene mechanism was recently suggested. In this mechanism (MIME v4) additional OH is generated during isoprene oxidation, which could not be verified in the conditions of the CHEERS experiment.

Contents

1

Introduction - The apple's skin

"The atmosphere is very thin - just like the skin of an apple" (Mario J. Molina, The Lindau Nobel Laureate Meeting 2012). Nevertheless this thin layer is essential for life on Earth. Composed of 78.1 % nitrogen and 20.9 % oxygen (Warneck and Williams, 2012), argon, neon, helium, various trace gases, water vapor as well as solid and liquid particles, it covers the Earth's surface. Although relatively small in volume (less than 1 %), the multitude of trace gases significantly impacts climate, weather and air quality.

1.1 Atmosphere-biosphere interactions

One big source of trace gases is the biosphere, which per definition provides the space for life on a planet. Oceans as well as terrestrial ecosystems host living organisms which release thousands of volatile organic compounds (VOCs) in the atmosphere (Goldstein and Galbally, 2007). These volatile organic compounds are composed of carbon and hydrogen atoms, and often contain other elements such as oxygen or nitrogen as well. Biogenic emissions dominate total global VOC emissions (1150 out of 1300 $\mathrm{Tg\,C\,yr^{-1}}$), while anthropogenic emission sources are of minor importance (142 $\mathrm{Tg\,C\,yr^{-1}}$) on global scale. Large areas on Earth are covered by forests (ca. 30 % of landmass (Bonan, 2008)). Forests interact in global carbon cycles, regional hydrology and atmospheric chemistry (Ozanne et al., 2003). Through photosynthesis plants convert light and carbon dioxide (CO_2) into energy and biomass. Via metabolic pathways they synthesize characteristic and species-specific biogenic volatile organic compounds (BVOCs) which are potentially released to the atmosphere (e.g. Kesselmeier and Staudt (1999), Dudareva et al. (2006)). Prominent BVOCs, copiously emitted by vegetation, are isoprene (570 $\mathrm{Tg\,yr^{-1}}$), methanol (160 $\mathrm{Tg\,yr^{-1}}$), monoterpenes (97 $\mathrm{Tg\,yr^{-1}}$), sesquiterpenes (12 $\mathrm{Tg\,yr^{-1}}$), and aldehydes (e.g. acetaldehyde 11 $\mathrm{Tg\,yr^{-1}}$) (Warneck and Williams, 2012).

The strength and composition of plant's emissions vary with the influence of different environmental factors: temperature is an important driving force, as is light, humidity in air and soil, season, or stress to extreme events such as heat, drought, herbivoral attack (Fehsenfeld et al., 1992, Laothawornkitkul et al., 2009, Loreto and Schnitzler, 2010). The function of vegetational emissions is still poorly understood. Released chemical compounds act to attract or repel insects, stabilize photosynthesis pathways or reduce oxidant levels close by (Dudareva et al., 2004). An overview of biological feedback mechanisms is pictured in Figure 1.1.
Once emitted to the atmosphere biogenic VOCs undergo photochemical reactions, mixing, advection, deposition, or become involved in heterogeneous processes (Finlayson-Pitts and Pitts, 1986). Biogenically released compounds are initially oxidized in the atmosphere by hydroxyl radicals (OH), ozone (O_3) or nitrate radicals (NO_3). Reaction products are formed via various mechanisms, depending on the atmospheric mixture such as radical concentration levels, or available nitrogen oxide (NO), solar irradiation, and structure of the reacting molecules. The lifetimes of atmospheric constituents vary over a wide range, between seconds to hours (predominantly OH radical chemistry), to days (ozone and NO_3 chemistry), and months or years (e.g. involving relatively unreactive molecules such as methane). During daytime OH is the predominant oxidant. Due to its high reactivity it attacks VOCs and after a subsequent reaction with oxygen, peroxy radicals (RO_2) are generated (Figure 1.1). Depending on the available NO, two reaction pathways are then possible. In low NO conditions (such as in forested environment) typical photooxidation products are peroxides, alcohols and carbonyls. Ozone is lost in these reactions (as can be seen in the following example for CO).

$$\begin{gathered}
OH + CO \rightarrow H + CO_2 \\
H + O_2 \rightarrow HO_2 \\
HO_2 + \mathbf{O}_3 \rightarrow OH + 2O_2 \\
\hline
CO + O_3 \rightarrow CO_2 + O_2
\end{gathered}$$

If atmospheric NO is available (as is in urban areas) ozone can form:

$$\begin{gathered}
OH + CO \rightarrow H + CO_2 \\
H + O_2 \rightarrow HO_2 \\
HO_2 + NO \rightarrow OH + NO_2 \\
NO_2 \overset{h\nu}{\rightarrow} NO + O \\
O + O_2 + M \rightarrow \mathbf{O}_3 + M \\
\hline
CO + 2O_2 \rightarrow CO_2 + O_3
\end{gathered}$$

Heavy molecules and oxygenated compounds can be part of the formation and growth of secondary organic aerosol (SOA) (Tunved et al., 2006). Not only chemistry impacts

the mixture and constitution of the atmosphere. Physical processes mix, transport, wash out chemicals and additionally impact the radiation budget. Closely linked to light and temperature, these physical effects represent major driving forces of biogenic emissions.

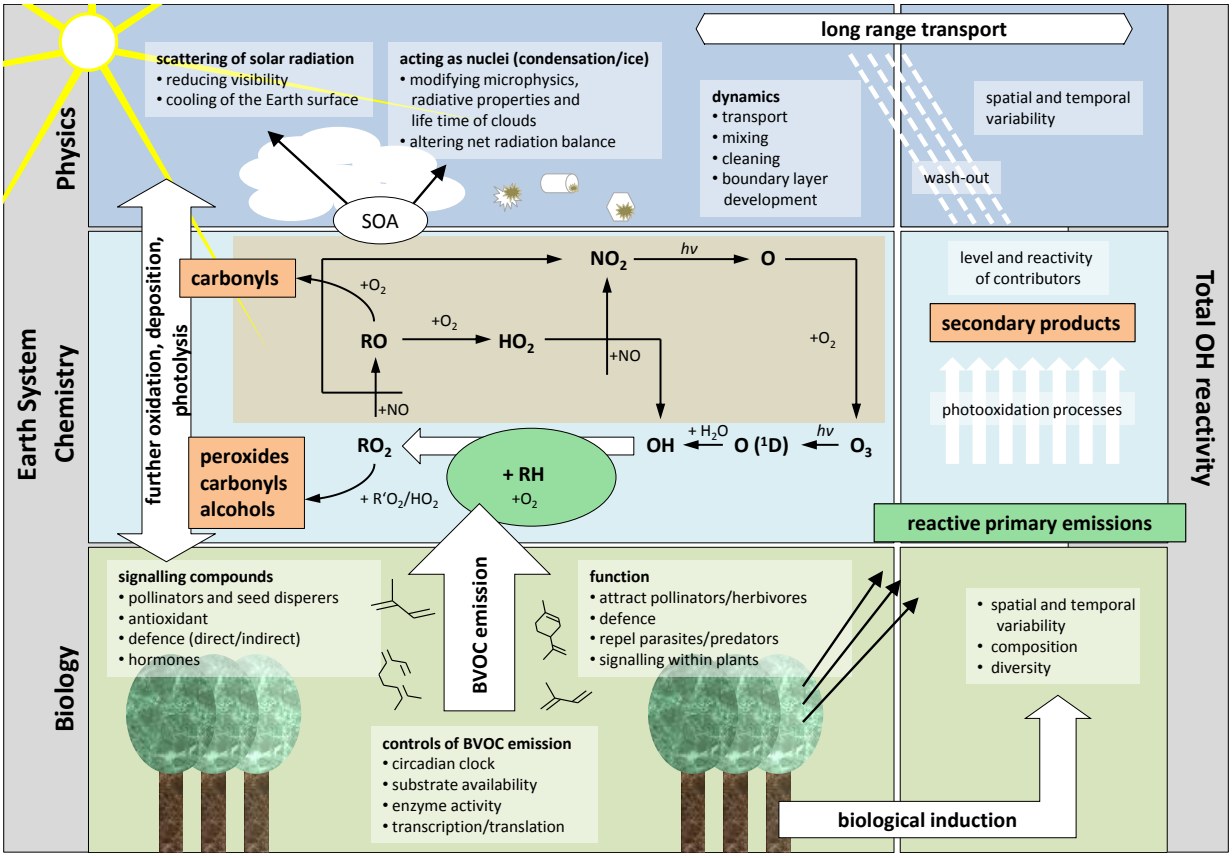

Fig. 1.1: Schematic adapted from Laothawornkitkul et al. (2009) and modified for total OH reactivity feedbacks: Included are biological driving forces, a simple schematic about daytime atmospheric photooxidation processes (OH chemistry), and physical influence and coupling. BVOCs are released due to various driving forces, oxidized and transformed into many products. Two principle pathways are presented for low (blue) and high (brown) NO levels. Both, primarily emitted compounds (green) and products (orange) can deposit on surfaces, condense on particles, or get involved in the formation of secondary organic aerosol (SOA). R is the placeholder for any organic group in the hydrocarbon RH, the peroxy radical RO_2 (R'O_2), and the alkoxy radical RO.

1.2 The big picture

Atmospheric observations classified more than 500 individual species in urban air (Lewis et al., 2000), and more than 650 compounds were identified (out of more than a thousand detected species) in Mediterranean air (Xu et al., 2003). Estimations consider

10^4 – 10^5 organic species (Goldstein and Galbally, 2007) in the atmosphere. The drastically increasing number of detected compounds in the air challenges the development of sophisticated measurement methods to monitor even more atmospheric VOCs. As those are removed again from the atmosphere, precise laboratory studies examine reaction rates and yields, and computational chemistry characterizes in detail atmospheric degradation processes.
It seems that great detail and high precision increases knowledge about the atmosphere. But it seems as well that with great detail and high precision research moves away from the initial focus of atmospheric chemistry (Williams, 2008). The importance of hydrocarbon oxidation for aerosol formation and as a photochemical source of ozone was initially discovered by Haagen-Smit (1953) with his studies of Los Angeles smog. That this is not only a matter of urban air, but also rural environments, was observed as blue haze, first reported by Went (1960). Tropospheric ozone and aerosols are key-players of the big atmosphere-biosphere picture. With this focus alternative approaches have been developed recently, such as the photochemical ozone creation potential (calculated e.g. by Derwent et al., 1996), the first direct measurements of ozone production rates by Cazorla et al. (2012), or determination of the potential aerosol mass (Kang et al., 2007).
In similar fashion, a method to measure the total OH reactivity was designed and recently included in various field studies (Di Carlo et al., 2004, Lou et al., 2010, Mao et al., 2012, Dolgorouky et al., 2012). Since the OH radical is the most important oxidant during daytime, one way to characterize the atmospheric oxidation capacity is to examine the total sink of OH, the total OH reactivity. A well determined total loss rate of OH can highlight important OH sinks, hence potentially relevant compounds for ozone and aerosol formation.

1.3 Total OH reactivity perspective

A novel method to investigate the exchange and balance between atmosphere and biosphere is the measurement of total OH reactivity. Total OH reactivity (R_{total} in s^{-1}) is the total loss rate of hydroxyl radicals (OH) due to all atmospheric reactive compounds. It is defined as the sum of all single compound reactivities which are calculated as the product of concentration $[X_i]$ (in molecules cm^{-3}) and reaction velocity with OH (k_{OH+X_i} in molecules^{-1} cm^3 s^{-1}).

$$R_{\mathrm{total}} = \Sigma\ k_{\mathrm{OH+X}_i} \times [\mathrm{X}_i] \tag{1.1}$$

To date measurements of total OH reactivity are conducted with three principle techniques. Two methods are based on Laser Induced Fluorescence (LIF), both of which detect OH after reaction with an air sample, either following the decay with time

("pump-and-probe LIF") or the response after variable reaction times ("flow tube LIF") (Sadanaga et al., 2004, Kovacs and Brune, 2001). The measurement principle used in this study is termed Comparative Reactivity Method (CRM). Using a Proton Transfer Reaction-Mass Spectrometer (PTR-MS) as detector, the levels of a reagent after reacting with OH alone and in the presence of the air sample (Sinha et al., 2008) are compared. Further details of the LIF instruments and the CRM measurement principle in particular are given in Section 2.

As presented in Figure 1.1 (right hand side) total OH reactivity easily embeds into the overall picture of biosphere and atmosphere in terms of physical, chemical and biological properties. Ambient field measurements for example show the impact of dynamics such as transport, mixing and boundary layer development on detectable VOC levels and observed total OH reactivity (Sinha et al., 2010, Lou et al., 2010). Both, the chemical composition and the budget of the atmosphere's primary oxidant OH are characterized by the measurement of total OH reactivity. The OH budget can be examined by analyzing sink and source terms (e.g. Mao et al., 2009). Ozone formation potential due to atmospheric reactive compounds can be determined via total OH reactivity measurements (Sinha et al., 2012). By comparing the contribution from individually measured compounds to the measured total OH reactivity, the size of any unaccounted for, or potentially "missing", sinks can be deduced. Recent publications pointed out, that biogenic environments contain high levels of missing total OH reactivity (e.g. Di Carlo et al., 2004, Ingham et al., 2009). A summary of recent field studies in forested regions is presented in Chapter 3. Hypotheses how to explain the large missing fraction of total OH reactivity embrace unmeasured and unknown biogenic primary emissions as well as a mixture of unmeasured and unknown photooxidation products (detailed in Chapters 3 and 4).

An overview of field campaigns including total OH reactivity measurements is given in Figure 1.2. The high variability of total OH reactivity depending on location and season can be recognized, as well as extremely high values in urban and tropical environments.

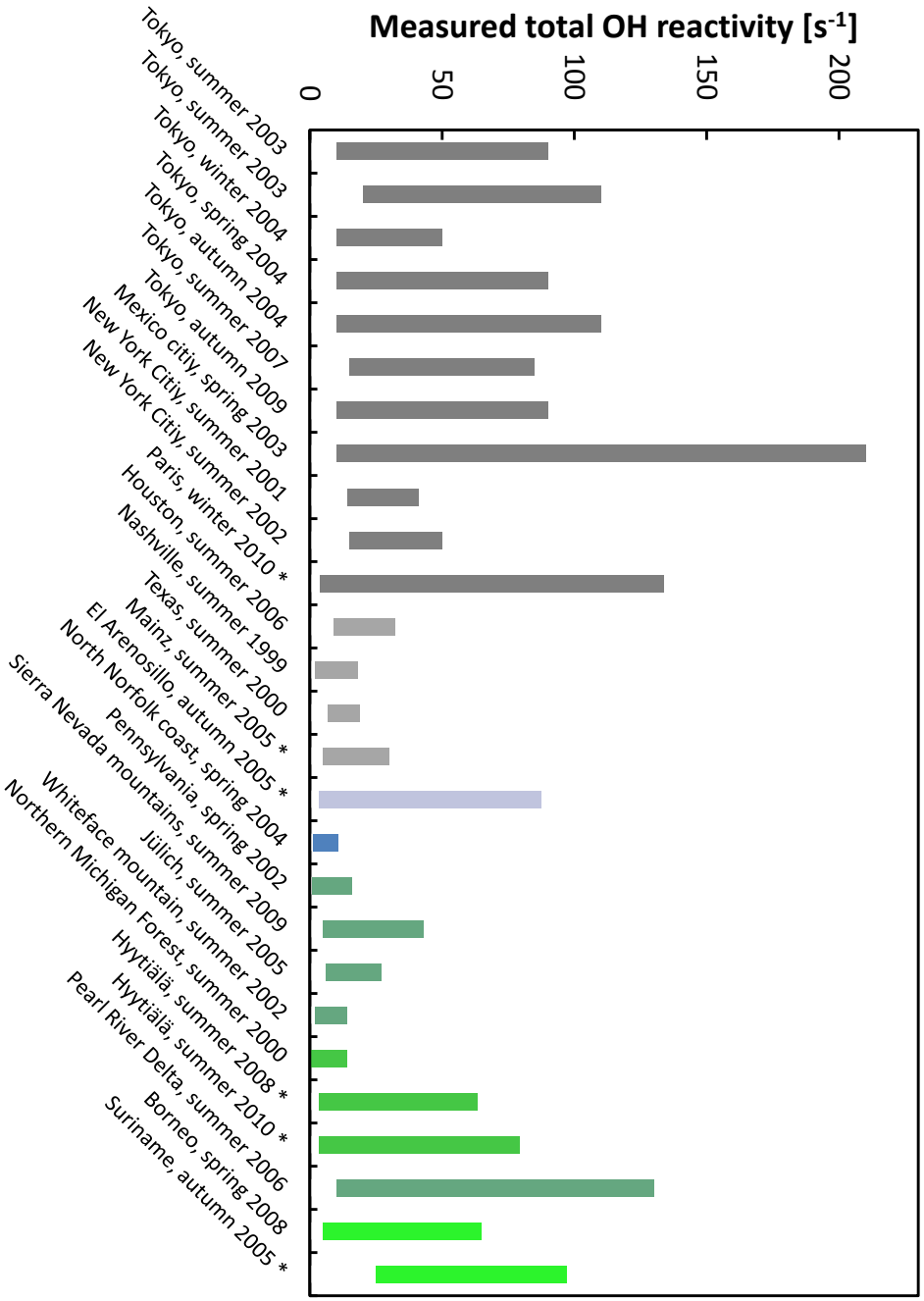

Fig. 1.2: Summary of observed total OH reactivity in urban (grey), coastal (blue) and natural (green) environments. The data is given as range from the lowest detectable total OH reactivities up to maximum peak values. Marked with * are measurements made by using CRM.

1.4 Open research questions and the total OH reactivity utility

Focus of current research is the characterization of biogenic emission mechanisms and the elucidation of atmospheric feedbacks. Different scales are investigated from leaf and branch level (e.g. enclosing cuvettes, Ruuskanen et al., 2005) to small trees (e.g. plant chambers, Niinemets et al., 2011), entire ecosystems (e.g. mesocosms, Jardine et al., 2012) or regional observations (e.g. measurement field campaigns, Williams et al., 2011). Biologists examine the function and trigger-mechanisms of vegetational biosynthesis forming and releasing compounds. Chemists are interested in reaction mechanisms involving biogenic reactive emissions, oxidants and other atmospheric constituents. Meteorologists include biosphere-atmosphere interactions in global models for simulations and predictions.

- Essential mechanisms inducing and controlling the release of many observed compounds by vegetation need to be elucidated in more detail. Functions inside the plants depending on enzymatic processes, circadian control, seasonality, signaling, and many more lack an explanation (Dudareva et al., 2006, Monson et al., 2012).
  Therefore, vegetational emissions as function of light and temperature, as well as other driving forces, need to be characterized in detail in controlled and natural conditions. The measurement of the total OH reactivity as a flux from direct plant emissions provides the direct response to essential driving factors.

- It remains uncertain if the diversity and variability of biogenic emissions is captured with current measurement devices. The knowledge about number and abundance of many reactive biogenic VOCs seems rather incomplete (Hewitt et al., 2011). This might be partly due to difficult sampling procedures, inaccessible ecosystems, unavailability of appropriate equipment, and inaccuracy in measurements.
  The comparison of total OH reactivity measurements, as budget of all OH sinks, to individually measured species could highlight the amount and properties of unknown or unaccounted for biogenic emissions.

- Photochemical processes in forested regions puzzle scientists. Ozone and OH chemistry in clean, biogenically influenced environment are poorly understood and need further investigation (e.g. Wolfe et al., 2010, Hofzumahaus et al., 2009).
  Ambient measurements of total OH reactivity picture both, the nature of primary biogenic emissions and the influence of secondary photooxidation products. Temporal and spatial variability in total OH reactivity measurements can be used as pieces to the photochemical puzzle in forested regions.

- A proper chemical description of atmospheric degradation processes of biogenic VOCs is crucial for understanding the system of biosphere and atmosphere. Hence, detailed chamber studies in controlled, but realistic atmospheric conditions need to be conducted (e.g. Paulot et al., 2009).
  Model and measurement comparisons for known oxidation products as well as for total OH reactivity observations could reveal gaps in the current understanding.

- Atmospheric models rely on a good description and parameterization of biological mechanisms, chemical processes, accurate and complete measurements. Uncertainties increase with the lack of knowledge about these, but also with an insufficient description of e.g. landscape types and meteorology. Future high precision and long-term measurements would be of great use for any regional or global climatological observation and modeling approach (e.g. Lelieveld et al., 2004, Guenther et al., 2012).
  Precise measurements of many atmospheric observables are difficult to conduct and rely on expensive and fragile equipment. Observations of total OH reactivity, as sum of all sinks of OH, the most important oxidant of the atmosphere, helps to simplify, reduce errors, and complete the current model picture of the atmosphere-biosphere system.

This thesis highlights total OH reactivity as tool to investigate exchange processes between biosphere and atmosphere. In order to adequately access these open questions from the total OH reactivity point of view, ambient temporal and spatial variability, direct biogenic emissions, and controlled photochemical reactions have been investigated in the course of this thesis work.
The Comparative Reactivity Method (CRM) was further improved and an alternative detection system was tested and validated (detailed in Chapter 2). Summertime measurements of total OH reactivity in a boreal forest environment (Hyytiälä, Finland) at two different levels (in and above the canopy) highlighted the impact of various factors on atmospheric composition and reactivity, such as heat stress, transport of biomass burning pollutants, and normal boreal forest emissions. The level of unaccounted for OH reactivity during this study was high, despite the comprehensive set of atmospheric measurement instruments during the HUMPPA-COPEC campaign 2010 (Chapter 3). The role of primary emissions from vegetation for the high missing total OH reactivity in forests was explored by seasonal branch enclosure measurements during spring, summer and autumn 2011. Total OH reactivity emission rates were observed for the first time in parallel to emission rate measurements of BVOCs by Proton Transfer Reaction-Mass Spectrometer (PTR-MS) from a Norway spruce on Kleiner Feldberg,

Germany. Results and discussion are presented in Chapter 4. Atmospheric photooxidation processes were simulated in the reaction vessel EUPHORE (Valencia, Spain) in autumn 2011, in order to compare modeled expectations and measurements. The formation of secondary products and the temporal development of total OH reactivity was studied in low NO conditions similar to those in forests (Chapter 5).

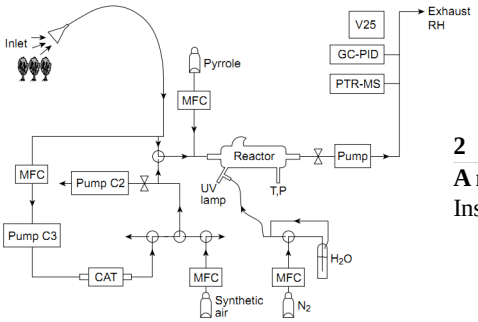

2

A new instrument for total OH reactivity measurements
Instrumental development, automation and detector validation

3

Summertime total OH reactivity measurements
In and above canopy observations during a comprehensive field measurement campaign

4

Seasonal measurements of total OH reactivity fluxes
Branch enclosure observations of directly emitted OH reactive compounds and comparison to PTR-MS detected VOC fluxes

5

A total OH reactivity perspective on isoprene photooxidation
Chamber analysis of total OH reactivity during the controlled oxidation of isoprene and comparison to PTR-TOF-MS measurements and model prediction

2

A new instrument for total OH reactivity measurements using a fast Gas Chromatographic Photo-Ionization Detector (GC-PID)

A. C. Nölscher[1], V. Sinha[1,2], S. Bockisch[3], T. Klüpfel[1], and J. Williams[1]

[1]Department of Atmospheric Chemistry, Max Planck-Institute for Chemistry, Mainz, Germany
[2]Indian Institute of Science Education and Research Mohali, Punjab, India
[3]Environics-IUT GmbH, Berlin, Germany

Manuscript published in Atmospheric Measurement Techniques Discussion

Summary. The primary and most important oxidant in the atmosphere is the hydroxyl radical (OH). Currently OH sinks, particularly gas phase reactions, are poorly constrained. One way to characterize the overall sink of OH is to measure directly the ambient loss rate of OH, the total OH reactivity. To date direct measurements of total OH reactivity have been either performed using a Laser Induced Fluorescence (LIF) system ("pump-and-probe" or "flow reactor") or the Comparative Reactivity Method (CRM) with a Proton Transfer Reaction Mass Spectrometer (PTR-MS). Both techniques require large, complex and expensive detection systems. This study presents a feasibility assessment for CRM total OH reactivity measurements using a new detector, a Gas Chromatographic Photo-Ionization Detector (GC-PID). Such a system is smaller, more portable, less power consuming and less expensive than other total OH reactivity measurement techniques.
Total OH reactivity is measured by the CRM using a competitive reaction between a reagent (here pyrrole) with OH alone and in the presence of atmospheric reactive molecules. The new CRM method for total OH reactivity has been tested with parallel measurements of the GC-PID and the previously validated PTR-MS as detector for the reagent pyrrole during laboratory experiments, plant chamber and boreal field studies. Excellent agreement of both detectors was found when the GC-PID was operated under optimum conditions. Time resolution (60–70 s), sensitivity (LOD 3–6 s^{-1}) and overall uncertainty (25 % in optimum conditions) for total OH reactivity were equivalent to PTR-MS based total OH reactivity measurements. One drawback of the GC-PID system was the steady loss of sensitivity and accuracy during intensive measurements lasting several weeks, and a possible toluene interference. Generally,

the GC-PID system has been shown to produce closely comparable results to the PTR-MS and thus in suitable environments (e.g. forests) it presents a viably economical alternative for groups interested in total OH reactivity observations.

2.1 Introduction

The hydroxyl radical (OH) is the most effective oxidant in the atmosphere. Due to it's high reactivity, OH is thought to act as a cleaning agent, initiating the photochemical processes leading to removal of chemicals from the atmosphere. The tropospheric OH radical budget has been analyzed in several atmospheric studies via simultaneous measurements of OH sources (photolysis of ozone (O_3), formaldehyde (HCHO), nitrous acid (HONO), e.g. Logan et al., 1981, Mahajan et al., 2011, Kleffmann et al., 2005), the in-situ OH concentration using Laser Induced Fluorescence (LIF), Chemical Ionization Mass Spectrometry (CIMS) or Differential Optical Laser Absorption Spectroscopy (DOAS), (Schlosser et al., 2009) and the sum of all OH sinks (total OH reactivity). The total OH reactivity is the total loss rate of OH due to all atmospheric OH reactive species (Di Carlo et al., 2004). This total sink has proven most difficult to constrain and direct measurements of total OH reactivity have become an important and much coveted technique for studying atmospheric chemistry.
As a direct approach for the total sink of OH, total OH reactivity measurements help to understand the role of various sinks and sources that balance the OH budget (Martinez et al., 2003). Furthermore the relative contribution of various reactive volatile organic compounds (VOCs) to the total loss rate of OH may be examined (Lou et al., 2010, Sinha et al., 2010, Kato et al., 2011). By comparing the OH reactivity contribution from individually measured compounds, model results and the measured total OH reactivity, completeness of measured species can be investigated. Unknown or unmeasured constituents may play an important role in tropospheric OH and ozone budgets (e.g. Di Carlo et al., 2004, Mao et al., 2009, Sinha et al., 2012).
Total OH reactivity measurements are currently performed with three methods which are described below and summarized in Table 2.1.
The first direct measurements of atmospheric total OH reactivity were carried out by Calpini et al. (1999) and Jeanneret et al. (2001). Later the "pump-and-probe" technique was improved by Sadanaga et al. (2004). In this configuration, a pump laser photolyzes ozone to produce artificially high OH. Due to the reaction with reactive atmospheric molecules the OH decays. The rate of decay is detected by Laser Induced Fluorescence (LIF) in a low pressure cell, and can be used to derive the lifetime of atmospheric OH, hence the total OH reactivity. The "pump-and-probe" LIF is capable of operating fast (30–180 s averaging time), with a detection limit of 1–2 s^{-1}, and an overall uncertainty of 10–12 % (Sadanaga et al., 2004, Lou et al., 2010).

Kovacs and Brune (2001) reported a second method to directly monitor the total OH reactivity which was also based on LIF, but employed a different system of generating OH namely a discharge flow technique. In the first step OH is produced by a mercury UV lamp in a movable inlet and injected into a large flow-tube. After mixing with ambient air, OH is analyzed downstream using LIF. Then, the injector is pulled back in multiple steps. Due to longer mixing- and hence longer reaction-times the detected OH concentrations change. Observing the decay of OH at different reaction times, allows the determination of the overall loss rate of OH down to a detection limit of $1\,s^{-1}$ within a time resolution of 210 s. The uncertainty for this technique is roughly 16–25 % (Kovacs and Brune, 2001, Mao et al., 2009).
A third method, proposed by Sinha et al. (2008), uses a competitive reaction of artificially produced OH radicals with a reagent which is not present in ambient air and all OH reactive atmospheric species. The Comparative Reactivity Method (CRM) compares the reagent's mixing ratio after reacting with OH in zero air and in the presence of ambient air. A suitable detector is used to measure the mixing ratio of the reagent before and after the competitive reactions. Different combinations of reagent and detector can be chosen for the CRM according to the required instrumental characteristics (Sinha et al., 2008). Pyrrole was found to be reasonable for ground based ambient continental measurements. However, for biomass burning emissions (which contain pyrrole) and airborne based or marine studies (low total OH reactivities) a different reagent would be valuable. Hence, based on the user's needs and the available detection system, another suitable reagent can be chosen.

Table 2.1: Three basic principles for direct total OH reactivity measurements, the uncertainties, detection limit and time resolution.

	Basic principle	Uncertainty	Detection Limit	Time resolution
Pump-and-probe LIF	Production of artificially high OH with a flash photolysis beam and detection of the OH decay with LIF	10–12 %	1–2 s^{-1}	30–180 s
Discharge flow tube LIF	Inject high OH levels with a movable inlet and monitor OH with LIF after different reaction times (different inlet positions)	16–25 %	1 s^{-1}	210 s
Comparative Reactivity Method	Monitor the change in a reagents concentration for the reaction of the reagent+OH with and without the presence of atmospheric reactive molecules	16–20 %	3–4 s^{-1}	10–60 s

In the current CRM based instruments under atmospheric conditions pyrrole functions as the reagent and a PTR-MS (IONICON, Austria) as the detector. Using a PTR-MS for total OH reactivity measurements provides a time resolution of 10–60 s, sensitivity

down to 3–4 s^{-1} detection limit, overall relative uncertainty of 16–20 % and good stability (Sinha et al., 2012, Nölscher et al., 2012b). However, the PTR-MS instrument is big (650 × 1660 × 550 mm), heavy (150 kg) and expensive (ca. 180 000 €). For field measurements it would be desirable to use a small, more portable and less expensive measurement device in order to make the total OH reactivity measurement accessible to more practitioners.
The potential of a custom built GC-PID (VOC-Analyzer from IUT-Berlin, now Environics-IUT GmbH) for total OH reactivity measurements using CRM is assessed in this study. The GC-PID is small (260 × 160 × 400 mm), light (8 kg), provides a good time resolution (60–70 s) and is less expensive (18 000 €). It requires no external carrier gas, and an internal battery provides power for ca. 12 h making it suitable for field campaigns. The detection limit for pyrrole is 3 ppbV, and total OH reactivity can be measured under best conditions down to 3 s^{-1} (6 s^{-1} worst case, see Sect. 2.3.3). The new GC-PID set-up has been tested in parallel to previously validated PTR-MS measurements for CRM in laboratory experiments, a plant chamber, and boreal forest field studies (Sect. 2.3.2). Advantages and drawbacks of the new technique are discussed.

2.2 Experimental

2.2.1 The Comparative Reactivity Method – basic principle

Total OH reactivity measurements by the Comparative Reactivity Method (CRM) are based on the competitive reaction between OH and a reagent, which is not present in ambient air, and atmospheric OH reactive compounds. The reagent is introduced into a Teflon coated glass reactor, diluted with zero-air and quantified with a suitable detector (concentration level C1). Next, OH molecules are generated by photolyzing water-vapor with a pen-ray mercury UV lamp and introduced into the reactor. The reaction of the reagent with OH decreases the amount of detectable molecules leading to a second concentration level (C2). By exchanging zero-air with ambient air multiple other OH reactive molecules are introduced into the reactor and these compete with the reagent for the OH present. This results in a concentration change (concentration level C3) which depends on the OH reactivity of the atmospheric composition. The following equation provides the total OH reactivity of air R_{air} (Sinha et al., 2008).

$$R_{\mathrm{air}} = C1 \times k_{R+OH} \times \frac{(C3 - C2)}{(C1 - C3)} \tag{2.1}$$

Where C1, C2, C3 are the different concentration levels and k_{R+OH} is the reaction rate coefficient of the reagent with OH. For ambient measurements a range of total OH reactivity from 0 to 100 s^{-1} (unpolluted) and 200 s^{-1} (polluted) has been measured (Shirley et al., 2006, Lou et al., 2010). In this range pyrrole (C_4H_5N) acts as

suitable reagent molecule. It's reaction rate coefficient to OH is comparable to many atmospheric constituents. The exact value has recently been measured by Dillon et al. (2012) and found to be weakly temperature and pressure dependent. For a more precise examination in a low-OH reactivity environment another reagent, which reacts more slowly with OH, could be used. Typical mixing ratios of pyrrole before the reaction with OH are 30–100 ppbV, after the reaction 10–30 ppbV depending on flow rates, humidity and intensity of the UV lamp. This corresponds to an OH field in the reactor of ca. 10^{12} molecules cm^{-3}. The ratio of pyrrole to OH usually ranges from 1.7 to 3.0. To calculate the total OH reactivity from the different measurement steps, each concentration level needs to be evaluated:
(1) Hysteresis, due to switching valves, unsynchronized detectors (inducing transitory changes in the signal of typically 0.5–10 s), or turning on the UV lamp initially (at least half an hour for warming up), causes artificial and misleading data-points. These need to be excluded from any analysis.
(2) Sensitivity changes of the detector in general complicate the measurements. Rapid jumps need to be excluded, while slowly decreasing sensitivity must be accounted for by calibrations.
(3) To correct for different humidity levels in C2 and C3, a humidity-response-calibration needs to be done. For this, different water levels can be applied to the measurement of C2, which result in variations of the UV production. This calibration can be used to correct parts of the data, where baseline (C2) and measurements (C3) consistently show different humidity levels. Sharp peaks in ambient humidity and rapid changes should be filtered from the data-set.
(4) A correction to account for deviations from pseudo first order conditions is necessary using CRM as was already described by Sinha et al. (2008). Since CRM measurements usually contain a mixture of pyrrole/OH about 1.7–3.0 a small correction (ca. 8 %) can be calculated and applied.
(5) NO might interfere in CRM total OH reactivity measurements due to its OH recycling potential. As presented in Sinha et al. (2008), levels higher than 10 ppbV NO need to be present in ambient air in order to impact total OH reactivity measurements via CRM. A detailed discussion of a CRM set-up used for highly polluted environments is given in Dolgorouky et al. (2012).
(6) Flows inside the CRM system need to be regularly checked and monitored. Thus a dilution factor for ambient air probes due to the addition of nitrogen and pyrrole is easily obtained.
The uncertainty of CRM measurements is calculated through a propagation of errors and depends on the uncertainty of the reagent's gas mixture, the error of the rate coefficient, the flow variations, and the detector's uncertainty.

2.2.2 Proton Transfer Reaction Mass Spectrometer (PTR-MS) measurements for CRM

In situ ambient measurements of total OH reactivity using CRM require a precise, stable, and reasonably fast detector with good linearity over the measurement range. Thus, in it's first configuration, total OH reactivity was measured by CRM as described above using PTR-MS (Sinha et al., 2008). This detector offers a fast response, reasonably precise measurements and an indication of water levels in the analyzed gases (which is helpful for ambient, hence humid measurements). The PTR-MS has been applied in various fields of scientific and industrial interest (Lindinger et al., 1998, de Gouw et al., 2004, Blake et al., 2009).
The basic principle can be described as follows: A hollow-cathode discharge source generates H_3O^+ ions from water vapor, which are introduced into a drift tube and mixed with the air sample. Proton transfer from the H_3O^+ to the gas molecules of interest occurs for compounds with higher proton affinity than water. The instrument is thus blind to N_2 and O_2, the main constituents of the atmosphere, but detects a wide range of organic compounds. Proton transfer is a relatively soft ionization method which limits the fragmentation of ions. In the drift tube an electric field accelerates the positive ions through the gas mixture. The operating pressure within the drift tube is typically 2.2 mbar and the total voltage across the drift tube 600 V. A quadrupole mass spectrometer separates ions according to their protonated mass to charge (m/z) ratios and a secondary electron multiplier detects them.
For total OH reactivity measurements the protonated reagent pyrrole is detected on m/z 68. In addition, primary ions H_3O^+, water clusters, markers for impurities (such as oxygen [m/z 32], methanol [m/z 33] and acetone [m/z 59]) and for noise (such as [m/z 24]) are monitored. An accurate calibration for pyrrole is needed not only in dry but also for humid air. It is known that the sensitivity of the PTR-MS varies for several compounds with humidity. Sinha et al. (2009) reported that the PTR-MS response to pyrrole is weakly dependent on the water concentration. It's sensitivity increases with relative humidity up to 30 %, but for higher relative humidities the sensitivity of the PTR-MS to pyrrole remains reasonably constant. Since total OH reactivity measurements are deployed for variably humid ambient air, the sensitivity dependence on humidity needs to be determined through calibration beforehand and applied during data-analysis.

Using the PTR-MS as a detector provides measurement points with a time resolution between 10–60 s and a limit of detection of 3–4 s^{-1} for total OH reactivity. This was calculated as 2σ of the C2 noise and tested empirically by introducing known OH reactivities to the system. CRM measurements use relatively high levels of pyrrole (10 ppbV–100 ppbV), so the absolute sensitivity towards the pyrrole signal is not crucial. More important is the signal to noise ratio and the stability of the detected concentrations levels (C1, C2, C3) which are compared to each other for the calculation (Eq. 2.1).

2.2.3 A new detector for CRM total OH reactivity measurements: a Gas Chromatographic Photo-Ionization Detector (GC-PID)

A custom-built GC-PID system (VOC-Analyzer from IUT-Berlin, now Environics-IUT GmbH) for total OH reactivity measurements has been developed to measure the mixing ratio of pyrrole comparable in quality and quantity to those obtained by PTR-MS. Compared to commercially available systems, sensitivity was improved, interferences were minimized, and the separation between peaks of interest (here:pyrrole) was optimized.
The instrument operates as follows: a small sampling pump continuously draws air through a particle-filter into the system (50–250 sccm). For analysis a sample is swept through a short capillary GC column to separate the various volatile organic compounds (VOCs) and water. In the detection cell the separated molecules are selectively ionized by UV light (e.g. aromatics, alkenes). Ions are formed and accelerated to a collector electrode by a weak electric field. In this system the ambient air itself acts as carrier gas eliminating the need for compressed gases. Due to a switching valve the inlet flow stops briefly after each sampling period, i.e. after each chromatogram. This does not impact the stability of the GC-PID and the detection of pyrrole. Column, valves and the detector are situated in a temperature controlled box to keep it isothermal. One chromatogram is generated, monitored and automatically saved every 60–70 s. The instrument records the raw signal of the chromatogram as well as a calibrated value in ppbV using the peak height and a previously determined calibration factor. The peak area was analyzed off-line using a custom-made IDL software provided courtesy of the University Frankfurt ("IAU chrom") which fits Gaussian curves to the peak and integrates the area of this Gaussian fit. Given an accurate calibration for pyrrole, the mixing ratio can be reliably determined from the peak area.

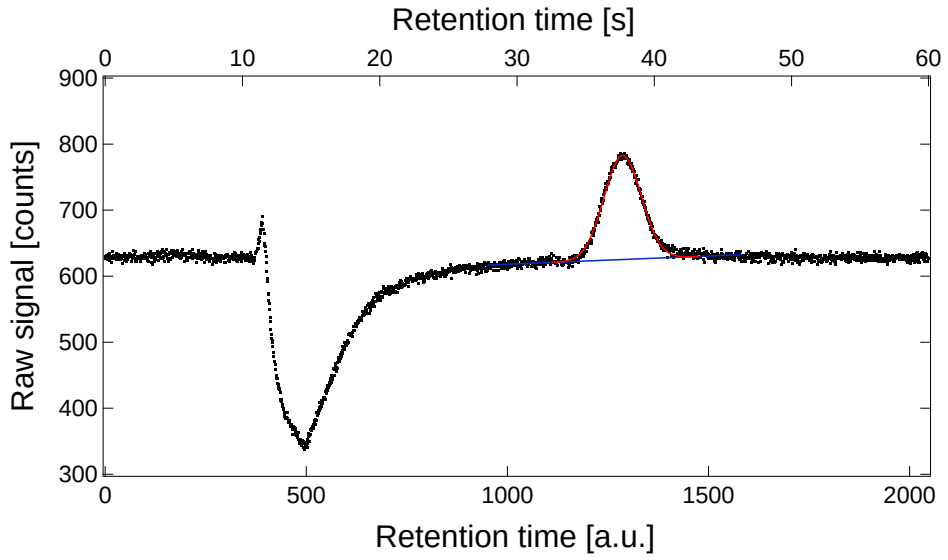

Fig. 2.1: Typical GC-PID chromatogram of pyrrole in humid air. Pyrrole is detected in a retention window of 1000–2000 a.u. (35–55 s) and needs to be well separated from the water peak (400–1000 a.u.). Added is the Gaussian fit for peak integration in red and the applied baseline in blue. It can be noted that the baseline is slightly tilted due to the water peak.

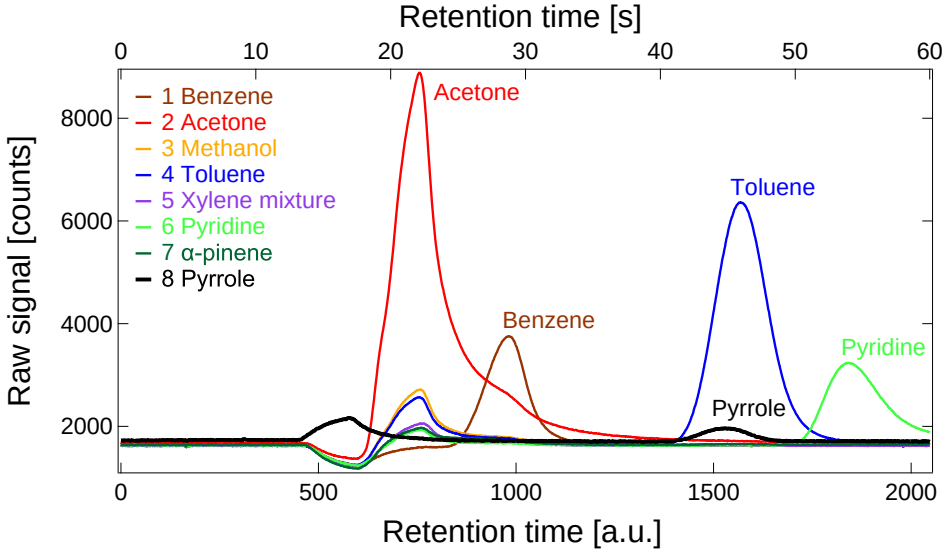

Fig. 2.2: Seven tested compounds (high ppbV to low ppmV levels) for interference on the pyrrole (black: 1000–2000 a.u.) retention time window. Four peaks are identified: acetone (red: 600–1000 a.u.), benzene (brown: 800–1200 a.u.), toluene (blue: 1300–1800 a.u.) and pyridine (green: 1700–2050 a.u.). Only toluene was overlapping with the pyrrole retention time window. Chromatograms for substances tested subsequently to acetone show a rest-acetone peak.

A typical chromatogram is presented in Fig. 2.1. An offset of 500–2000 counts was observed, which depended on the condition of the instrument. The offset is typically caused by several effects: (1) Traces of ionizable compounds, e.g from out-gasing material, are detected in addition to the analyzed sample. (2) UV radiation induces a photo-effect on the collector. (3) The detector has some electrical noise. The retention time of pyrrole ranged between 1000–2000 in the given units (corresponding to 35–55 s). When operating in ambient air additionally a water peak was found at 400–1000 a.u. retention time. This water peak was inverted with respect to pyrrole (it decreased the signal) and needs to be well separated from the pyrrole peak. Water absorbs in the UV and shields energy available for ionization causing the background signal (offset) in the detection cell to drop.
Many other chemicals are in principal detectable by the GC-PID. These include toluene, benzene and acetone, all of which are common compounds of ambient air. Because of the fast sampling and the relatively short chromatogram, the separation is not perfect and substances besides pyrrole can potentially interfere within the same retention time window. As can be seen in Fig. 2.2, four substances show clear peaks: acetone, benzene, toluene and pyridine. Other compounds such as α-pinene, methanol and a xylene-mixture did not show peaks in the analyzed sample. To identify the peak positions as shown in Fig. 2.2 head space of the pure liquid compounds, hence extremely high levels (about several hundred ppbV to low ppmV), were introduced to the instrument. By comparing Fig. 2.1 and Fig. 2.2, it can be noted that the pyrrole peak is shifted in retention time. Depending on temperature, different sampling conditions, and the state of the instrument, pyrrole might occur at slightly different times. The analysis software takes this effect into account, and has no problem, since pyrrole is the only significant peak to integrate.
For total OH reactivity measurements the pyrrole retention time window needs to be free of significant interferences. Atmospheric interference candidates are toluene (ambient concentrations 0.1–1 ppbV), since it's retention time overlaps with pyrrole, or pyrrole itself when being emitted by biomass burning (Karl et al., 2007). It is worth noting that pyrrole concentrations for CRM measurements are significantly higher (see Sect. 2.2.1). If necessary a background correction can be easily made by alternating between ambient measurements (without introducing pyrrole to the system) and total OH reactivity measurements. This assumes that the interference species does not vary significantly between the background tests.
Two calibration plots for pyrrole are given in Figs. 2.3 and 2.4. For both calibrations good linearity could be found, the fit-quality, the Pearson correlation coefficient R, is almost 1. The linear fit provides a slope which is a proxy for the sensitivity of the instrument and an offset which is caused by the level of noise. Standard tests have shown that pyrrole mixing ratios down to 3 ppbV are detectable by the instrument,

when it is running in optimum conditions (e.g. as was for Fig. 2.3). This is sufficient for CRM measurements where pyrrole is expected in the range of 10–100 ppbV.

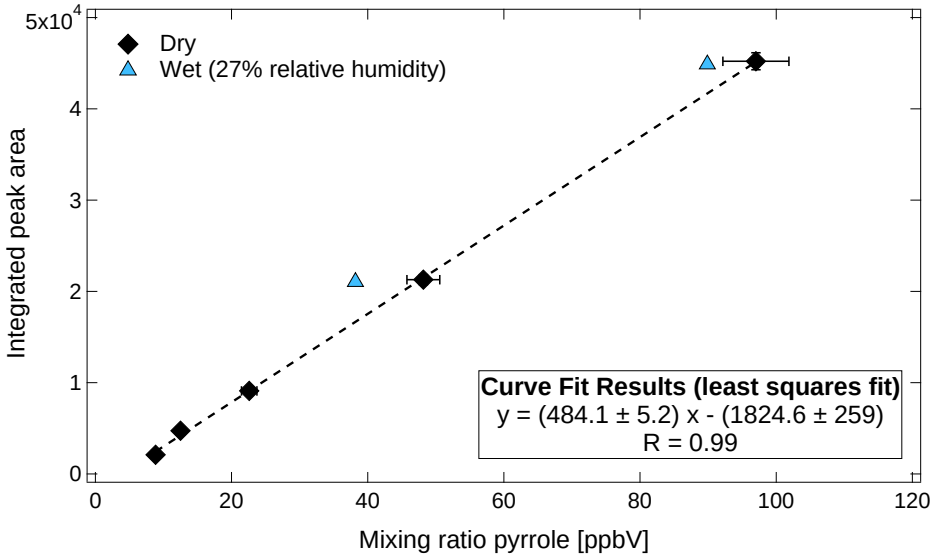

Fig. 2.3: Calibration plot for pyrrole which was introduced in different mixing ratio levels and detected with the GC-PID. The peak area was monitored and peak area integration averages were used to receive a calibration factor. Standard deviations of the averaged peak areas were less than 4 %. Two points (blue) were monitored in humid air and compared to dry results (black).

For ambient, hence humid air the instrument must provide the same linear performance in pyrrole detection as for dry conditions (as in Fig. 2.3). The characteristic water peak (Fig. 2.1) drives the signal negative at a retention time of 400–1000 a.u. and has the potential to drag down the baseline which is used to fit the pyrrole peak. In such cases the integrated peak area of pyrrole could be overestimated. This can be seen in Fig. 2.3 where two additional calibration points were recorded in humid conditions, and pyrrole was not well separated from the water peak. For a relative humidity of 27 % the integrated peak area was increased by 12 %. To correct the humidity depedency, in case of not well separated peaks, a factor can be determined through calibration beforehand. This correction is easy to apply as long as humidity in measured alongside with the GC-PID. For independent measurements a good separation is mandatory. This can be achieved by lenghtening the chromatographic separation (e.g. to 60–70 s), which improves the division of water and pyrrole but lowers the sampling frequency.
During an intensive field campaign frequent calibrations proved, that over several (ten) days the sensitivity of the instrument did not change much. The GC-PID was started in optimal conditions and ran non-stop for ambient measurements. As can be seen from Fig. 2.4, a repetition of pyrrole calibration after five days matches exactly the

previous results (less than 10 % deviation of the first calibration), while after ten days the sensitivity has slightly decreased (deviation of 35 %). Sensitivity can possibly be lost because of three reasons: (1) the particle-filter loses it's efficiency with time, (2) the PID window gets coated by photopolymerizing pyrrole (Cruz et al., 1999, Yang and Lu, 2005) weakening the ionization efficiency, (3) on the long term the detector ages and shows decreasing sensitivity. During field campaigns it is possible to exchange the particle-filter and to regularly calibrate. Decreasing sensitivity can be compensated by extending averaging times for a while. However, after intensive measurements over a long period (e.g. 1 year) the instrument needed maintenance such as cleaning the PID window and exchanging the detector to remain operational.

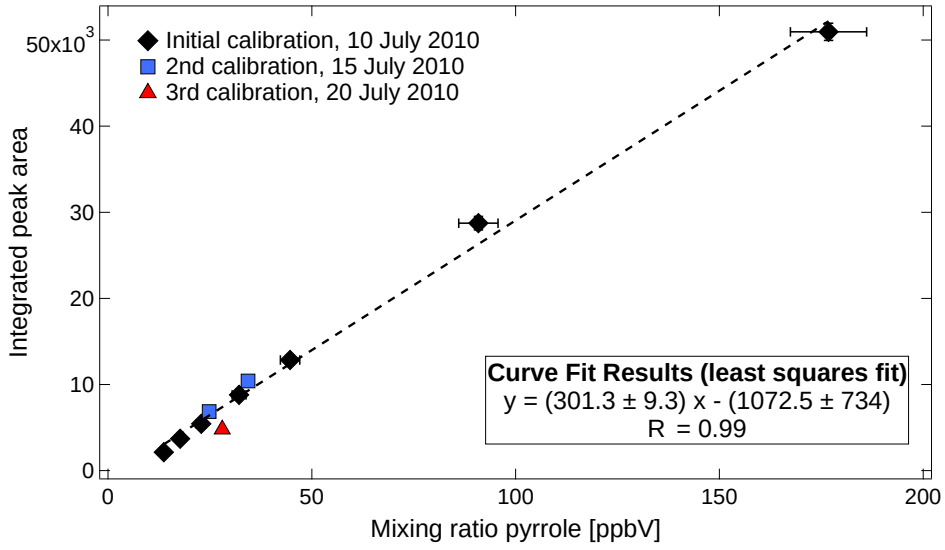

Fig. 2.4: Three different calibrations for pyrrole within ten days intensive measurements at the HUMPPA-COPEC 2010 field campaign: for optimized conditions at the start of the campaign (black), five days later (blue) and after ten days intensive measurement campaign (red). After five days less than 10 % deviation of the first calibration curve could be observed. After ten days sensitivity was decreased by 35 %.

2.2.4 Modifications to the CRM-set-up

Since the original publication of the CRM method, a number of design improvements have been realized. Figure 2.5 presents a schematic of the current operated CRM set-up.

A process controlling device (V25) switches automatically between different concentration levels (C1, C2, C3). Pyrrole is introduced directly before the reactor into the air stream which either provides clean air for baseline measurements (C2) or ambient air (C3). To produce OH another arm to the reactor contains a pen-ray mercury UV

lamp (184.9 nm) which is sheathed in a flow of either dry (no OH production, e.g. C1) or humidified nitrogen (OH production, e.g C2 or C3).
One major change to the original set-up (Sinha et al., 2008) is the position of the sampling pump (Pump). It is now installed downstream of the reactor, and draws ambient air samples into the reactor without passing through a pump beforehand. This avoids possible total OH reactivity loss in the pump. Thus ambient air is introduced unperturbed into the system and reacts with the generated OH. Downstream of the reactor, only the quantification of the pyrrole mixing ratio is necessary for total OH reactivity measurements. The Teflon pump which is used here has been proven to not affect the amount of pyrrole led through it. Pyrrole levels up and downstream to the pump were detected to be equal in several tests.

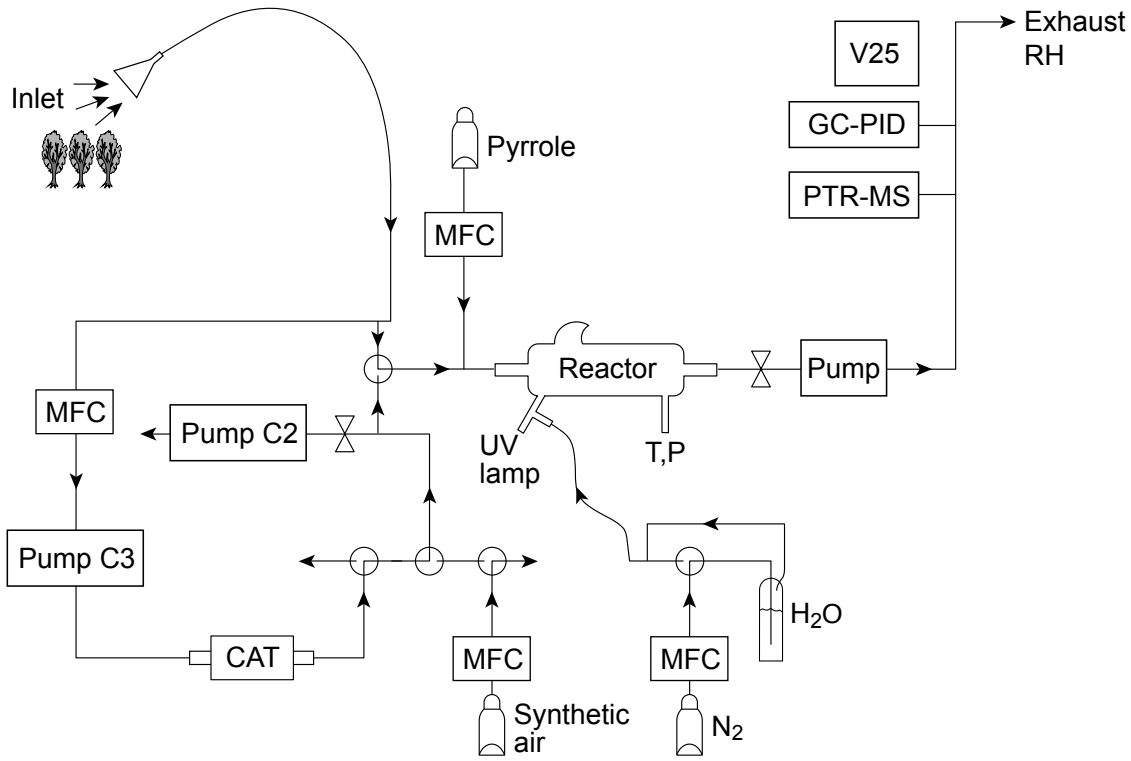

Fig. 2.5: Schematic of the Comparative Reactivity Method (CRM), as it was set-up for all presented tests and field campaigns. Two detectors (PTR-MS, GC-PID) were probing in parallel the outflow of the reactor. Mass flow controllers (MFC), valves and a catalytic converter (CAT) were operated by a controlling devise V25. This also recorded the measurement positions (C1, C2, C3) as well as temperature (T) and pressure (P) inside the system and relative humidity (RH).

These changes cause the reactions to proceed at slightly lower pressure in the reactor than ambient (1–4 hPa lower). Therefore it has to be ascertained that the system is leak-free, which was routinely controlled by injecting methanol at connecting parts, and checking the flow rates. All concentration levels (C1, C2, C3) need to be equal in pressure and flow conditions inside the reactor.
In Fig. 2.5 it can be seen, that a three-way-valve (Teflon) upstream of the reactor provides clean air (C2) or the ambient sample (C3). Both, the pump controlling the inlet flow (Pump C3) and another pump at the zero-air side (Pump C2), have to be adjusted carefully in order to provide the same pressure and flow through the reactor for all concentration levels. The additional pump (Pump C2) is needed to reduce the pressure at the clean-air, the C2 side. Otherwise, clean-air would be pushed with ambient pressure into the reactor through the catalytic converter by Pump C3, or the mass flow controller for synthetic air.
To avoid humidity effects in the reactor, meaning different water concentrations in measurements (C3) and baseline (C2) leading to different OH concentrations, a catalytic converter (CAT) was used to generate zero air with ambient humidity levels. The catalytic converter effectively transformed ambient molecules to corresponding oxides, e.g. CO_2 and H_2O. The resulting water was minor in comparison to ambient air levels. A sensor for humidity (RH) in the exhaust and the PTR-MS water signal (e.g. m/z 37) showed equal humidity levels for both C2 and C3 measurements. For extremely rapid changes of the humidity between two baseline C2 measurements, data was excluded from analysis later. The scrubbing efficiency was found to be high for all operating conditions. Please note, that the CRM used here was optimized to operate in natural, biogenically influenced, high reactivity environments. At such sites VOCs, which are effectively destroyed in the converter, dominate the total OH reactivity. For measurements in polluted regions with high levels of SO_2 and NO_2, which cannot be scrubbed by a typical catalytic converter, another set-up is necessary. As an alternative to the catalytic converter, synthetic air can be humidified to ambient water levels, and used for background measurements.
Temperature and pressure have been monitored and applied in the total OH reactivity calculations afterwards.
As in the original set-up, short Teflon lines and Teflon valves were implemented. In addition the glass reactor was coated with Teflon, to minimize surface induced hysteresis of humidity and pyrrole levels. The Teflon coating also minimizes the loss of OH reactive species to the walls of the reactor. The lines providing pyrrole from the gas standard (10.1 ppmV in Nitrogen) were shielded from light in order to avoid photolytic loss.
The inlet flow of the CRM can be chosen in a range between 350 sccm (chamber measurements) and 5000 sccm (fast flushing inlets). Overall 330 sccm were pumped through

the reactor, including 100 sccm Nitrogen and 1.8 sccm pyrrole. Under these conditions the reactor mixture contained 70 % of the ambient air sample, which optimized the CRM for operation in relatively clean, biogenic environments.

2.3 Results

Parallel measurements of PTR-MS and GC-PID as detector for CRM total OH reactivity observations were carried out in the laboratory, the Finnish boreal forest and a plant chamber. The instruments' limitations and advantages were revealed through comparison under different conditions. As visual intercomparison both detectors are pictured in Fig. 2.6.

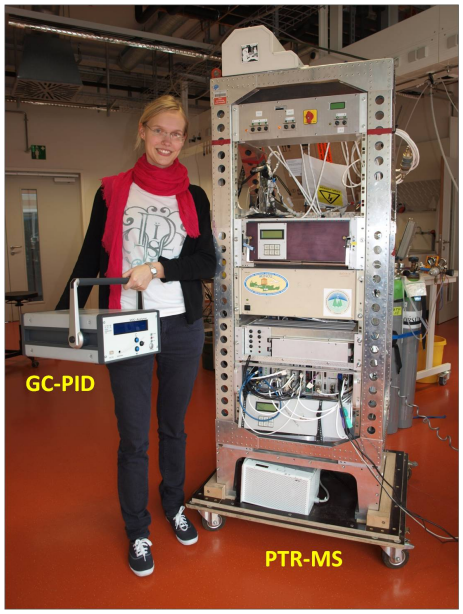

Fig. 2.6: Two detectors for CRM total OH reactivity measurements: To the right the IONICON PTR-MS, to the left the GC-PID.

2.3.1 Standard measurements

To verify the reliability of the two detector systems for CRM total OH reactivity measurements, standard tests were conducted in a series of laboratory and field experiments spanning over one year. The calibration gases employed for determination of OH reactivity were propane and propene (32890 ppbV, 596 ppbV, respectively) in Nitrogen. Both were diluted in zero air and individually introduced into the reactor of the system. Comparing the theoretically expected OH reactivity and the measured

OH reactivity established that both methods generated reasonable and comparable results. With respect to the theoretically expected total OH reactivity from the standard gas mixtures, the PTR-MS measurements reached 97 % and the GC-PID values 92 %. Both instruments slightly underestimated the true total OH reactivity (as compared to the stated values on the calibration bottle) by less than 10 % in the presented tests. Hence, both detectors responded accurately and within the uncertainty when used for CRM measurements.
Figure 2.7 compares the response of the two detectors in a OH reactivity range from 3–30 s^{-1}. A linear regression gives a slope of $m = 0.92$ and a low offset, which is smaller than the limit of detection for both instruments. Both detectors show very good correlation to each other, hence agree in the measured total OH reactivity from standard measurements.

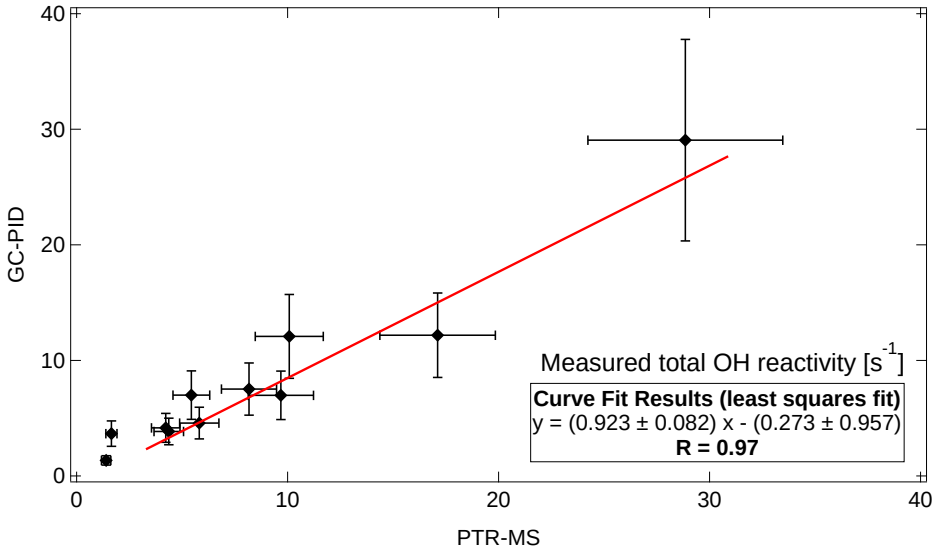

Fig. 2.7: Correlation plot and linear least squares fit for standard measurements of PTR-MS and GC-PID in parallel as detector for total OH reactivity. As standard gas propane and propene have been introduced into the system in a known amount and the total OH reactivity was detected with both instruments.

2.3.2 Field measurements – HUMPPA-COPEC 2010

In summer 2010 an intensive field measurement campaign (HUMPPA-COPEC 2010) at the Finnish boreal forest station SMEAR II in Hyytiälä took place in order to characterize direct biogenic emissions and photochemical reaction products in the gas-phase as well as the particulate phase. A detailed description of the field site, instruments and an overview of some results can be found in Williams et al. (2011). During this campaign the CRM was implemented to monitor total OH reactivity at two different

heights (in and above the forest canopy). These results are presented in Nölscher et al. (2012b). The HUMPPA-COPEC campaign in summer 2010 provided an excellent opportunity for the first intensive tests within a field campaign of the GC-PID in parallel with a PTR-MS as detector for total OH reactivity measurements.
Since the measurement site was surrounded by boreal forest, little toluene-interference was expected as toluene is thought to be predominantly anthropogenically emitted. Nevertheless frequent tests (several times a day) without pyrrole were performed but did not show any significant enhanced background within the pyrrole retention window. Even during the influence of an aged biomass burning plume no pyrrole or pyrrole interfering peak could be detected (Nölscher et al., 2012b). Furthermore, independent ambient PTR-MS measurements made in parallel showed extremely low toluene mixing ratios (less than 0.4 ppbV) and no evidence for pyrrole either. Figure 2.8 presents a comparison of the directly measured total OH reactivity inside the canopy for both instruments at the end of the campaign (7 August 2010–8 August 2010).
Diel variation was weak for 7 Aug 2010, a rainy and turbulent day. Total OH reactivity reached highest values shortly after a storm, as the boundary layer height started to decrease. A stronger signal for total OH reactivity was found the following day when maximum values of $40\,s^{-1}$ were observed in the late afternoon. As the day before, this day was stormy but warmer. Between strom rain showers high boreal forest emissions due to irradiation and high temperatures (which typically drive the VOC emissions) are likely causing the measured total OH reactivity to be high.
The GC-PID was operated in optimal conditions after a break for maintenance during the campaign, meaning a re-newed particle-filter and a brand new detector. In this manner, good time resolution and sensitivity could be achieved. The PTR-MS ran stably for the four week intensive field campaign. The two data-sets have been handled equivalently and averaged to 5 min values. The typical relative uncertainty for total OH reactivity measured with GC-PID in this campaign was 25 %, whereas the PTR-MS uncertainty was 16 %. These values are calculated through a propagation of errors: Three of the four parameters contributing to the measurement uncertainty are the same for both detectors (uncertainty of the reagent's gas mixture (5 %), error of rate coefficient (14 %), flow variations (2 %)). The instrumental error derived as standard deviation of the averaged noise is for PTR-MS results 5 %, and for the GC-PID 20 %. Both instruments operated with the same detection limit of $3\,s^{-1}$, which is the 2σ of the baseline (C2) noise during total OH reactivity measurements.

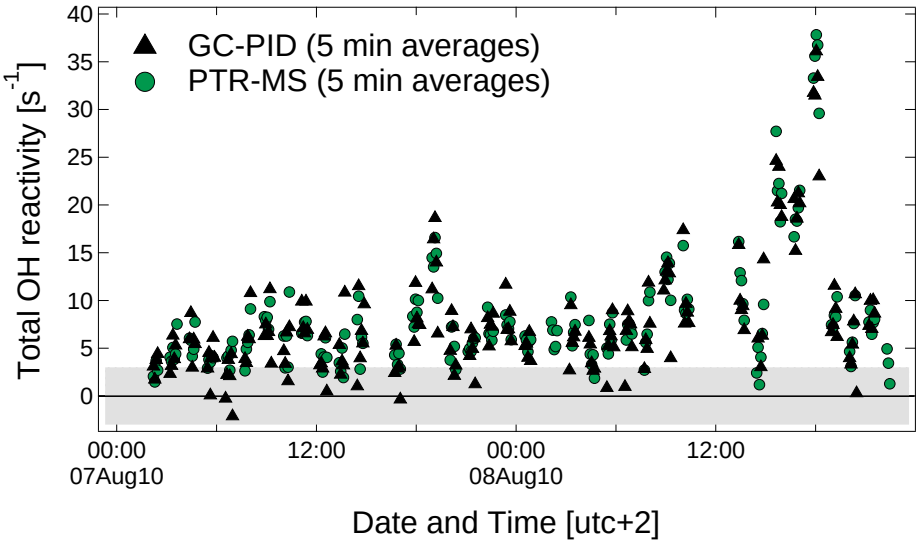

Fig. 2.8: Direct total OH reactivity measurements within the summertime boreal forest canopy during HUMPPA-COPEC 2010. Both detectors were operated in parallel for CRM, the data was analyzed and averaged to 5 min. PTR-MS (green) and GC-PID (black) show good agreement in a total OH reactivity range from the limit of detection to 40 s^{-1}. The detection limit for both instruments during this study was 3 s^{-1} and is highlighted in the graph as grey shaded area.

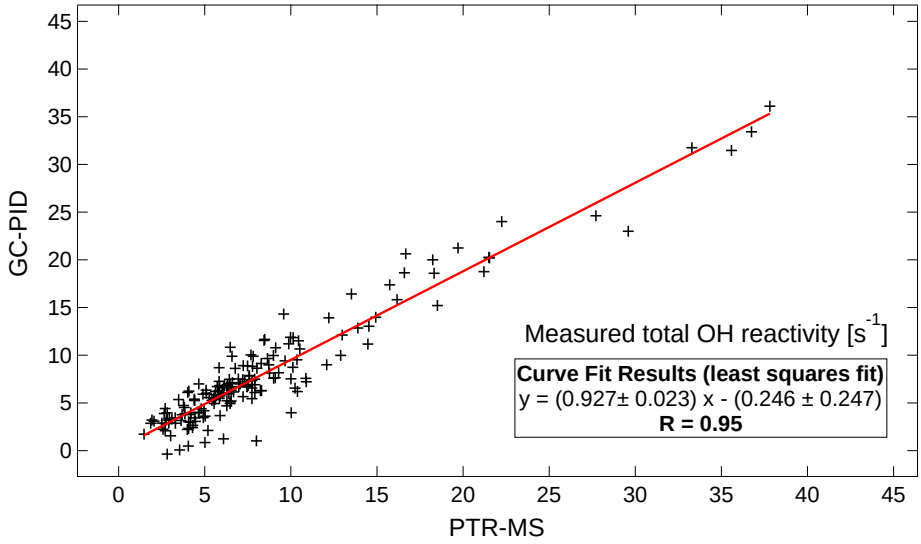

Fig. 2.9: Correlation of PTR-MS and GC-PID results for summertime boreal forest total OH reactivity during HUMPPA-COPEC 2010. A linear least squares curve fit is given, it's slope and the Pearson R of the correlation between the two instruments.

Generally PTR-MS and GC-PID values agree well with each other within the observed total OH reactivity levels from the limit of detection up to $40\,s^{-1}$. This can also be seen in Fig. 2.9 which presents the correlation and a linear fit of the 5 min averaged data from PTR-MS and GC-PID for total OH reactivity. The linear least squares fit shows good agreement between the two detectors with a slope of $m = 0.93$. The offset of the linear fit lies within the error. The quality of the correlation, given by Pearson R, is close to 1. Hence, both instruments were able to detect total OH reactivity using CRM and were in good agreement. Moreover the instruments operated at comparable time resolution, detection limit, and sensitivity.

2.3.3 Plant chamber measurements

The same set-up as deployed in the HUMPPA-COPEC 2010 campaign was operated at the Jülich Plant Atmospheric Chamber (JPAC) in September 2010. The total OH reactivity system was installed at the plant chamber facility to examine primary boreal tree emissions under controlled conditions. Figure 2.10 shows the results of both detectors' measured total OH reactivity, averaged to 5 min (PTR-MS) and 15 min (GC-PID) in a range of $15\,s^{-1}$ down to the limit of detection. The plant emissions show a weak diel variation in total OH reactivity and overall low levels, which are for most points below $8\,s^{-1}$. Because of decreased sensitivity, lower offset and higher noise the GC-PID results had to be averaged over a longer time period, and lost therefore in time resolution. Still the GC-PID results fluctuate more, but show the same overall trend as PTR-MS measurements. The detection limit of the GC-PID for these measurements was $6\,s^{-1}$, compared to $4\,s^{-1}$ detection limit of the PTR-MS total OH reactivity measurements. Again the limit of detection was calculated as the 2σ of the baseline (C2) noise. The GC-PID showed a less sensitive response to pyrrole when compared to previous conditions. Directly after maintenance with a new water-filter system (6 August 2010, Finland) the conversion factor of peak area to pyrrole mixing ratio was 289.04 peak area $ppbV^{-1}$, while after one month (9 September 2010) in Jülich it decreased to 276.89 peak area $ppbV^{-1}$. Because of a more noisy signal the overall uncertainty for the plant chamber results was 46 % for the GC-PID. After one month intensive field measurements in Finland during the HUMPPA-COPEC campaign, shipping and re-installation the plant chamber experiments present a worst case study for the new GC-PID detector.

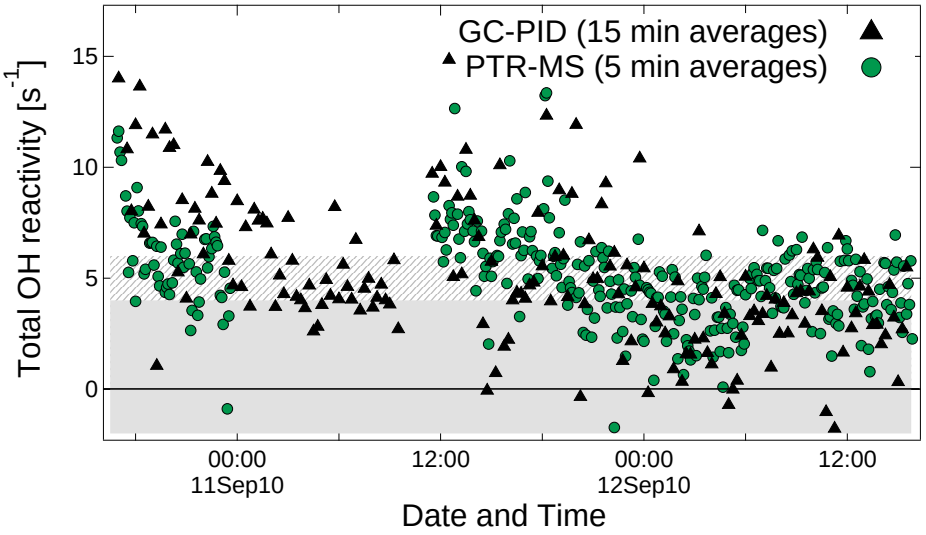

Fig. 2.10: Direct total OH reactivity measurements in the Jülich Plant Atmospheric Chamber (JPAC) for primary boreal tree emissions. The 15 min averaged results of the GC-PID (black) show the same trend but a higher variability than the PTR-MS (green) 5 min averages. The grey shaded area marks the range of the PTR-MS detection limit ($4\,s^{-1}$) and the grey pattern the GC-PID detection limit of $6\,s^{-1}$.

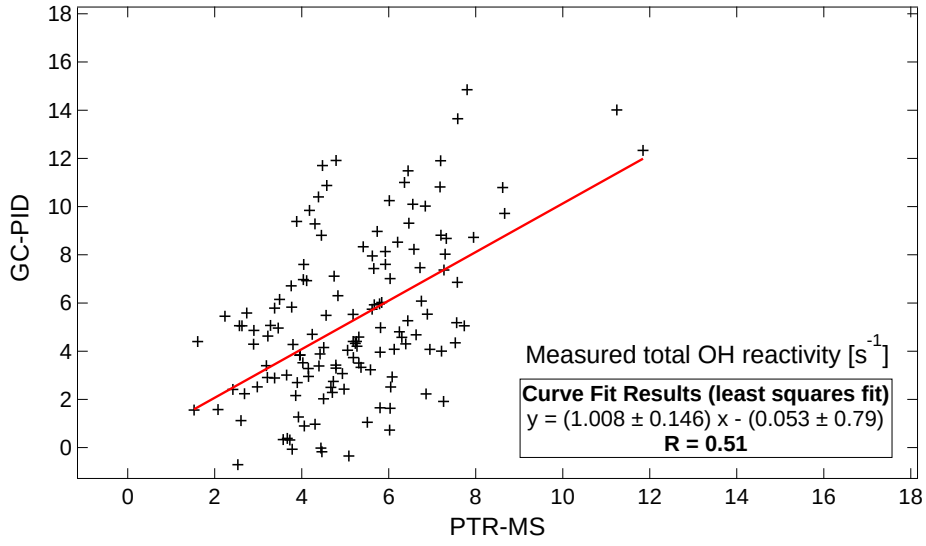

Fig. 2.11: Correlation of PTR-MS and GC-PID results (15 min averages) for total OH reactivity measured from boreal tree species in the JPAC plant chamber. A linear least squares curve fit, it's slope and the quality of the correlation (Pearson R) are given.

The correlation (Fig. 2.11) of both detectors is more scattered and the Pearson R coefficient shows positive but not strong correlation ($R = 0.51$). A linear regression fit has a slope of 1.01 but is not of good quality. This is mainly because of the generally low level of detectable total OH reactivity and less optimized conditions of the GC-PID. When examining the instrument subsequently of the campaign a layer on the detection PID window was observed and removed by cleaning. With time pyrrole polymerized due to UV radiation at the detection PID window, blocked transmission and hence ionization. The instrument lost sensitivity and noise increased. After the cleaning the GC-PID operated again with improved sensitivity and accuracy.

2.4 Discussion and comparison

A new detector for total OH reactivity measurements, a GC-PID, using CRM was tested under various (optimum and worst case) conditions. In general, the previously validated PTR-MS results and the new GC-PID measurements showed excellent agreement for standard tests and field observations within the boreal forest (HUMPPA-COPEC 2010). For the plant chamber experiments acceptable correlation was found. Decreasing sensitivity and accuracy in the GC-PID instrument were identified to be caused by polymerizing pyrrole at the detection PID window.
Table 2.2 summarizes technical and operational advantages and disadvantages of both instruments. When compared to the PTR-MS, the GC-PID is a smaller, lighter and less expensive instrument. The inlet flows for both instruments are adjustable and comparable. Both systems show slight humidity dependent sensitivity. This has been well characterized by Sinha et al. (2009) for the PTR-MS and so the measurements can be corrected. Calibrating with humid and dry air also provides a correction factor for GC-PID ambient (wet) measurements. For a good separation between the water and pyrrole peaks, the GC-PID results are not influenced by water. Lengthening the chromatogram improves the separation but reduces the sampling frequency unless multiple detectors are used asynchronously.

Table 2.2: Detailed comparison of technical, instrumental and operational parameters of PTR-MS and GC-PID

	PTR-MS	GC-PID
Size	$650 \times 1660 \times 550$ mm	$260 \times 160 \times 400$ mm
Weight	150 kg	8 kg
Power	max. 1500 W	max. 50 W (+ internal battery for ca. 12 h)
Inlet flow	30–300 sccm (continuously, adjustable)	50–250 sccm (not continuously, adjustable)
Interferences/Challenges	changing sensitivity with humidity	changing sensitivity with humidity possible toluene interference
Cost	ca. 180 000 €	ca. 18 000 €
Limit of detection	3–4 s^{-1}	3–6 s^{-1}
Uncertainty	16–20 %	25–46 %
Stability	very good over several weeks	decreasing after several weeks
Time resolution – raw	10–60 s	60–70 s
Time resolution – average	1–5 min	5–20 min

The second part of Table 2.2 highlights details of the application as detector for total OH reactivity measurements. The overall uncertainty is lower in the PTR-MS and it also shows good stability over long periods of measurement. The time resolution of the PTR-MS raw signal can be very short, i.e. only 10 s (when focusing on only a few detected masses). In most applications it is averaged to 1 to 5 min. With this time resolution the limit of total OH reactivity detection is 3–4 s^{-1} for PTR-MS. Compared to this, under optimum conditions, the GC-PID reaches the same detection limit and time resolution, but has a higher overall uncertainty (25 %). With less well optimized conditions, which can be expected when running the instrument continuously over several weeks, the uncertainty increases sharply (46 %) as well as the detection limit (6 s^{-1}). Then a longer averaging time is needed to gain reasonable accuracy. However, a full maintenance of the GC-PID prior to a campaign is advisable.
It should be noted that direct biomass burning emissions (Warneke et al., 2011), urban emissions (Fortner et al., 2009) and some biogenic emissions (White et al., 2009) could effect total OH reactivity measurements using GC-PID due to high and variable toluene emissions which may interfere on the pyrrole retention window. Under such conditions regular background determinations would be necessary with the same (or a second GC-PID), detracting from the measurement frequency (or doubling the costs). The boreal forest environment appears to be suitable for GC-PID determined total OH reactivity. Mao et al. (2012) recently reported concerns, involving interferences on the OH measurements using LIF techniques particularly in forests, where the GC-PID-CRM performed well. It remains to be determined whether this also impacts LIF total OH reactivity results.
Since the GC-PID coupled CRM is a small and light instrument, even airborne related total OH reactivity measurements could be possible in the future. Deploying the GC-PID as detector for direct total OH reactivity measurements using CRM offers a

robust, portable and less expensive alternative to PTR-MS measurements. Under optimized conditions very good agreement between both instruments could be examined. A technically improved version of the prototype GC-PID should also ensure that the detector provides good sensitivity for a long time, it is easy to handle and maintain regularly, and interferences with water and toluene diminish. The newest version is already smaller, lighter, better protected against water, optimized to separate compounds of interest (pyrrole, water, toluene), and most importantly, the lamp as well as the PID window are easily accessible. This way, maintenance of the instrument during a field campaign can be performed by the operator at the site. This makes the GC-PID a potentially useful method for total OH reactivity measurements in field studies.

Acknowledgments

We thank the IAU Team (Andreas Engel, Harald Bönisch, Stephan Sala) for providing the peak integration software, and the Jülich JPAC Team (Jürgen Wildt, Astrid Kiendler-Scharr) who hosted the plant chamber measurements. The entire HUMPPA-COPEC team is grateful for the support of the Hyytiälä site engineers and staff. Support of the European Community – Research Infrastructure Action under the FP6 "Structuring the European Research Area" Programme, EUSAAR Contract No. RII3-CT-2006-026140 is gratefully acknowledged.

3

Summertime total OH reactivity measurements from boreal forest during HUMPPA-COPEC 2010

A. C. Nölscher[1], J. Williams[1], V. Sinha[1,2], T. Custer[1], W. Song[1], A. M. Johnson[1,*], R. Axinte[1], H. Bozem[1], H. Fischer[1], N. Pouvesle[1], G. Phillips[1], J. N. Crowley[1], P. Rantala[3], J. Rinne[3], M. Kulmala[3], D. Gonzales[4], J. Valverde-Canossa[4], A. Vogel[5], T. Hoffmann[5], H. G. Ouwersloot[1,6], J. Vilà-Guerau de Arellano[6], and J. Lelieveld[1]

[1]Department of Atmospheric Chemistry, Max Planck-Institute for Chemistry Mainz, Mainz, Germany
[2]Indian Institute of Science Education and Research, Mohali, Punjab, India
[3]Department of Physics, University of Helsinki, Helsinki, Finland
[4]School of Environmental Sciences, Universidad Nacional, Heredia, Costa Rica
[5]Johannes Gutenberg-University Mainz, Mainz, Germany
[6]Meteorology and Air Quality Section, Wageningen University, Wageningen, The Netherlands
*now at: Department of Chemistry, Brigham Young University, Rexburg, Idaho, USA

Manuscript published in Atmospheric Chemistry and Physics

Summary. Ambient total OH reactivity was measured at the Finnish boreal forest station SMEAR II in Hyytiälä (Latitude 61°51′ N; Longitude 24°17′ E) in July and August 2010 using the Comparative Reactivity Method (CRM). The CRM – total OH reactivity method – is a direct, in-situ determination of the total loss rate of hydroxyl radicals (OH) caused by all reactive species in air. During the intensive field campaign HUMPPA-COPEC 2010 (**H**yytiälä **U**nited **M**easurements of **P**hotochemistry and **P**articles in **A**ir – **C**omprehensive **O**rganic **P**recursor **E**mission and **C**oncentration study) the total OH reactivity was monitored both inside (18 m) and directly above the forest canopy (24 m) for the first time. The comparison between these two total OH reactivity measurements, absolute values and the temporal variation have been analyzed here. Stable boundary layer conditions during night and turbulent mixing in the daytime induced low and high short-term variability, respectively. The impact on total OH reactivity from biogenic emissions and associated photochemical products was

measured under "normal" and "stressed" (i.e. prolonged high temperature) conditions. The advection of biomass burning emissions to the site caused a marked change in the total OH reactivity vertical profile. By comparing the OH reactivity contribution from individually measured compounds and the directly measured total OH reactivity, the size of any unaccounted for or "missing" sink can be deduced for various atmospheric influences. For "normal" boreal conditions a missing OH reactivity of 58 %, whereas for "stressed" boreal conditions a missing OH reactivity of 89 % was determined. Various sources of not quantified OH reactive species are proposed as possible explanation for the high missing OH reactivity.

3.1 Introduction

Boreal forests are among the largest terrestrial ecosystems on Earth covering 15 million km^2 (FAO, 2010). Vegetation is a significant source of reactive biogenic volatile organic compounds (BVOCs) (Guenther et al., 1995) including a hemiterpene (isoprene), monoterpenes (e.g. α-pinene) and sesquiterpenes (e.g. α-farnesene) (Fehsenfeld et al., 1992, Kesselmeier and Staudt, 1999). These various reactive emissions represent a strong potential sink for the main tropospheric oxidant, the hydroxyl radical (OH). Moreover, these species also react in the atmosphere with ozone (O_3) or nitrate radicals (NO_3) (Atkinson and Arey, 2003). The resulting photochemical products can influence ambient ozone, contribute to particle formation and growth processes, and therefore impact air quality and climate.

Biogenic volatile organic compounds are produced in plant organs and released depending on physical (e.g. mechanical and meteorological stimuli) and physiological (e.g. natural respiration) processes. It has been established that the chemical composition of the BVOCs and the emission rates are highly dependent on the plant species (Niinemets et al., 2004, Laothawornkitkul et al., 2009, Yassaa et al., 2012). In warmer regions, e.g. the tropics, isoprene is the strongest BVOC emission (Guenther et al., 2006) while in temperate and boreal regions monoterpenes, such as α-pinene, β-pinene and Δ-3-carene, predominate (Williams et al., 2007, Rinne et al., 2009). Monoterpene emissions are mainly temperature dependent, because resin duct storage pools in which the terpenes are located release these chemicals primarily according to the ambient temperature (Tingey et al., 1980, Guenther et al., 1993). Some monoterpene emissions are also driven by light (Shao et al., 2001, Ghirardo et al., 2010) when de novo biosynthesis is initiated. Another factor influencing plant emissions is the reaction to stress (Niinemets, 2010, Loreto and Schnitzler, 2010), including physical damage (Juuti et al., 1990, Yassaa and Williams, 2007, Haase et al., 2011), herbivoral attack (Wu and Baldwin, 2010), drought and heat (Rennenberg et al., 2006).

Total OH reactivity presents an excellent way to investigate the exchange and balance between atmosphere and biosphere, in terms of both the chemical composition and the budget of the atmosphere's primary oxidant (OH). It is defined as the total OH loss rate

calculated as the sum of all sink terms due to OH reactive species X_i, which depends on their ambient concentrations $[X_i]$ and the respective reaction rate coefficients k_{OH+X_i}.

$$R_{total} = \Sigma\ k_{OH+X_i} \times [X_i] \tag{3.1}$$

Alternatively, total OH reactivity can be measured directly (Kovacs and Brune, 2001, Sadanaga et al., 2004, Sinha et al., 2008) and compared to the calculated total OH reactivity as in Eq. (3.1). Previous studies have shown that this comparison can reveal gaps in the general understanding of local atmospheric chemistry, in particular of unquantified OH radical sinks. Especially in forested regions total OH reactivity has been observed to be significantly higher than expected from measurements of individual species. Thus, in ambient air there is often a "missing", and hence unexplained fraction of OH reactivity. Di Carlo et al. (2004) observed for two campaigns in the Michigan forest (northern hardwood forest) 1998 and 2000 an exponential dependence between temperature and missing OH reactivity. It was therefore suggested that unmeasured, terpene-like BVOCs contributed to this missing OH sink. In contrast, Ren et al. (2006) found similar absolute total OH reactivity, but no missing OH reactivity at a comparable forest site. In the tropical rainforest direct total OH reactivity measurements have indicated a significant missing fraction of total OH reactivity (Sinha et al., 2008, Ingham et al., 2009). Similarly, Sinha et al. (2010) found within the canopy of a boreal forest 50 % missing OH reactivity which did not correlate significantly with light or temperature. These results and other total OH reactivity measurements of forest field campaigns are summarized in Table 3.1.

Several hypotheses have been developed over the last decade concerning the identity and nature of the missing OH reactivity. In addition to unmeasured primary emissions suggested by Di Carlo et al. (2004), a significant contribution from secondary products has been proposed (Lou et al., 2010, Taraborrelli et al., 2012). A strong contribution to ambient missing OH reactivity from secondary oxidation products appears to be supported by branch enclosure measurements that showed no missing fraction in primary emissions (Kim et al., 2011). However, accounting for the reaction products of previously measured compounds at the Hyytiälä site (boreal forest) using Chemical Master Mechanism modeling did not explain the discrepancy between calculated and directly measured total OH reactivity (Mogensen et al., 2011).

Table 3.1: Total OH reactivity field studies in forest environments, typical measured values, the mean missing (unexplained) fraction and a hypothesis to explain this missing OH reactivity.

Publication	OH reactivity [s^{-1}]	Missing fraction[a]	Hypothesis
Di Carlo et al. (2004) PROPHET Northern Michigan, mixed forest[b] Summer 1998/2000	1–12	temp. dependent	unmeasured terpene-like emissions
Ren et al. (2006) PMTACS-NY Whiteface Mountain, mixed forest[b] Summer 2002	2–12	0 %	no significant missing OH reactivity
Sinha et al. (2008) GABRIEL Surinam, tropical forest Summer 2005	28–72	70 %	unmeasured compounds
Ingham et al. (2009) OP-3 Borneo, tropical forest Spring 2008	10–60	50 %	unmeasured direct biogenic emissions and isoprene oxidation products
Sinha et al. (2010) BFORM Hyytiälä, boreal forest Summer 2008	5–12	50 %	primarily unmeasured direct biogenic emissions

[a] Note that the missing fraction of total OH reactivity depends on the available single compound's measurements.

[b] Inconsistent results in missing OH reactivity were found although the measurement sites were similar. The PROPHET mixed forest is characterized by northern hardwood, mixed aspen, bog conifers, pines and red oaks. The PMTACS-NY mixed forest is composed of hardwood and conifer species with birch, sugar maple, beach, some red spruce and balsam fir. It was suggested that there is a significant difference in BVOC emissions between these two sites (Ren et al., 2006).

In this study total OH reactivity measurements for a boreal forest during summer are presented. Measurements were taken both within the canopy (where primary emissions likely predominate) and above the canopy (with a higher fraction of photooxidation products). Ambient conditions varied between unusually hot periods, periods influenced by biomass burning and typical summertime boreal forest meteorological conditions. Simultaneous comprehensive observations of ambient gas-phase compounds and aerosols, allowed the missing OH reactivity at the Hyytiälä field station SMEAR II to be examined in detail through a comparison with concurrently measured primary emissions and secondary products.

3.2 Experimental

For the HUMPPA-COPEC campaign in summer 2010 the total OH reactivity instrument was installed at the SMEAR II station in Hyytiälä, Finland. Measured at the same site were precursors such as anthropogenic and biogenic VOCs, their oxidation products, and the main oxidants OH, O_3 and NO_3 as well as aerosol distributions, other inorganic chemical constituents, and meteorological parameters.

3.2.1 Measurement site in Hyytiälä

Boreal forest surrounds the Hyytiälä SMEAR II station which has been set up to routinely monitor ecological, meteorological and plant physiological parameters as well as gas-phase chemistry, new particle formation and aerosol growth throughout the year. In summer 2010 an additional tower (HUMPPA-COPEC tower) was built to house further photochemical instrumentation. A comprehensive description of the measurement site, typical vegetation and land-use characteristics, campaign instrumentation and meteorological parameters are described elsewhere (Williams et al., 2011).
The height of the predominantly Scots pine canopy is around 20 m from the ground, the trees being approximately 50 yr old. Two inlet lines of identical length were positioned adjacent to the forest at 18 m and 24 m on the HUMPPA-COPEC tower within a small clearing to provide air samples from within and above canopy.

3.2.2 Comparative Reactivity Method – a total OH reactivity instrument

During HUMPPA-COPEC 2010 the total OH reactivity was measured directly using a modified version of the Comparative Reactivity Method (CRM) described by (Sinha et al., 2008). Total OH reactivity can be determined based on competitive reactions between OH and a selected reagent, which is not present in ambient air, and other atmospheric reactive compounds. The reagent (pyrrole in this case) is diluted with zero air, introduced into a Teflon coated glass reactor and detected with a Proton Transfer Reaction Mass Spectrometer (PTR-MS). Next, OH is produced by photolyzing water vapor (humidified nitrogen) and mixed into the reactor. The initial pyrrole concentration (C1) is reduced by the amount of generated OH radicals, which can be seen in the detector's signal (C2). By exchanging zero air with ambient air, atmospheric reactive molecules enter the reactor and react with OH. The competitive reaction between those atmospheric molecules and pyrrole for OH results in a higher amount of detectable pyrrole molecules (C3). The following equation provides the total OH reactivity in air R_{air}.

$$R_{\mathrm{air}} = \mathrm{C1} \times k_{\mathrm{pyr+OH}} \times \frac{(\mathrm{C3–C2})}{(\mathrm{C1–C3})} \tag{3.2}$$

Where $k_{\mathrm{pyr+OH}}$ is the rate coefficient of pyrrole with OH. The reaction rate of pyrrole with OH has recently been measured (Dillon et al., 2012). The rate coefficient used here

(1.2×10^{-10} cm^3 molecules^{-1} s^{-1}) corresponds to the temperature and pressure regime of the reactor. Corrections for the influence of humidity to the PTR-MS sensitivity (Sinha et al., 2009), pseudo-first order conditions and dilution are applied. Although these corrections are small in comparison to the overall signal, they are essential for the reliable quantification of the total OH reactivity by this method. The data has been averaged into 5 min intervals. The threshold for NO interference has been previously determined to be 10 ppbV in ambient air (Sinha et al., 2008). Since NO levels detected were lower than 0.4 ppbV for the entire field campaign no significant interference on the CRM measurements occurred and no correction was needed. The instrument switched between the above and in canopy inlet lines (both 30 m length) in a 20 min cycle. The dwell time for an air sample in these lines was $\pm$ 23 s. The residence time for the reactor was less than 10 s, the PTR-MS sampling time 12 s.

In comparison to the system described by Sinha et al. (2008), the set-up used here is more fully automated. To avoid humidity effects in the reactor, meaning different water levels in measurement (C3) and baseline (C2) leading to different OH concentrations, a catalytic converter was used to generate zero air with ambient humidity. The catalytic converter effectively converted VOC mixtures to CO_2+H_2O. However, the resulting water vapor was minor in comparison with ambient humidity levels. A pump, which has been installed downstream of the reactor (in contrast to the previously described set-up (Sinha et al., 2008)), draws the ambient air samples into the reactor. This way the atmospheric air sample entered the reactor without passing through a pump beforehand, eliminating possible OH reactivity loss due to removal of OH reactive compounds in the pump. Temperature and pressure in the reactor as well as ambient temperature, pressure and humidity were recorded during the entire campaign and used for OH reactivity calculations. The detection limit was found to be 3–4 s^{-1} with respect to the 2σ of the baseline pyrrole concentration level (C2). Errors in the detector (5 %), rate coefficient (14 %), gas standard (5 %) and dilution (2 %) lead to an overall uncertainty of 16 %. A detailed description of the modified instrument and the applied corrections is given in Nölscher et al. (2012a).

In order to check the accuracy of the system, standard-tests were regularly performed throughout the campaign as well as in subsequent experiments (Jülich, September 2010; Paris (COMPOH), June 2011). Both propane and propene standards were introduced and the measured OH reactivity matched the expected value within the respective uncertainties (Fig. 3.1). The results showed good linearity in all tests over a long time period and the atmospherically relevant total OH reactivity regime.

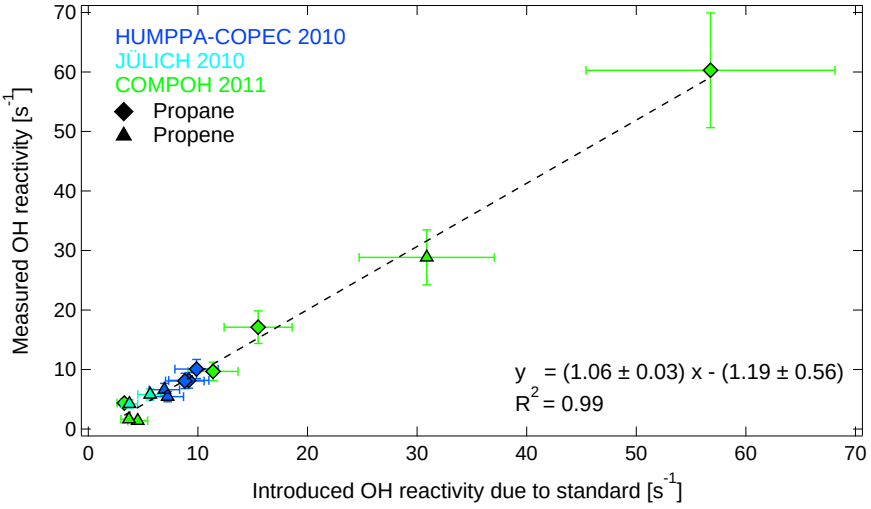

Fig. 3.1: Standard tests with propane and propene at different days for the HUMPPA-COPEC campaign (summer 2010), experiments in Jülich (autumn 2010) and the COMPOH campaign in Paris (spring 2011). Given is a linear fit, with slope and the quality of the fit.

3.3 Results

In the course of the campaign, the site was impacted by a variety of emission sources including the surrounding forest, transported biomass burning pollutants, and occasional urban influences. The campaign can be subdivided into three parts based on the meteorological conditions and total OH reactivity characteristics (see Fig. 3.2). Prior to the start of the campaign the forest had been exposed to unusually high temperature conditions (14–30 °C) for several weeks and showed symptoms of heat (but not drought) stress (Bäck et al., 2012). The regime "**stressed boreal**" (18–25 July 2010) was defined as the period of the elevated temperature ($T_{average} = 19.78 \pm 0.10$ °C) extending into the field campaign. Within this period, boreal forest emissions were mixed with anthropogenic pollutants transported by south-westerly winds. The highest ambient concentrations of biogenic VOCs such as isoprene (peak concentration: 680 pptV) and monoterpenes (α-pinene peak concentration: 936 pptV) were observed during this period of the campaign. At the end of this period wind from the north brought clean, cool air to the measurement site for circa 2 days. Under these conditions the minimum anthropogenic influence was detected. The second regime, named "**transported pollution**", was defined for 26–29 July 2010. Within this time wildfire pollution plumes from Russia were advected to the measurement site (Williams et al., 2011). Strongly enhanced mixing ratios of biomass burning tracers, such as CO (peak concentration: 438 ppbV) and acetonitrile (peak concentration: 551 pptV), were used to define the **transported pollution** period. A HYSPLIT-back-trajectory analysis indicated wild-

fires 400 km east of Moscow as the source burning region. Local temperatures remained high throughout this period (14–32 °C, $T_{average} = 23.68 \pm 0.10$ °C). Note that although ambient temperatures during the **transported pollution** regime are higher, the first period is termed **heat stress** regime due to the extended period of high temperatures preceding the campaign. The **transported pollution** regime represents a combined effect of heat stress and transported biomass burning emissions.
Following this period, at the beginning of August (1–7 August 2010) temperatures varied between 14–27 °C ($T_{average} = 18.98 \pm 0.06$ °C) and wind directions changed between south-west and south-east. The meteorological conditions here are comparable to previous summertime observations (2007: 8–24 °C, 2008: 6–24 °C, 2009: 12–22 °C – Williams et al., 2011) and hence this regime is termed "**normal boreal**". Since the conurbations Tampere and Helsinki lie to the south-west and St Petersburg to the south-east it is likely that this **normal boreal** regime represents a boreal forest signal with occasional anthropogenic influence. It should be noted that peak ozone concentrations (50–76 ppbV) were always coupled with southerly winds. Therefore the potential for ozonolysis products was higher during these periods. Storms and precipitation events happened more frequently during the **normal boreal** regime compared to the beginning of the campaign.

3.3.1 In canopy – above canopy comparison of total OH reactivity

Using total OH reactivity measurements at both heights, a deviation from average total OH reactivity for above (R_{above}) and in (R_{in}) canopy can be calculated. Therefore, two hour averages of both total OH reactivity measurements (in and above canopy) are compared to the original individual measurements in and above the canopy.

$$\Gamma = \frac{R_{above/in}}{R_{ave}} - 1 \tag{3.3}$$

Equal total OH reactivity above and in the canopy leads to a value $\Gamma = 0$. When total OH reactivity in the canopy is higher than above, Γ is negative. For higher total OH reactivity above the canopy, Γ is positive. Figure 3.2 also presents the in canopy – above canopy comparison Γ for the entire measurement period. The green colored bars indicate total OH reactivity was higher in the canopy (negative values), the bars are blue when total OH reactivity was higher above the canopy (positive values). Additionally, two hour averaged data is included (black line) for a smoothed picture of the highly variable atmospheric total OH reactivity.
The previously characterized regimes show distinct differences: predominantly green during **stressed boreal**, predominantly blue during **transported pollution** and mixed for the **normal boreal** regime. On several occasions short spikes in the comparison between in and above canopy OH reactivity occurred due to local pollution or

rapid mixing from above the canopy. High total OH reactivity inside the canopy was usually observed in the afternoon with high light and temperature conditions.

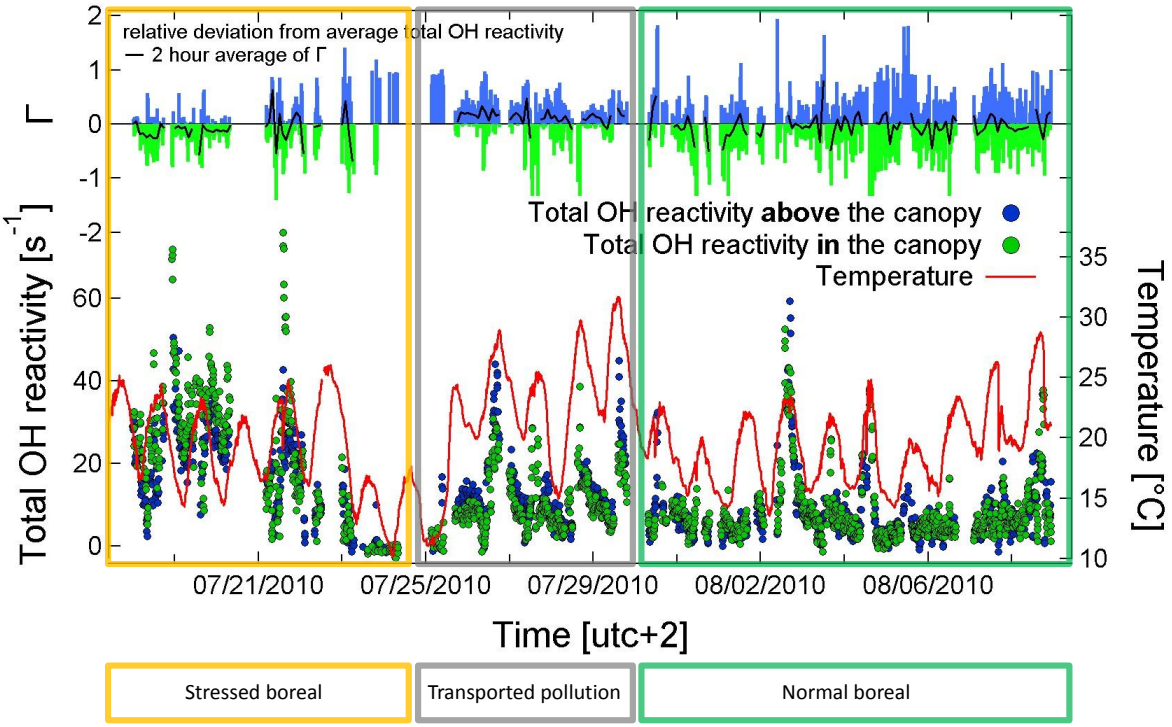

Fig. 3.2: Overview of total OH reactivity measurements in (green markers) and above (blue markers) the canopy, temperature (red) and superimposed (green and blue bars) the in canopy – above canopy comparison of total OH reactivity Γ. Three periods of different influences and conditions are defined, marked and labeled.

3.3.2 Missing OH reactivity

In addition to direct measurements from the CRM instrument, total OH reactivity was calculated using single compound measurements. Summing up each of the single compound OH reactivities (Eq. 3.1) leads to the total calculated OH reactivity. The difference between this calculated and the directly measured total OH reactivity provides the missing OH reactivity.

Table 3.2: Compounds, instruments and locations of the measurements which have been used for the calculation of total OH reactivity. The rate coefficients were taken from the literature and listed here in $cm^3\,molecules^{-1}\,s^{-1}$.

Compound	Method	Location	rate coefficient
α-pinene[a]	GC-MS	HUMPPA-COPEC tower	5.30×10^{-11}
β-pinene[b]			7.43×10^{-11}
Δ-3-carene[b]			8.80×10^{-11}
isoprene[a]			1.00×10^{-10}
β-myrcene[c]			3.34×10^{-10}
benzene[a]			1.19×10^{-12}
m-xylene[b]			2.31×10^{-11}
p-xylene[b]			1.43×10^{-11}
ethylbenzene[b]			7.00×10^{-12}
methanol[a]	PTR-MS	SMEAR II meteo tower	9.00×10^{-13}
acetonitrile[a]			2.20×10^{-14}
acetaldehyde[a]			1.50×10^{-11}
formic acid[a]			4.50×10^{-13}
acetone[a]			1.80×10^{-13}
MVK/MACR[a]			3.00×10^{-11}
MEK[a]			1.20×10^{-12}
toluene[a]			5.60×10^{-12}
iso-butane[b]	Fast GC-MS	SMEAR II meteo tower	2.10×10^{-12}
n-butane[b]			2.35×10^{-12}
iso-pentane[b]			3.60×10^{-12}
n-pentane[b]			3.70×10^{-12}
methane[a]	GC-FID	SMEAR II meteo tower	6.40×10^{-15}
NO_2[c]	BLC+CLD	HUMPPA-COPEC tower	1.10×10^{-11}
NO[a]	CLD		1.29×10^{-11}
O_3[a]	UV absorption		7.30×10^{-14}
CO[a]	VUV absorption		1.44×10^{-13}
H_2O_2[a]	Dual enzyme		1.70×10^{-12}
HCHO[a]	Hantzsch		8.50×10^{-12}
SO_2[a]	UV absorption	SMEAR II meteo tower	1.30×10^{-12}
pinonic acid[c]	APCI-IT-MS		1.04×10^{-11}
pinic acid[c]			8.70×10^{-12}
HONO[a]	Marga		6.00×10^{-12}
MHP[b]	HPLC	HUMPPA-COPEC tower	5.50×10^{-12}
PAA[c]	CIMS		1.88×10^{-12}
PAN[a]			3.00×10^{-14}

[a] IUPAC preferred value; [b] Atkinson and Arey (2003); [c] others: β-myrcene (Hites and Turner, 2009), NO_2 (Mollner et al., 2010), pinonic & pinic acid (Vereecken and Peeters, 2002), PAA (Jenkin et al., 1997).

Single compound measurements from a GC-MS instrument drawing air on the same inlet line as the CRM (HUMPPA-COPEC tower), PTR-MS vertical gradient measurements from the SMEAR II meteo tower, Fast GC-MS observations from SMEAR II meteo tower, and other measurements from nearby towers (less than 200 m distant) associated with the SMEAR II station were used to calculate a theoretical value for total OH reactivity above the canopy. For the purpose of this calculation it is assumed that all measurements are co-located. Overall 35 compounds contributed to the total calculated OH reactivity. Compounds, method, location and the applied rate coefficients are listed in Table 3.2.

In Fig. 3.3 the above canopy measured total OH reactivity (marked in blue), the calculated OH reactivity (red) and the missing fraction (color-coded by itself) are included. The missing fraction indicates how much of the measured OH reactivity remains unexplained by the calculated OH reactivity. Clearly, the sum of these 35 compounds was less than the total measured OH reactivity for most of the time. Only 17 % of all results are found to have lower than 50 % missing fraction of total OH reactivity. Also included in Fig. 3.3 is the overall uncertainty (grey shaded) of the calculated OH reactivity. This is estimated as the root square propagation of the uncertainties in the reaction rate coefficients and the single compound measurements.

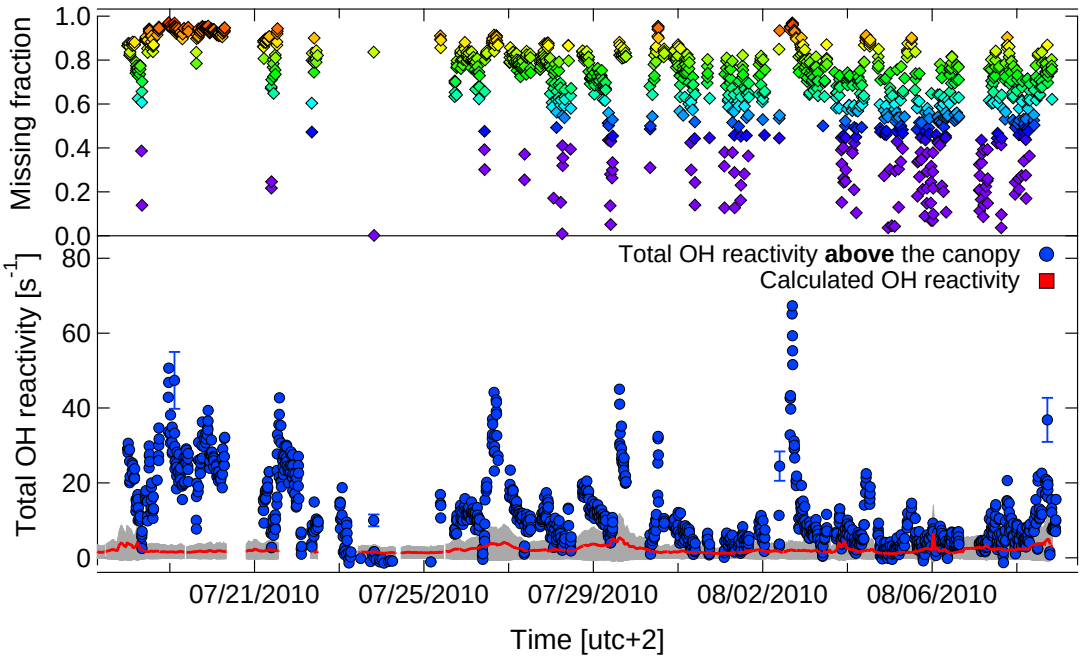

Fig. 3.3: Overview of total OH reactivity measurements above the canopy (blue markers), calculated OH reactivity (red) and superimposed the missing fraction of total OH reactivity (color-coded by itself). High missing fraction indicates a high percentage of unaccounted for OH reactivity when comparing single compound ambient measurements to the results of CRM. Error bars in grey show the uncertainty in the total OH reactivity calculation.

3.3.3 Characteristics of boreal summertime OH reactivity

A detailed analysis of the results in terms of absolute values, in canopy – above canopy comparison (Γ) and missing OH reactivity for all previously characterized regimes is given in the following paragraphs:

Whole campaign:
Results for the entire HUMPPA-COPEC campaign (18 July–9 August 2010) are illustrated in Figs. 3.2 and 3.3 and summarized in Table 3.3. Total OH reactivity was observed to vary between values at the limit of detection ($3\,s^{-1}$) and $76\,s^{-1}$. The ambient air temperature, which is also shown in Fig. 3.2, fluctuated during summer 2010 between 10–32 °C.
Mean results for the entire campaign do not show a significant difference between in and above canopy measured total OH reactivity. Within the canopy $12.4 \pm 0.1\,s^{-1}$ was detected and $11.5 \pm 0.1\,s^{-1}$ above the canopy. Values close to zero were found on average for Γ (-0.01 ± 0.004). The large range of total OH reactivity over the campaign is apparent in high standard deviations, around $10\,s^{-1}$. High short-term variability was noted in the BFORM campaign during summer 2008 at the same measurement site (Sinha et al., 2010). In HUMPPA-COPEC the measured total OH reactivity in summer 2010 shows a diel pattern in short-term variability when calculating the relative standard deviation (RSD) (standard deviation over mean value) for night and day (30 min mean values). Daytime total OH reactivity measurements above the canopy showed an overall high variability ($RSD_{day} = 1.22$). A lower short-term variability ($RSD_{night} = 0.84$) was found during the night.
For the entire measurement period the calculated OH reactivity (sum of measured compound contributions, see Sect. 3.3.2) is on average $2.2 \pm 0.01\,s^{-1}$. Here CO ($0.406\,s^{-1}$), methane ($0.280\,s^{-1}$) and acetaldehyde ($0.248\,s^{-1}$) are the most dominant contributors. Biogenic emissions like isoprene ($0.222\,s^{-1}$), Δ-3-carene ($0.130\,s^{-1}$), α-pinene ($0.101\,s^{-1}$) and methanol ($0.073\,s^{-1}$) also contributed significantly to the calculated OH reactivity along with NO_2 ($0.096\,s^{-1}$) and HCHO ($0.098\,s^{-1}$). From Fig. 3.3 it is clear that the calculated OH reactivity does not reflect the high variability of the measured total OH reactivity. Since the calculated OH reactivity remains broadly constant, the trend of the missing total OH reactivity is similar to the measured.

Table 3.3: Characteristic regimes during HUMPPA-COPEC 2010, average values for total OH reactivity measured in the canopy (18 m) and above the canopy (24 m), the mean in canopy – above the canopy comparison Γ, average calculated and missing OH reactivity and the average missing fraction of total OH reactivity. Uncertainties are given as standard error.

	Whole campaign	Stressed boreal	Transported pollution	Normal boreal
measured OH reactivity (in canopy)	$(12.4 \pm 0.1)\,s^{-1}$	$(30.7 \pm 0.4)\,s^{-1}$	$(10.9 \pm 0.2)\,s^{-1}$	$(7.8 \pm 0.2)\,s^{-1}$
measured OH reactivity (above canopy)	$(11.5 \pm 0.1)\,s^{-1}$	$(23.6 \pm 0.3)\,s^{-1}$	$(13.0 \pm 0.2)\,s^{-1}$	$(6.8 \pm 0.2)\,s^{-1}$
Γ	-0.01 ± 0.001	-0.14 ± 0.01	0.10 ± 0.01	0.13 ± 0.01
calculated OH reactivity (above canopy)	$(2.2 \pm 0.01)\,s^{-1}$	$(2.0 \pm 0.02)\,s^{-1}$	$(2.8 \pm 0.02)\,s^{-1}$	$(2.0 \pm 0.01)\,s^{-1}$
missing OH reactivity (above canopy)	$(8.9 \pm 0.1)\,s^{-1}$	$(21.6 \pm 0.3)\,s^{-1}$	$(10.3 \pm 0.2)\,s^{-1}$	$(4.8 \pm 0.2)\,s^{-1}$
missing fraction (above canopy)	68 %	89 %	73 %	58 %

Stressed boreal regime:

This regime represents the boreal forest under conditions of prolonged heat stress (see Sect. 3.3). Wind speeds were lower than $6\,m\,s^{-1}$ which enhances the impact of local forest sources on the measurement site. Measured total OH reactivity in the canopy reached $76\,s^{-1}$ for high temperatures and southerly winds, and dropped below detection limit ($3\,s^{-1}$) for low temperatures and northerly winds. On average the measured total OH reactivity was highest during this period (in canopy: $30.7 \pm 0.4\,s^{-1}$, above canopy: $23.6 \pm 0.3\,s^{-1}$, Table 3.3).

During this period 78 % of the Γ values (on average $\Gamma = -0.14 \pm 0.01$) are negative and the total OH reactivity observed in the canopy is elevated compared to the above canopy OH reactivity. This indicates that the direct biogenic emissions have likely had a strong impact on total OH reactivity at this time. The diel median profile of Γ, absolute values and missing fraction of OH reactivity are presented in Fig. 3.4 (left panel). In canopy total OH reactivity was higher than measured above canopy during daytime. In contrast to Γ, the diel profile of total OH reactivity observations was highest during nighttime. This is in good agreement with measured diel cylces of monoterpenes which are major primary biogenic emissions of the boreal forest (Fig. 3.5, second row). These show minimum values during daytime and elevated concentrations during the night due to suppressed turbulent mixing. The minimum measured total OH reactivity could be found in the morning hours (08:00 [UTC+2]). This agrees well with the minimum missing fraction of total OH reactivity which is 60 % in the morning hours as the stable nocturnal boundary layer breaks up and mixing into a higher residual boundary layer starts (Fig. 3.4).

In general at the beginning of the campaign, during **stressed boreal** conditions (see also Table 3.3), the highest fraction of missing OH reactivity was observed. In this period 89 % are missing or unaccounted for, meaning that barely 10 % of the measured total OH reactivity can be explained by other ambient observations.

Transported pollution regime:
During biomass burning influence, on average the above canopy OH reactivity was higher ($13.0 \pm 0.2\,s^{-1}$) than within the canopy ($10.9 \pm 0.2\,s^{-1}$). Exceptional were days with unusually high temperatures (up to 32 °C), when in canopy measurements were higher with maximum values of $39\,s^{-1}$. Accordingly, Γ was found to be predominantly positive (on average 0.10 ± 0.01) (Figs. 3.2 and 3.4). For 75 % of the measurements in this period, the measured total OH reactivity above the canopy was higher than within the canopy. The higher OH reactivity above the canopy level was likely due to the myriad transported pollutants from biomass burning. The diel profile of total OH reactivity for this regime (Fig. 3.4, medium panel) has a maximum in the late afternoon, in contrast to the **stressed boreal** regime. However, similar to the **stressed boreal** regime, the minimum in measured OH reactivity occurs in the morning. On average the unexplained fraction of OH reactivity is 73 %, the closest agreement being at 09:00–12:00 [UTC+2] with only 30 % missing. Since pyrrole is known to be produced by biomass burning (Karl et al., 2007, Yokelson et al., 2007) it is important to exclude possible interferences for CRM measurements in this period. During the biomass burning influenced period in summer 2010 at the Hyytiälä measurement site, a second PTR-MS observing $m/z = 68$ and frequent tests with a GC-PID, configured to measure pyrrole, both found no detectable pyrrole in ambient air.

Normal boreal regime:
Total OH reactivity varied from the limit of detection ($3\,s^{-1}$) to $30\,s^{-1}$ (with one exceptional peak up to $67\,s^{-1}$) within this period. On average in canopy measurements showed slightly higher ($7.8 \pm 0.2\,s^{-1}$) OH reactivity than above the canopy ($6.8 \pm 0.2\,s^{-1}$). Hence, Γ (on average 0.13 ± 0.01) fluctuated around 0 and showed no consistent vertical distribution in total OH reactivity. In comparison to the previously discussed **stressed boreal** and **transported pollution** regime, the **normal boreal** forest shows less diel variation in total OH reactivity (Fig. 3.4). These results are consistent with in canopy measurements during summer 2008 at the same site (Sinha et al., 2010).
The overall short-term variability in total OH reactivity changed significantly, as can be seen in Fig. 3.4 (right panel), from 21:00–12:00 [UTC+2] (relatively quiescent, $RSD_{night} = 0.61$) to 14:00–19:00 (highly variable, $RSD_{day} = 1.22$). During the night the stable nocturnal boundary layer confines the weak forest emissions and the signal shows little short-term variability. In the daytime, frequent and effective mixing processes and turbulence bring down less reactive air into the forest canopy to mix with the strong emissions, causing rapid variations in the total OH reactivity.
During **normal boreal** conditions an average missing fraction of 58 % was observed. No significant trend in the missing fraction of total OH reactivity and high short-term variability were seen during this period.

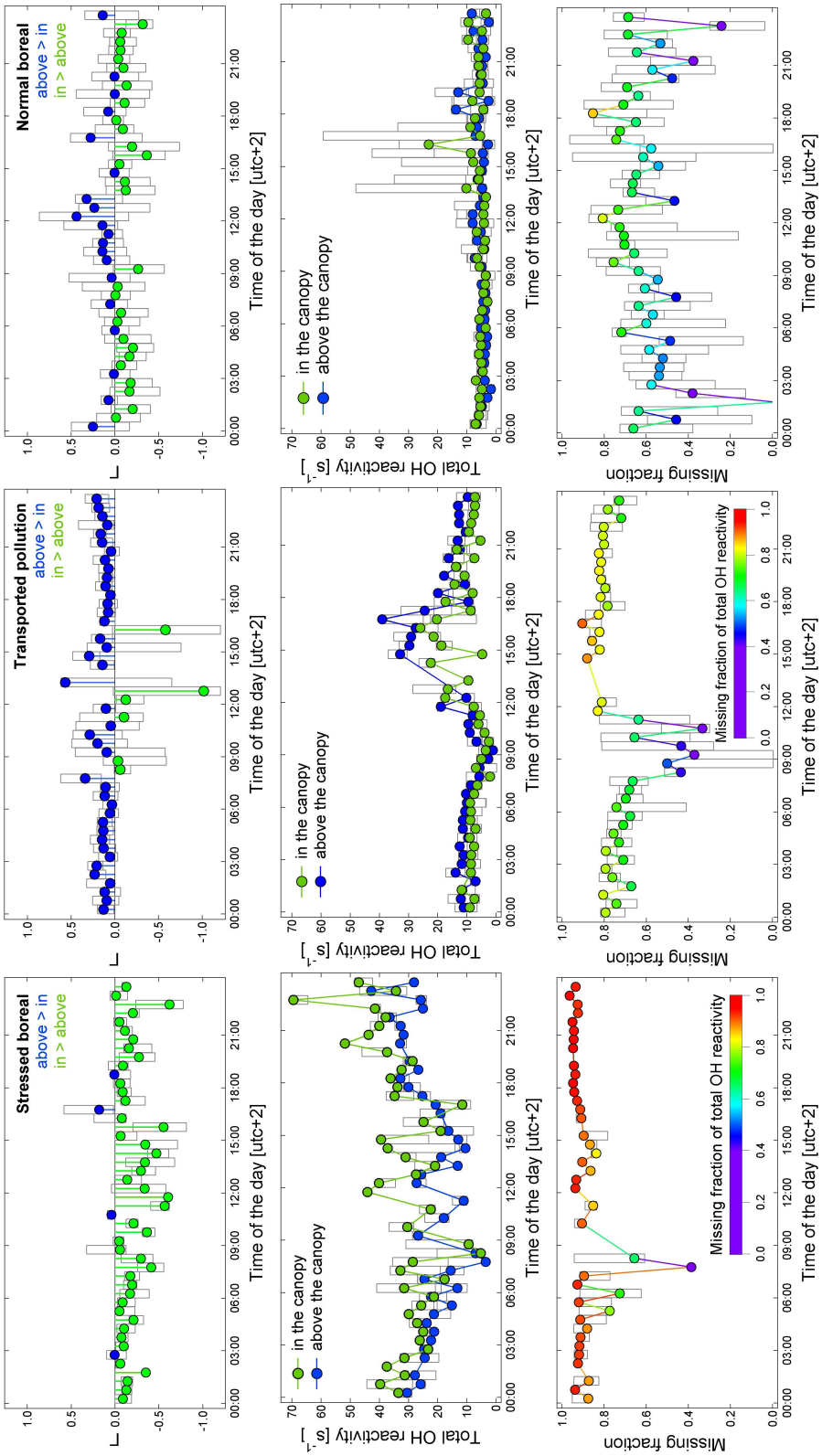

Fig. 3.4: Median diel variation for Γ, total OH reactivity measurements (in and above canopy) and missing fraction. Three characteristic regimes are shown: stressed boreal, transported pollution and normal boreal.

3.4 Discussion and conclusions

During HUMPPA-COPEC 2010 the missing OH reactivity was consistently high (58–89 %). This suggests that the total sink of OH was not well characterized despite the comprehensive suite of atmospheric measurements at the HUMPPA-COPEC campaign (see Table 3.2). A summary of the missing OH reactivity fraction for three characteristic regimes as a function of time of the day can be found in Fig. 3.6. Remarkably high is the missing fraction of total OH reactivity found above canopy during the influence of prolonged high temperatures (on average 89 %) and low wind speeds, hence local **stressed boreal** conditions (orange line). During the **transported pollution** period (black line), on average 73 % missing total OH reactivity was observed above the canopy. **Normal boreal** conditions (green line), with moderate temperatures and changeable winds, led to on average 58 % unexplained total OH reactivity. For the **stressed boreal** and the **transported pollution** periods, total OH reactivity was best accounted for by individual measurements during the morning hours (05:30–10:30 [UTC+2]) and worst in the late afternoon (13:00–18:00 [UTC+2]). In the morning, the stable nocturnal boundary layer broke up and air entrained from the residual layer and then the free troposphere (Nilsson et al., 2001). The measured total OH reactivity could be accounted for up to 70 %. In the **normal boreal** forest conditions, more mixing occurred due to frontal passages and no diel variation could be observed.
One low missing total OH reactivity event was observed during this period (01:00 [UTC+2]). This corresponded to an occasion when exceptionally high monoterpene mixing ratios were measured at the site. The event was associated with emissions from a local saw mill. Since monoterpenes dominated the emissions and were measured at the site, this had the effect of reducing the missing fraction of total OH reactivity.

Ambient monoterpene mixing ratios were determined via two different methods during the HUMPPA-COPEC campaign 2010. A GC-MS monitored selected monoterpenes which were included in total OH reactivity calculations as can be seen in Table 3.2. The sum of all monoterpenes was detected by a PTR-MS, however, the measurement was not included in the total OH reactivity calculations. The PTR-MS total monoterpene signal is difficult to use for total OH reactivity calculations, since the exact monoterpene composition is unknown and the rate coefficient (which varies considerably within the monoterpene family) , can only be estimated. Nevertheless, we have attempted to calculate the total OH reactivity including the total monoterpenes measured by PTR-MS using a weighted rate coefficient (based on the GC-MS speciation: $4.24 \times 10^{-11}\,\mathrm{cm^3\,molecules^{-1}\,s^{-1}}$). The average missing total OH reactivity decreased by 2 % using this approach. Similarly, the measurement of total organic peroxides and total organic acids was used with estimated rate coeffi-

cients (5.50×10^{-12} cm^3 molecules^{-1} s^{-1}, 9.55×10^{-12} cm^3 molecules^{-1} s^{-1}, respectively) to re-calculate the total OH reactivity. The largest improvement, found during the **transported pollution** regime, was about 5 %. The inclusion of the measured total monoterpenes, organic peroxides and organic acids does not significantly impact the proportion of missing total OH reactivity.
In order to understand the origin of the boreal summertime missing OH reactivity, tracers representative of primary biogenic emissions, directly processed photochemical products and transported pollutants are compared. Figure 3.5 presents diel median values of temperature, photosynthetically active radiation (PAR) and O_3 mixing ratios in the first row for the three defined regimes (**stressed boreal, transported pollution, normal boreal**). Light levels reached a maximum at 12:00 [UTC+2], whereas the temperature maximum was in the late afternoon (16:00 [UTC+2]). Ozone mean values for the three regimes were 38.5 ± 0.2 ppbV in the **stressed boreal**, 46.8 ± 0.4 ppbV during the **transported pollution** period, and 42.6 ± 0.2 ppbV in **normal boreal** conditions. NO (not included in the graph) did not vary significantly throughout the course of the campaign. The mixing ratios of NO were on average 30.3 ± 1.0 pptV, 26.7 ± 0.7 pptV and 30.5 ± 0.8 pptV for the **stressed boreal**, **transported pollution** and **normal boreal** regimes respectively.

The second row of Fig. 3.5 focuses on median primary emissions. As boreal forest strongly emits monoterpenes, Δ-3-carene is presented as a typical boreal primary emission. Isoprene is shown on the same graph. Both species are very reactive to OH and hence important for total OH reactivity. The diel development of ambient monoterpene mixing ratios depends on the direct emission strength, the lifetime due to oxidants and dynamical processes. For all shown periods in the campaign ambient levels of monoterpenes are higher during the night due to a small temperature-coupled release from the trees, a shallow stable nocturnal boundary layer (ca. 200–400 m) and low levels of oxidants. A decrease in the morning (06:30–08:30 [UTC+2]) was coupled to mixing of clean residual air and increasing oxidants (see O_3 in Fig. 3.5). Minimum ambient mixing ratios during daytime are caused by dilution through turbulent mixing into a larger boundary layer (ca. 900–2000 m) and a higher oxidation capacity of the atmosphere. This is despite the trees emitting monoterpenes at higher rates during the day because of high temperatures and light (Eerdekens et al., 2009b; Yassaa et al., 2012). Highest ambient mixing ratios of isoprene are found in the afternoon (16:00–18:00 [UTC+2]). This is because isoprene emission is coupled to both temperature and light (Guenther et al., 2006).

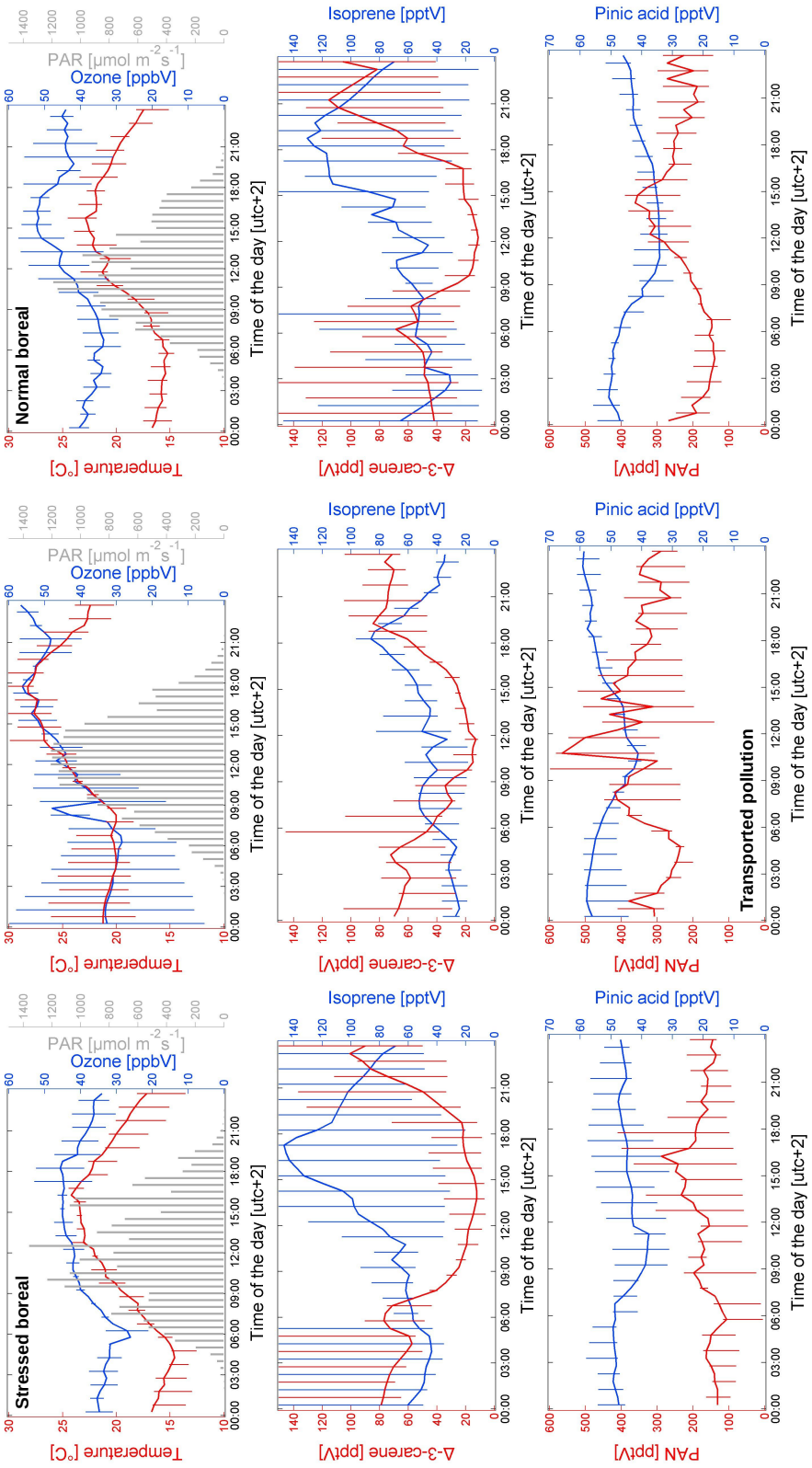

Fig. 3.5: Median diel variation for several measured parameters during HUMPPA-COPEC 2010 in stressed boreal, transported pollution and normal boreal forest conditions. Temperature, O_3 mixing ratios and PAR are presented in the first row for all regimes. The second row pictures the diel variation of primary biogenic emissions (Δ-3-carene and isoprene) and the lowermost row shows secondary products such as PAN and pinic acid.

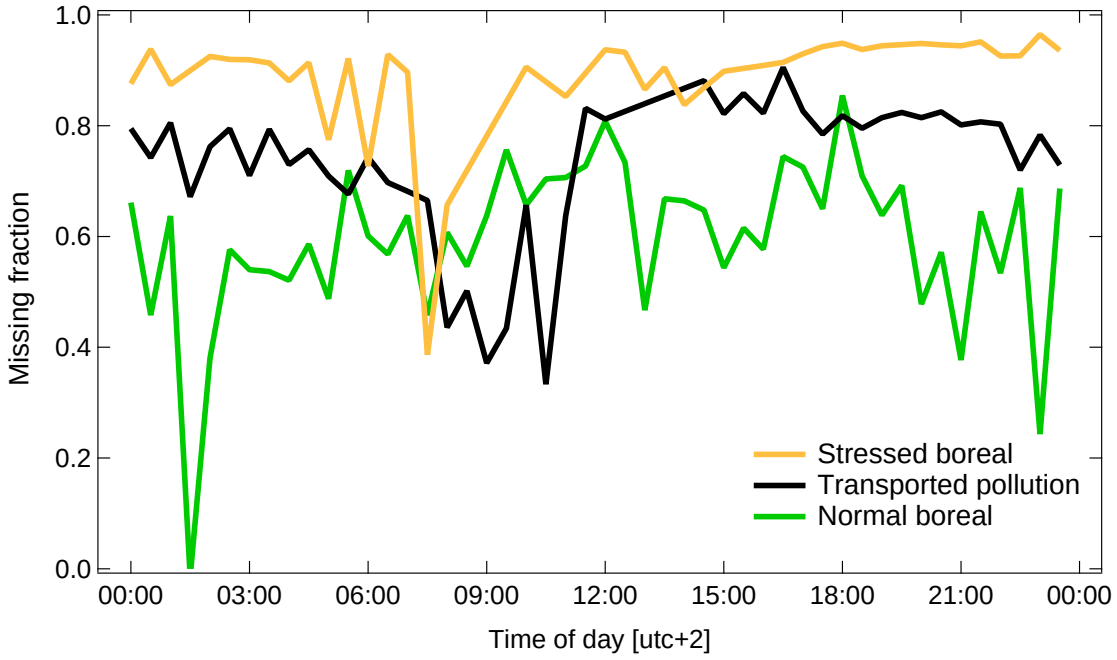

Fig. 3.6: Summary of missing fraction of total OH reactivity for all characteristic regimes as diel median profile: normal boreal (green), transported pollution (black), stressed boreal (orange).

In the third row of Fig. 3.5, two types of secondary products are shown. Primary biogenic emissions are effectively oxidized into secondary products once they are exposed to the atmosphere. The boreal forest provides a low NO_x environment where oxidation products like peroxides (from OH oxidation during day), aldehydes and organic acids (O_3 oxidation during night and day) can form (Atkinson and Arey, 2003). During the HUMPPA-COPEC campaign, some secondary products have been found to peak during daytime, coincident with the highest temperature, insolation and oxidants levels. The median PAN mixing ratio is given as example of a secondary product in Fig. 3.5. Other secondary compounds peak during the night due to reaction processes in the stable nocturnal boundary layer with O_3 or NO_3 yielding compounds such as pinic acid, which is presented here. Coupling and feedback between dynamical diel processes and chemistry is discussed further in Ouwersloot et al. (2012).

In the **normal boreal** forest primary biogenic emissions peak at different times of the day (Fig. 3.5, right panel). In terms of total OH reactivity, high monoterpene levels by night and elevated isoprene by day act to stabilize total OH reactivity throughout the day. Secondary products also exhibit maxima, both by day and night. For example pinic acid peaks at night, showing similar diel profile as its precursor monoterpene (Fig. 3.5). In contrast peak concentrations of PAN were measured around midday. The diel profile of the missing total OH reactivity fraction during the **normal boreal** forest period shows high variability and no diel dependency (Fig. 3.4, right panel). A weak

correlation (the best in this regime) between missing OH reactivity and ozone ($R = 0.39$) indicates influence of pollutants and ozonolysis products originating from nearby cities. It is likely that the missing contributors are of both primary and secondary origin.

In addition to total OH reactivity provided by the **normal boreal** forest, biomass burning plumes impacted the **transported pollution** period. Secondary products, such as PAN (Fig. 3.5, middle panel) were elevated in concentration and peaked in the afternoon. Since this coincides temporally with the measured total OH reactivity diel median profile (Fig. 3.4, middle panel), it is likely that the multitude of unmeasured secondary products contribute significantly to the 73 % average missing total OH reactivity during this period. Missing total OH reactivity was significantly correlated with H_2O_2 ($R = 0.71$) and the measurement of total organic peroxides ($R = 0.73$) in this regime. These are typical low NO_x environment photochemical products. During the influence of **transported pollution** the temperature reached extremely high values at daytime. This enhanced the biogenic emissions which could be seen in the in and above canopy comparison in Fig. 2. The combined effect of transported pollutants, unmeasured biogenics and their photooxidation products are likely to contribute to the missing OH reactivity on these occasions. Correlation of missing OH reactivity with secondary products such as acetic acid ($R = 0.56$), formic acid ($R = 0.52$) and the peroxides suggests a dominant role of photochemistry for total OH reactivity. Possibly, at this time the forest showed reaction to this pollution stress (Loreto and Schnitzler, 2010).

As the stable nocturnal boundary layer breaks up in the morning (07:00–10:00 [UTC+2]) both absolute measured total OH reactivity and missing fraction decrease. This is despite total OH reactivity being measured as higher above the canopy for most of the **transported pollution** regime (Fig. 3.4, middle panel). Possibly, vertical mixing of air masses with different characteristics, such as the residual layer (containing low reactivity levels) and free tropospheric air (affected by measured transported pollutants) influenced the total OH reactivity instrument during this period.

The missing total OH reactivity was significantly enhanced for **stressed boreal** conditions. While in the **normal boreal** forest period 58 % was missing, during heat-stress it was 89 %. During the long heat-stress period for HUMPPA-COPEC 2010 parallel enclosure studies showed that the emission rates increased and the composition became more diverse (Yassaa et al., 2012). No ambient air measurements of these reactive primary emissions or their secondary products were available, although they are likely contributors to missing total OH reactivity. This contention is supported by elevated total OH reactivity inside the canopy and the diel profile, which compares well with the profile of monoterpenes and their products (Figs. 3.4 and 3.5, left panel). Despite having similar diel variation, missing total OH reactivity and monoterpenes showed no

significant correlation ($R = -0.22$). The missing fraction of total OH reactivity in this regime was weakly dependent on wind direction ($R = 0.54$) and the solar zenith angle ($R = 0.46$).

Overall, total OH reactivity measurements in the summertime boreal forest showed impact of chemical and dynamical processes. Diel boundary layer height development, local meteorological conditions and long range transport were reflected in short-term variability, vertical distribution, measured and missing total OH reactivity. The best agreement between calculated and measured total atmospheric OH reactivity was found under **normal boreal** forest conditions. A mixture of boreal primary biogenic emissions, photooxidation products and occasional anthropogenic pollutants likely contributed to the missing fraction of total OH reactivity of on average 58 %. This is comparable to the values obtained by Sinha et al. (2010), for the same site. If the missing total OH reactivity of $4.8\,s^{-1}$ on average during **normal boreal** forest impact was caused by compounds at very low ambient mixing ratios (below a limit of detection of 5 pptV) which react with OH with the rate coefficient $5 \times 10^{-11}\,cm^3\,molecules^{-1}\,s^{-1}$, 780 of these compounds would be needed to explain the budget discrepancy. If the assumed rate coefficient is taken to be equal to isoprene ($1 \times 10^{-10}\,cm^3\,molecules^{-1}\,s^{-1}$) this reduces to 390 unmeasured reactive compounds.
Transported biomass burning secondary products enhanced the average missing total OH reactivity to 73 %. Even more total OH reactivity was missing (on average 89 %) in the **stressed boreal** forest. Using the same assumption as for **normal boreal** conditions (limit of detection 5 pptV, $k = 5 \times 10^{-11}\,cm^3\,molecules^{-1}\,s^{-1}$) 3500 compounds would be necessary to explain the average missing reactivity of $21.6\,s^{-1}$ above the canopy during the influence of heat stress. It is likely that a greater variety of more reactive compounds were emitted in higher rates under stress, which were detected with the total OH reactivity instrument but not with regular measurement devices. High emissions of various stress-induced compounds (e.g. sesquiterpenes, aldehydes) and their large number of photooxidation products were not quantified in the atmosphere. The in canopy – above canopy comparison of total OH reactivity suggests, that under these heat-stress conditions enhanced and more diverse primary biogenic emissions, and their secondary products, contribute strongly to the high missing OH reactivity.

Acknowledgments

The entire HUMPPA-COPEC team is grateful for the support of the Hyytiälä site engineers and staff. Support of the European Community – Research Infrastructure Action under the FP6 "Structuring the European Research Area" Programme, EUSAAR Contract No. RII3-CT-2006-026140 is gratefully acknowledged. Special thanks to Thomas Klüpfel and Rolf Hofmann for technical support, Laurens Ganzeveld, Domenico Taraborrelli and Jaana Bäck for helpful discussions. We thank the two referees for helpful comments on this manuscript.

Supplementary material

Compound	Whole campaign	Stressed boreal	Transported pollution	Normal boreal
temperature	0.2738	-0.2266	0.5821	0.3456
wind direction	0.1192	0.5356	0.1260	-0.0827
wind speed	0.0262	-0.2997	0.0368	-0.1456
PAR	0.0565	-0.3170	0.1360	0.1339
global radiation	0.0606	-0.2961	0.1513	0.1381
solar zenith angle	-0.0687	0.4609	-0.1396	-0.1909
J (NO_2)	0.0614	-0.3209	0.1697	0.1183
water vapour flux	0.0732	-0.3006	0.3210	0.0783
CO_2 flux	-0.0200	0.3927	0.0343	-0.1261
relative humidity	-0.1244	0.0956	-0.1443	0.0032
NO_2	-0.1079	-0.0260	-0.1701	-0.0374
NO	-0.0073	-0.3656	-0.1571	0.0766
O_3	0.2174	0.1684	0.4617	0.3869
CO	0.0785	-0.4915	0.3090	0.0946
SO_2	0.1249	-0.1657	0.3007	0.1588
iso-butane	0.0550	0.2691	0.0292	0.0808
iso-pentane	0.2477	-0.5508	0.0092	0.0167
n-butane	0.0063	-0.3132	-0.0380	0.1032
n-pentane	0.0233	-0.5084	-0.0633	0.0368
propene	0.1559	0.0454	0.3627	0.0382
methane	-0.0964	-0.5195	0.2532	0.1338
H_2O_2	0.4175	-0.1141	0.7110	0.3005
HCHO	0.1869	-0.1272	0.2787	0.1982
MHP	0.2135	0.0423	0.5888	0.1016
organic peroxides	0.3599	0.0258	0.7349	0.2090
m-xylene	0.1151	0.2187	0.4473	0.2021
p-xylene	0.1711	0.1931	0.4846	0.1992
toluene	0.0010	0.1289	0.2768	0.0194
ethylbenzene	0.0321	0.3086	0.5063	0.0254
benzene	0.0910	-0.4439	0.3949	-0.0458
isoprene	0.1753	-0.2470	0.4486	0.0736
α-pinene	-0.0596	-0.2313	-0.0229	-0.0918
β-pinene	-0.1327	-0.2027	0.2423	-0.2176
Δ-3-carene	-0.0826	-0.1805	-0.1332	-0.1044
myrcene	-0.0893	-0.1682	0.4527	-0.1383
total monoterpenes (GC-MS)	-0.1101	-0.2166	0.0547	-0.1369
m31 (formaldehyde)	0.3228	-0.1485	0.5340	0.3177
m33 (methanol)	0.2008	-0.2519	0.4218	0.2806
m42 (acetonitrile)	0.0944	0.0704	0.5433	0.1249
m45 (acetaldehyde)	0.2082	-0.3403	0.4719	0.2139
m47 (formic acid)	0.2699	-0.3775	0.5231	0.1919
m59 (acetone)	0.1319	-0.4695	0.4201	0.1562
m61 (acetic acid)	0.2643	-0.1771	0.5647	0.2362
m69 (isoprene)	0.2849	-0.2389	0.4994	0.2756
m71 (MVK/MACR)	0.1913	-0.4861	0.4122	0.2189
m73 (MEK)	0.1903	-0.3558	0.3715	0.1798
m79 (benzene)	0.1429	-0.2847	0.4687	0.1368
m81*	0.0660	-0.2795	0.1669	-0.0226
m83*	0.3250	-0.0908	0.3697	0.1968
m85*	0.1843	-0.4057	0.2100	0.1081
m87*	0.2417	-0.3091	0.4251	0.2485
m93 (toluene)	0.0427	-0.4155	0.0308	0.1016
m99*	0.1971	-0.1758	0.3097	0.1597
m101*	0.2397	-0.1657	0.3916	0.1678
m103*	0.1509	0.0583	0.2144	-0.0999
m113 (chlorobenzene)	0.2427	-0.2055	0.5450	0.2069
m137 (α-pinene)	0.1199	-0.2910	0.1520	-0.0350
m141*	0.1991	-0.0606	0.0502	0.2373
m153*	0.1580	-0.2006	0.0649	0.1127
m155*	0.1796	-0.1208	0.0762	-0.0350
m169*	0.2314	-0.1003	0.2360	-0.0013
m205*	0.1406	-0.1442	-0.0153	0.0965
m263*	0.1732	0.0158	-0.0048	-0.0804
PAA	0.2075		0.3110	0.2207
PAN	0.0888	0.1248	0.1997	0.2994
pinonicacid	0.1312	0.0149	0.1623	-0.0969
pinicacid	0.1519	-0.0151	0.2189	-0.0596

* un-calibrated PTR-MS measurements

Table S1. Correlations (Pearson R coefficients) for missing OH reactivity and the suite of other measurements for the three defined regimes (stressed boreal, transported pollution and normal boreal conditions) as well as for the whole campaign.

4

Seasonal measurements of total OH reactivity fluxes, total ozone loss rates and missing emissions from Norway spruce in 2011

A.C. Nölscher[1], E. Bourtsoukidis[2,3], B. Bonn[2], J. Kesselmeier[4], J. Lelieveld[1], and J. Williams[1]

[1]Department of Atmospheric Chemistry, Max Planck-Institute for Chemistry, Mainz, Germany
[2]Institute for Atmospheric and Environmental Sciences, J.W. Goethe University, Frankfurt/Main, Germany
[3]International Max Planck Research School for Atmospheric Chemistry and Physics, Max Planck-Institute for Chemistry, Mainz, Germany
[4]Department of Biogeochemistry, Max Planck-Institute for Chemistry, Mainz, Germany

Manuscript accepted for publication in Biogeosciences Discussion

Summary. Numerous reactive volatile organic compounds (VOCs) are emitted into the atmosphere by vegetation. Most biogenic VOCs are highly reactive towards the atmosphere's most important oxidant, the hydroxyl (OH) radical. One way to investigate the chemical interplay between biosphere and atmosphere is through the measurement of total OH reactivity, the total loss rate of OH radicals. This study presents the first determination of total OH reactivity emission rates (measurements via the Comparative Reactivity Method) based on a branch cuvette enclosure system mounted on a Norway spruce (Picea abies) throughout spring, summer and autumn 2011. In parallel separate VOC emission rates were monitored by a Proton Transfer Reaction-Mass Spectrometer (PTR-MS), and total ozone (O_3) loss rates were obtained inside the cuvette. Total OH reactivity emission rates were in general temperature and light dependent, showing strong diel cycles with highest values during daytime. Monoterpene emissions contributed most, accounting for 56-69 % of the measured total OH reactivity flux in sping and early summer. However, during late summer and autumn the monoterpene contribution decreased to 11-16 %. At this time, a large missing fraction of the total OH reactivity emission rate (70-84 %) was found when compared to the VOC budget measured by PTR-MS. Total OH reactivity and missing total OH reactivity emission rates

reached maximum values in late summer corresponding to the period of highest temperature. Total O_3 loss rates within the closed cuvette showed similar diel profiles and comparable seasonality to the total OH reactivity fluxes.
Total OH reactivity fluxes were also compared to emissions from needle storage pools predicted by a temperature-only dependent algorithm. Deviations of total OH reactivity fluxes from the temperature-only dependent emission algorithm were observed for occasions of mechanical and heat stress. While for mechanical stress, induced by strong wind, measured VOCs could explain total OH reactivity emissions, during heat stress they could not. The temperature driven algorithm matched the diel course much better in spring than in summer, indicating a different production and emission scheme for summer and early autumn. During these times, unmeasured and possibly unknown primary biogenic emissions contributed significantly to the observed total OH reactivity flux.

4.1 Introduction

The Earth's atmosphere contains thousands of reactive biogenic volatile organic compounds (VOCs) (Goldstein and Galbally, 2007). These are important players for chemical processes consuming oxidants, forming products, radicals, and organic aerosol (Atkinson and Arey, 2003, Hoffmann et al., 1997, Williams et al., 2001, Pöschl et al., 2010). The reasons why vegetation emits VOCs so copiously (globally ca. $1.15\,\mathrm{Pg\,yr^{-1}}$, Guenther et al., 1995), are various and not yet fully understood (Kesselmeier and Staudt, 1999). Through photosynthesis plants convert light and carbon dioxide (CO_2) into energy and biomass. Based on this primary metabolism, vegetation forms, stores, transforms and releases a large variety of volatiles (such as isoprene, monoterpenes, sesquiterpenes or even diterpenes, e.g. Dudareva et al. (2006), Laothawornkitkul et al. (2009)). Such emissions can be useful to the plant for signaling, attracting and guiding pollinators (Fehsenfeld et al., 1992), or reducing oxidant levels close to the plant (Jardine et al., 2012). Other compounds may be regarded as a reaction to stress, e.g. heat, drought, oxidant, mechanical, herbivores and pollution (Vickers et al., 2009, Niinemets, 2010, Loreto and Schnitzler, 2010). Oxygenated compounds such as formaldehyde, acetaldehyde, formic acid, acetic acid, acetone, methanol and methyl vinyl ketone (MVK) are also released (Kesselmeier et al., 1997, Rinne et al., 2007, Goldstein and Galbally, 2007, Jardine et al., 2012) but may be taken up by vegetation as well (e.g. Kesselmeier, 2001). Emissions of biogenic VOCs can be categorized into two groups: compounds which are emitted immediately following synthesis, and compounds which are released from storage pools (see Kesselmeier and Staudt, 1999). Isoprene and monoterpenes are synthesized and immediately released under light conditions if not stored in special organs such as resin ducts (coniferous trees) or glands (fragrant plants). This kind of VOC synthesis and emission can be simulated by a light and temperature related algorithm adapted by Guenther et al. (1993) and (1995). A simpler algorithm de-

scribes the release from storage organs exponentially depending on temperature only (Tingey et al., 1980, Guenther et al., 1993). This algorithm is often used to simulate the emission of monoterpenes stored in the resin ducts of coniferous needles or the light independent synthesis and release of sesquiterpenes. Oxygenated VOC species can be described by a light and temperature dependent algorithm due to the light regulated stomatal opening.

Several recent field studies have shown the importance of plant emissions for understanding the chemistry of the atmosphere and it's most important oxidant, the hydroxyl radical (OH) (e.g. Lelieveld et al., 2008, Heard and Pilling, 2003). Most biogenic VOCs are highly reactive towards OH and hence contribute significantly to its overall sink. The loss frequency of OH is termed total OH reactivity, and can be measured directly (using a pre-reactor and Proton Transfer Reaction-Mass Spectrometer - PTR-MS, or Laser Induced Fluorescence - LIF, e.g. Sinha et al. (2008), Kovacs and Brune (2001)) along with ambient OH radical concentrations, and levels of atmospheric trace gases such as VOCs and inorganics. Especially in forests, OH sources and sinks seem to be poorly understood. Field campaigns have found missing OH sources (e.g. Lelieveld et al., 2008, Hofzumahaus et al., 2009, Tan et al., 2001) as well as missing sinks (e.g. Di Carlo et al., 2004, Nölscher et al., 2012b) when comparing the production and loss terms for OH of commonly monitored atmospheric compounds. While theories have been developed to explain the observed high OH concentrations in forests based on the OH recycling potential (Peeters et al., 2009, Taraborrelli et al., 2012), the identity of the missing sinks, the missing OH reactivity, remains elusive. On the one hand the biosphere might directly emit missing OH reactive compounds. This hypothesis is supported by a terpene-like temperature dependency of missing OH reactivity (Di Carlo et al., 2004), the high unexplained fraction in biogenic environment (Lou et al., 2010), a typically biogenic diel variation and a positive flux from the forest canopy for high temperatures (Nölscher et al., 2012b). On the other hand, unknown and unmeasured oxidation products of biogenic VOCs are likely to contribute to the high missing OH reactivity in forests. This hypothesis is based on good model-measurement agreement at daytime when accounting for hydrocarbon oxidation products (Lou et al., 2010), and on first observations of branch level total OH reactivity. Kim et al. (2011) found no missing OH sinks when comparing total OH reactivity and VOC measurements within an enclosing branch system from four different tree species (red oak, white pine, beech, red maple).

This study presents first trans-seasonal total OH reactivity emission rate measurements from a branch enclosure system using the Comparative Reactivity Method (CRM). The cuvette was installed on a Norway spruce in its natural environment. Furthermore seasonal branch-level total ozone (O_3) loss rates have been investigated. The applied cuvette system enabled direct tree emission rates for VOCs to be examined via PTR-MS

in parallel to total OH reactivity emissions. Fluxes for known Norway spruce emissions such as monoterpenes, acetone, isoprene, acetaldehyde and methanol (Cojocariu et al., 2004, Filella et al., 2007) could be characterized throughout the year 2011. Total OH reactivity emission rates were monitored in May/June and August/September. In this way the role of known VOCs as OH sinks could be determined. Additionally, the question whether biogenic emissions are a source of missing OH reactivity can be addressed directly and as a function of season.

4.2 Field site description and instrumentation

A mature Norway spruce (Picea abies, 80 years old, 13 m tall, healthy), located at Kleiner Feldberg, Taunus, Germany (50° 13' 18" N, 8° 26' 45" E, 825 m asl), was selected for the installation of a branch enclosure system from which the measurements were made. The tree was part of a small stand of Norway spruce close to the top of the mountain. Norway spruce is the dominant tree in the Taunus region at higher altitudes (> 600 m). To the north and west of the site the land was predominantly covered with coniferous and mixed forest, with few roads or small towns. To the south of the site lies the heavily populated Rhein-Main area (pop. ca. 2 million) including a dense motorway system, the airport and large cities such as Frankfurt (ca. 25 km distant), Wiesbaden (ca. 30 km distant) and Mainz (ca. 40 km distant).

Fig. 4.1: Cuvette set-up in the field on Kleiner Feldberg, Taunus, Germany: The enclosure system was fixed at a Norway spruce branch. The instruments (Sensors, PTR-MS, CRM) were located in the van underneath to keep inlet lines short. For 17 minutes the lid was kept open to allow contact with the natural atmospheric environment and closed automatically for 3 minutes.

4.2.1 Branch level cuvette

In order to determine the nature and rate of direct emissions from Norway spruce, a dynamic branch enclosure system (Ruuskanen et al., 2005, Bourtsoukidis et al., 2012) was mounted on a branch 5 m above ground (Figure 4.1). The branch enclosure system was a 15l, cylindrical plexi-glass cuvette which absorbed UV radiation and hence limited photochemical reactions inside the cuvette. A lid for opening and closing the cuvette was operated automatically for the measurements in 20 minute cycles, including a 3 minute closure for emission rate observations. Temperature, ozone (O_3), carbon dioxide (CO_2) and photosynthetic active radiation (PAR) (for summer onward only) were continuously monitored inside the cuvette. During closures, humidity and temperature levels increased by not more than 10% on average. CO_2 and O_3 decreased, with CO_2 values generally not falling below 250 ppmV. Hence, the branch did not show symptoms of being seriously impacted by the cuvette system, and therefore the emissions were considered to be natural. The measurement instruments were located directly underneath the tree within a van, and connected with 4.1 m long heated (70 °C) glass tubing to the cuvette. The residence time in the inlet was about 2 s. Biogenic VOCs were monitored by PTR-MS and total OH reactivity by a separate PTR-MS system using the Comparative Reactivity Method (Sinha et al., 2008).

4.2.2 Quantification of biogenic VOCs: PTR-MS

Measurements of VOC mixing ratios were made using a high sensitivity Proton Transfer Reaction-Mass Spectrometer (IONICON) (e.g. Lindinger et al., 1998). H_3O^+ ions are generated from water vapor in a hollow-cathode discharge source, and these protonate ambient gas molecules with higher proton affinity than water. This allows a wide range of gaseous organic compounds to be detected after acceleration through a drift tube and separation according to the mass-to-charge ratio (m/z) with a quadrupole mass spectrometer. In the set-up operated here, standard conditions were used for the drift tube voltage (600 V) and pressure (2.3 mbar). Optimization of the instrument resulted in sustained high sensitivity. More details of the PTR-MS configuration are presented in Bourtsoukidis et al. (2012). Amongst other VOCs (see Table 4.1) the sum of monoterpenes (m/z 137) and the sum of sesquiterpenes (m/z 205) were monitored and calibrated using gas standards (L4763, Ionimed analytic GmbH, Austria). Monoterpenes were calibrated with α-pinene, while for sesquiterpenes a permeation oven was used to produce stable β-caryophyllene concentrations (liquid β-caryophyllene standard: W225207, Sigma-Aldrich, Inc.).

Table 4.1: PTR-MS measured and calibrated VOCs, and the applied rate coefficients used for OH reactivity calculations. The reaction rate coefficients were taken from the IUPAC preferred values except for nopinone which was measured by Calogirou et al. (1999) and pinonaldehyde (Davis et al., 2007).

PTR-MS mass	compound	rate coefficient [$cm^3\,molecules^{-1}\,s^{-1}$]
m/z 33	methanol	9.00×10^{-13}
m/z 42	acetonitrile	2.20×10^{-14}
m/z 45	acetaldehyde	1.50×10^{-11}
m/z 47	ethanol	3.24×10^{-12}
m/z 59	acetone	2.19×10^{-13}
m/z 69	isoprene	1.00×10^{-10}
m/z 79	benzene	1.28×10^{-12}
m/z 137*	total monoterpenes	1.22×10^{-10}
m/z 139	total nopinone	1.70×10^{-11}
m/z 155	linalool	1.59×10^{-10}
m/z 169	pinonaldehyde	3.46×10^{-11}
m/z 205*	total sesquiterpenes	1.69×10^{-10}

* weighted rate coefficients used according to GC-MS composition analysis (see Section 4.3.1)

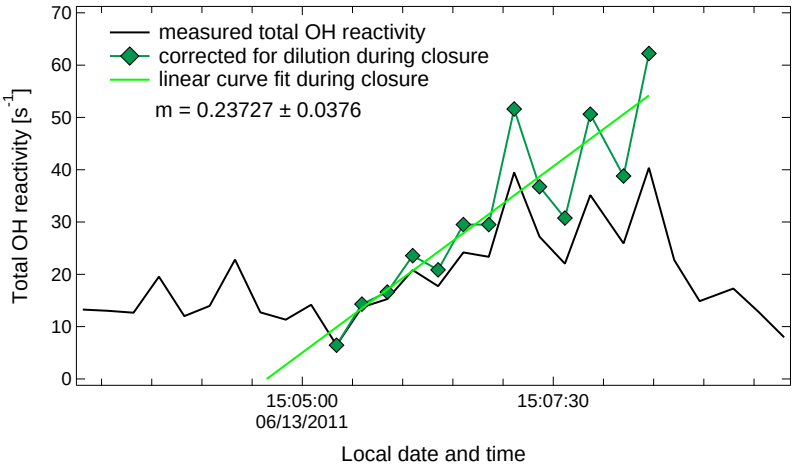

Fig. 4.2: Example for total OH reactivity emission (TOHRE) calculation: The originally measured total OH reactivity (black line) varied for open cuvette measurements between 10-20 s^{-1}, during closure it increased to 40 s^{-1}. The dilution during cuvette closure due to leaking in of atmospheric air suppresses the measured total OH reactivity stronger the longer the system is closed. A dilution correction is applied (green markers) before fitting the closure data with a linear regression line (green line). Slopes, uncertainty of the slopes, and fit quality are obtained for each closure.

4.2.3 Total OH reactivity measurements

Total OH reactivity (R_{total}) is the total loss rate of OH radicals due to atmospheric reactive molecules. It is defined as the sum of all single ambient compound reactivities, which can be calculated as product of the compound's concentration [X] and reaction rate with OH (k_{X+OH}) (Equation 4.1). If all atmospheric sink components of OH were known, the ambient concentration levels accurately measured and a rate coefficient determined, the calculation using Equation 4.1 and the direct measurement of total OH reactivity would agree. The difference between calculated and directly measured total OH reactivity is termed missing OH reactivity.

$$R_{total,calc} = \Sigma\ k_{X_i+OH} \times [X_i] \tag{4.1}$$

To date, total OH reactivity has been measured using three different techniques: 1) artificially generated OH in a flow tube reacts with the atmospheric composition and it's temporal decay is observed with Laser Induced Fluorescence (LIF) (e.g. Sadanaga et al., 2004); 2) a movable OH source in a flow tube reactor is used to vary reaction times of OH and the atmospheric constituents, and the OH signal is detected with LIF (e.g. Kovacs and Brune, 2001); 3) a competitive reaction between a reagent and OH alone, and then in the presence of atmospheric reactive molecules is observed by a suitable detector (e.g. Sinha et al., 2008). The last technique, termed Comparative Reactivity Method (CRM), was chosen in its latest configuration using a PTR-MS as detector (Nölscher et al., 2012a) for branch cuvette observations. It offers low sampling flow rates, a reasonably good time resolution (15 s), and good sensitivity for the expected high total OH reactivity levels (3-300 s^{-1}). The limit of detection for the CRM instrument operated during this campaign was 3-4 s^{-1} (2σ of the baseline noise), and the average overall uncertainty 16 %. This number is derived as propagation of errors and includes the uncertainties of the detector (PTR-MS, 5 %), the pyrrole gas mixture (5 %), error of rate coefficient (14 %), and flow variations (2 %).

4.2.4 VOC and total OH reactivity emission rate calculations

During closure, concentrations of continuously emitted species increased linearly in the cuvette. In the case of a single compound such as isoprene the rate of emission is normally expressed as the mass of species (ng) per unit needle dry weight ($g(dw)^{-1}$) per unit time (hr^{-1}). While the system was closed ambient air was drawn into the cuvette and diluted the mixture (Ruuskanen et al., 2005). After correcting for the modest dilution effect of ambient air ($k_{dil}=(2.9\pm0.2)\times10^{-3}\ s^{-1}$, see Bourtsoukidis et al. (2012)), the data were fitted by a linear regression. Mono- and sesquiterpene emission rates from the branch enclosure have been reported in Bourtsoukidis et al. (2012).
Total OH reactivity emission rates (TOHRE) were obtained in similar fashion to those of the single compounds. Increasing reactive tree emissions during closure lead to an

increasing total OH reactivity which is a property of the mixture's various component concentration levels and reaction rates with OH. Total OH reactivity emission rates were expressed as emitted total OH reactivity (R_{total} in s^{-1}) per unit needle dry weight ($g(dw)^{-1}$) per unit enclosure volume (m^{-3}) per unit time (s^{-1}). The resulting value for TOHRE has the dimensions [$s^{-2}\,g(dw)^{-1}\,m^{-3}$] and hence depends on the biomass (m_{bio}) and the volume of air enveloping the branch (V_{cuv}). As an example one cuvette closure is presented in Figure 4.2.

$$TOHRE = \frac{dR_{total}}{dt} \times \frac{1}{m_{bio} \times V_{cuv}} \tag{4.2}$$

By including the CRM measured total OH reactivity (R_{total}=$R_{total,meas}$) in Equation 4.2 the **measured TOHRE** was determined. It describes the flux of all OH reactive compounds being emitted from the examined Norway spruce branch. For comparison, the individual compounds measured by PTR-MS were singly transformed to OH reactivities and equivalently analyzed during cuvette closures. Inserting the single compound OH reactivity of e.g. isoprene (R_{total}=$R_{isoprene}$) in Equation 4.2 leads to the isoprene OH reactivity emission rate (IOHRE). The sum of all single compound OH reactivities (Eq. 4.1) generates the total calculated total OH reactivity, which was processed in the same manner (R_{total}=$R_{total,calc}$) to determine the **calculated TOHRE**. Please note, that the dynamic cuvette system uses the increase in total OH reactivity (and PTR-MS compounds) during closure, due to the continuous tree emissions, to determine biogenic fluxes. This method differs from ambient total OH reactivity measurements and calculations which must take account of background values of species such as CO and NO_2. Significant fluxes of the two aforementioned species were not expected from the spruce branch cuvette as they are typically anthropogenic in character.

Typical for total OH reactivity measurements were 13-15 data points per closure. Cuvette closures with less than 8 data points and a fit quality R^2 worse than 0.1 were excluded from the analysis (overall 20 % of the data was lost). The uncertainty is dominated by the fit error of the slope, which was on average about 35 % of the measured value.

As an example of how single compound and total OH reactivity flux measurements may be combined spring, 26 May 2011 at 11:00 [local time, utc+3] is examined in more detail. A good match between measured and calculated TOHRE was observed. CRM measured for TOHRE a value of $0.29\pm0.10\,s^{-2}\,g(dw)^{-1}\,m^{-3}$ and the PTR-MS sum of all reactive VOC emissions led to a value of $0.28\pm0.10\,s^{-2}\,g(dw)^{-1}\,m^{-3}$. The highest emission rate at that time was found in the monoterpene signal which was about $452.7\,ng\,g(dw)^{-1}\,hr^{-1}$. In terms of OH reactivity, emissions of monoterpenes contributed with $0.19\pm0.07\,s^{-2}\,g(dw)^{-1}\,m^{-3}$ to more than 50 % of the total measured signal of TOHRE. Due to its high reactivity, the isoprene OH reactivity emission rate is the second most important term for TOHRE with $0.05\pm0.02\,s^{-2}\,g(dw)^{-1}\,m^{-3}$, al-

though the isoprene emission rate was 64.5 ng g(dw)$^{-1}$ hr^{-1}. This is much less than the emission rates of acetone (285.3 ng g(dw)$^{-1}$ hr^{-1}), methanol (224.6 ng g(dw)$^{-1}$ hr^{-1}), acetaldehyde (105.7 ng g(dw)$^{-1}$ hr^{-1}) and sesquiterpenes (104.4 ng g(dw)$^{-1}$ hr^{-1}) which altogether have an OH reactivity emission of 0.03±0.01 s^{-2} g(dw)$^{-1}$ m^{-3} (11 % of measured TOHRE).

4.2.5 Total ozone loss rates

Ozone was monitored continuously inside the cuvette. The opening and closing dynamic branch cuvette system allowed an estimate of total ozone loss rates (Altimir et al., 2002, Wieser et al., 2012). Following closure, ambient concentrations decreased due to loss processes inside the system. To some extent this loss processes were gas phase reactions of ozone with the doubly bonded and highly reactive biogenic VOCs. In addition ozone deposited on walls and plant surfaces, underwent surface reactions and was stomatally-uptaken (Loreto et al., 2001). The values calculated directly from the decrease of ozone in pptV per time (s^{-1}) during closures are a very simple estimate of the total O_3 loss rate due to all possible loss mechanisms inside the cuvette. It was assumed, that deposition to the cuvette walls is a constant loss. Depletion of ozone by reactive tree emissions and through stomatal uptake can be related to physiological parameters, which are main driving forces for these time scales (Kulmala et al., 1999, Kurpius and Goldstein, 2003). In this study we cannot separate the ozone loss due to deposition on surfaces, stomatal uptake, and the gas phase loss to biogenic emissions. Presented results have to be taken as qualitative guide to the total O_3 loss rates, which are compared in diel profiles and trends.

4.3 Results

Total OH reactivity emission (TOHRE) rates in the Norway spruce mounted cuvette, varied during spring, summer and early autumn 2011 between no detectable emissions and 15.69 s^{-2} g(dw)$^{-1}$ m^{-3}. These trans-seasonal data are presented in Figure 4.3 alongside temperature, global radiation, wind speed and relative humidity. The two intensive measurement periods are separated visually into the first campaign (spring/early summer: 24 May – 14 June 2011) and the second campaign (late summer/autumn: 12 Aug – 07 Sept 2011) which was part of a comprehensive field campaign on top of Kleiner Feldberg (PARADE 2011). Covariation of TOHRE with temperature and light can be easily identified in Figure 4.3. Clear diurnal trends were seen for most days, with higher TOHRE during daytime (campaign average: 0.63±0.03 s^{-2} g(dw)$^{-1}$ m^{-3}) and lower values at night (campaign average: 0.32±0.01 s^{-2} g(dw)$^{-1}$ m^{-3}). Exceptional for the year 2011 was the unseasonably warm and dry spring. Typical early summertime conditions (1-14 June 2011) with moderate ambient temperatures and low levels of soil moisture

resulted in high TOHRE (on average $0.50\pm0.02\,s^{-2}\,g(dw)^{-1}\,m^{-3}$, Table 4.2). However, overall the summer was unusually rainy and cold (average ambient temperature in July was 12.2 °C, whereas 14.9 °C were typical for previous summers since 1997). The soil moisture during the second measurement period was significantly elevated in contrast to springtime and early summer. At the end of August (12 Aug – 26 Aug 2011, within the second campaign) the temperature increased to high levels and highest TOHRE was measured (late summer average: $0.83\pm0.07\,s^{-2}\,g(dw)^{-1}\,m^{-3}$). On the 26 Aug 2011, meteorological conditions changed drastically becoming cold and wet, which coincided with a drop of all VOC emission rates as well as total OH reactivity fluxes. Vegetation experienced early autumn conditions at this time (27 Aug – 7 Sept 2011). Lowest TOHRE was observed in early autumn with on average $0.16\pm0.01\,s^{-2}\,g(dw)^{-1}\,m^{-3}$ for cold and rainy weather. The calculated TOHRE (from PTR-MS measured VOCs, as introduced in Section 4.2.4) generally showed analogous temporal trends but lower absolute values, with the best agreement to measured values in spring and the worst in late summer (summarized in Table 4.2).

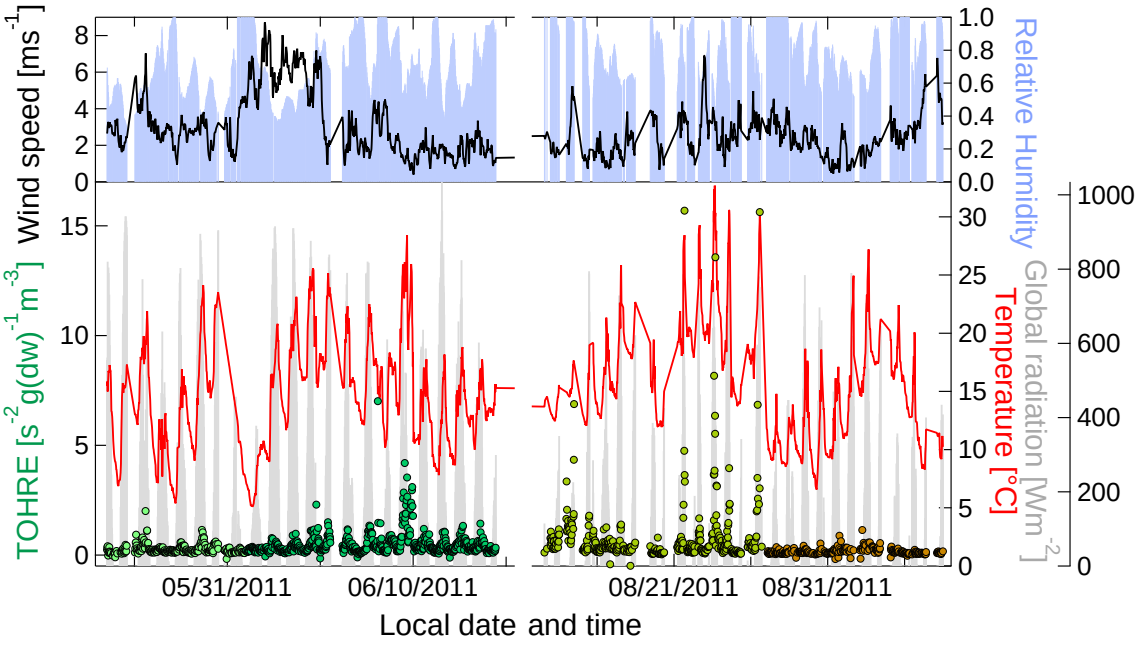

Fig. 4.3: Overview of the entire data set: Total OH reactivity emissions (TOHRE, green markers) were measured from 24 May to 14 June 2011 and 12 August to 7 September 2011 covering the seasonal impact from spring to early autumn. Temperature inside the cuvette (red line) and global radiation from a co-located mast (grey area) showed high variability throughout the measurement period as well as wind speed (black line, top panel) and relative humidity (blue area, top panel).

Table 4.2: Average values for meteorological parameters, total OH reactivity emissions (TOHRE), the single compound total OH reactivity emissions of monoterpenes (MTOHRE), isoprene (IOHRE) and acetaldehyde (AOHRE) and the unknown fraction of TOHRE (missing TOHRE). Data is averaged for the entire measurement period (all), for 24 May – 31 May 2011 (spring), 1 June – 14 June 2011 (early summer), 12 Aug – 26 Aug 2011 (late summer) and 27 Aug – 7 Sept 2011 (early autumn).

	all	spring	early summer	late summer ***	early autumn ***
temperature [°C] *	15.0±0.1	13.5±0.2	15.1±0.2	17.9±0.2	13.0±0.2
relative humidity [%] *	76.0±0.4	63.8±1.0	72.1±0.7	81.2±0.7	83.6±0.7
wind speed [$m\,s^{-1}$] *	2.8±0.03	2.9±0.06	3.3±0.08	2.4±0.05	2.4±0.05
soil moisture *	74.2±0.6	52.1±0.2	45.2±0.08	97.6±0.3	104.3±0.3
ambient ozone [ppbV] *	45.2±0.3	50.3±0.6	49.5±0.5	44.4±0.6	37.0±0.5
total ozone loss rate [$pptV\,s^{-1}$] *	-31.2±0.7	-27.0±1.2	-21.6±0.6	-40.9±1.6	-36.9±1.9
TOHRE (measured) [$s^{-2}\,g(dw)^{-1}\,m^{-3}$] *	0.4868±0.0206	0.2715±0.0127	0.5033±0.0205	0.8260±0.0722	0.1639±0.0063
TOHRE (calculated) [$s^{-2}\,g(dw)^{-1}\,m^{-3}$] *	0.1961±0.0121	0.2310±0.0165	0.3661±0.0338	0.1286±0.0066	0.0484±0.0020
MTOHRE (calculated) [$s^{-2}\,g(dw)^{-1}\,m^{-3}$] **	0.1453 (30 %)	0.1874 (69 %)	0.2806 (56 %)	0.0870 (11 %)	0.0268 (16 %)
IOHRE (calculated) [$s^{-2}\,g(dw)^{-1}\,m^{-3}$] **	0.0189 (4 %)	0.0186 (7 %)	0.0275 (5 %)	0.0189 (2 %)	0.0089 (5 %)
AOHRE (calculated) [$s^{-2}\,g(dw)^{-1}\,m^{-3}$] **	0.0230 (5 %)	0.0142 (5 %)	0.0491 (10 %)	0.0105 (1 %)	0.0074 (5 %)
missing TOHRE [$s^{-2}\,g(dw)^{-1}\,m^{-3}$] **	0.2907 (60 %)	0.0405 (15 %)	0.1372 (27 %)	0.6974 (84 %)	0.1155 (70 %)

* average ± standard error

** average (relative contribution to measured TOHRE)

*** average (applied monoterpene and sesquiterpene composition ratios of springtime GC-MS analysis)

4.3.1 VOC emission rates and OH reactivity contributions

Figure 4.4 presents the emission rates of the individually measured VOCs, and Figure 4.5 the contribution of each compound to OH reactivity fluxes for both field campaigns in 2011. The strongest emissions from Norway spruce were monoterpenes, acetone, methanol and acetaldehyde, which is consistent with previous assessments (Filella et al., 2007, Schürmann et al., 1993, Grabmer et al., 2006). The composition of monoterpenes, which was analyzed via GC-MS in the laboratory from both needle and cartridge samples, was similar to summertime Norway spruce emissions measured elsewhere (e.g. Yassaa et al. (2012)). Interestingly, the relative contribution of α-pinene and β-pinene did not change throughout the seasons, whereas limonene significantly increased in the second measurement period (Figure 4.4). Unfortunately other speciated monoterpenes such as β-phellandrene, camphene and β-myrcene were not quantified during the second measurement period although the chromatogram clearly showed more peaks than could be identified. Similarly, the speciation data for sesquiterpenes were only available from springtime/early summer probes (35 % β-caryophyllene, 29 % α-farnesene, 18 % longicyclene, 3 % α-humulene, and some minor contributors). However, total monoterpenes and total sesquiterpenes were monitored continuously by the PTR-MS. Most of the VOC emission rates stayed relatively constant for the two observed intensive periods. Only the emission rates of total monoterpenes and acetaldehyde decreased significantly in late summer and autumn (Figure 4.4), while sesquiterpenes were emitted in slightly higher ratios.

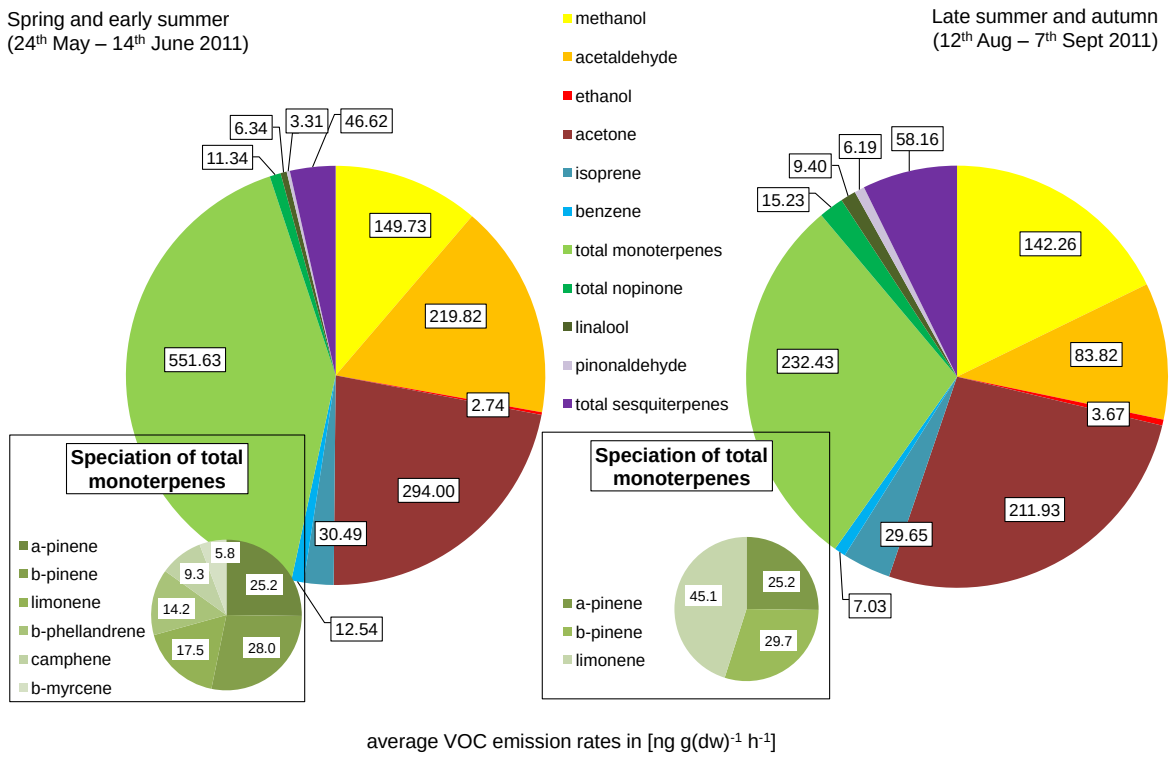

Fig. 4.4: The composition of biogenic VOC emissions and monoterpenes specified by GC-MS for both measurement periods a) springtime and early summer, b) late summer and autumn. Average emission rates are given in ng g(dw)$^{-1}$ hr^{-1}, the speciation is the relative contribution of single monoterpenes to the measured sum by PTR-MS.

For total OH reactivity, it is not necessarily the most abundant biogenic VOC that is the most important since the compound's reaction rate with OH must be factored in. From Figure 4.5 it is clear that the mixture of emitted monoterpenes on average contributed the most to calculated TOHRE rates. The reaction rate coefficient used for calculation of monoterpene OH reactivity emissions (MTOHRE) is a weighted average for compounds found in the springtime speciation ($k_{MT+OH} = 1.22\times10^{-10}$ cm^3 molecules^{-1} s^{-1}, Table 4.1). Since compounds were missing in the second speciation, no new reaction rate coefficient for summertime/autumn monoterpenes could be obtained. Assuming the mixture just contained the three measured compounds (α-pinene, β-pinene, limonene) a weighted reaction rate coefficient would be $k_{MT+OH} = 1.09\times10^{-10}$ cm^3 molecules^{-1} s^{-1} which is less reactive but similar to the springtime-monoterpene reaction rate coefficient. The impact of various reaction rate coefficients is briefly discussed in Section 5.5.2.

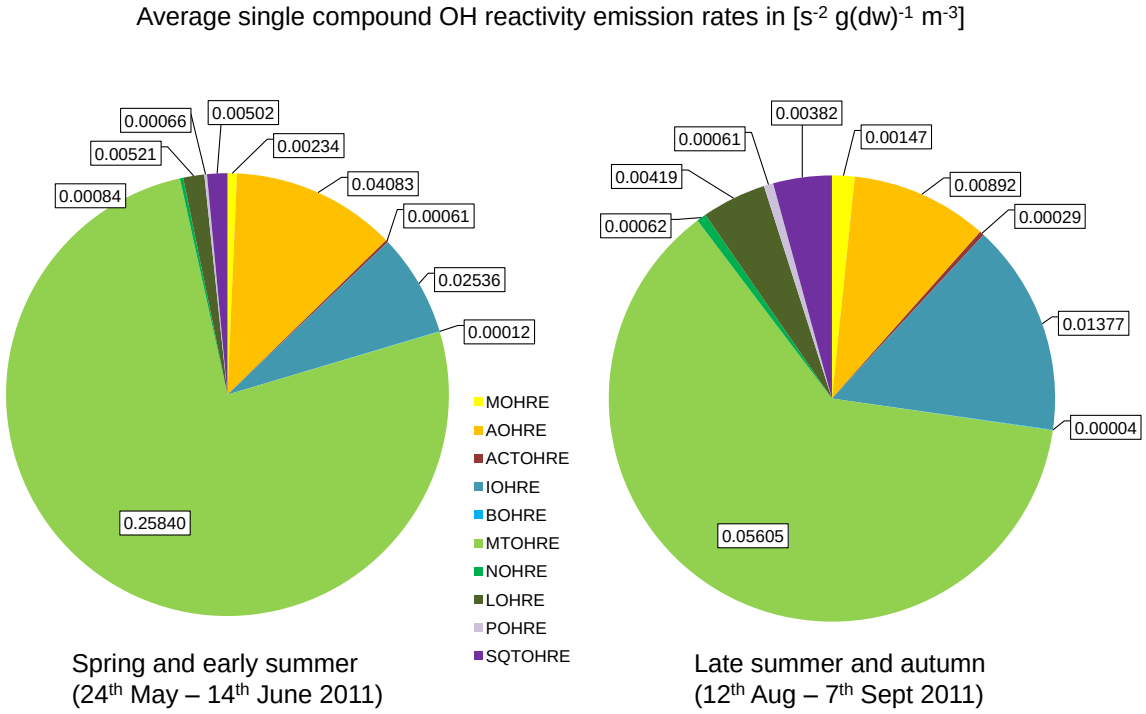

Fig. 4.5: Average contribution of PTR-MS measured compounds to total OH reactivity emission rates (calculated). Single compound OH reactivity emissions (OHRE) are calculated from the measured concentration levels and the reaction rate coefficients given in Table 4.1. The following compounds were included in the budget: methanol (MOHRE), acetaldehyde (AOHRE), acetone (ACTOHRE), isoprene (IOHRE), benzene (BOHRE), total monoterpenes (MTOHRE), total nopinone (NOHRE), linalool (LOHRE), pinonaldehyde (POHRE), total sesquiterpenes (SQTOHRE).

Two more relevant compounds for TOHRE were isoprene and acetaldehyde. Isoprene OH reactivity emissions (IOHRE) were seasonally stable (see Table 4.2) and explained about 2-7 % of the measured TOHRE. Acetaldehyde OH reactivity emission (AOHRE) rates varied with the season, being highest in early summer (10 % of measured TOHRE). As monoterpene emissions showed a significantly lower level in late summer and autumn, their relative contribution to measured TOHRE became minor during this period (11-16 %). During spring, monoterpenes accounted for 69 %, and early summer for 56 %. Compounds such as methanol, nopinone and sesquiterpenes were only minor contributors to total OH reactivity fluxes.

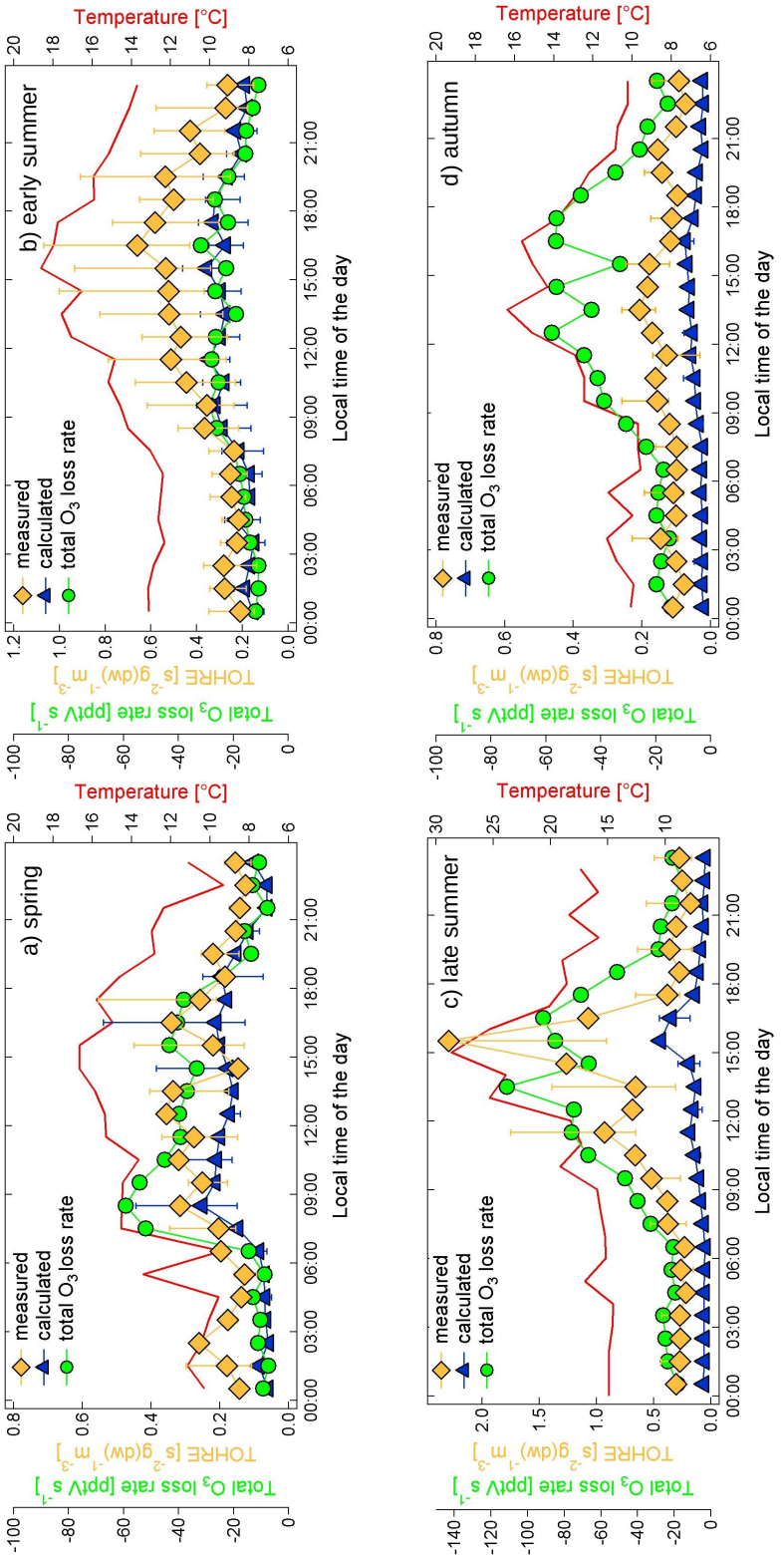

Fig. 4.6: Median diel profiles for four periods a) spring, b) early summer, c) late summer, d) autumn of total OH reactivity emissions (TOHRE) which were measured by CRM (orange markers) and calculated from PTR-MS data (blue markers) and of the observed total ozone loss rate (green markers). Additionally, the median temperature profile is included (red line). Uncertainties of the hourly median are given for measured and calculated TOHRE as 75 and 25 percentiles.

4.3.2 Median diel profiles of measured, calculated TOHRE and total O_3 loss rates

The seasonal variation of measured and calculated TOHRE is given as diel median profiles in Figure 4.6. Additionally, the ozone depletion inside the cuvette during closure was used as a proxy estimate of total O_3 loss rates and included for general comparison of diurnal trends, changing characteristics during seasons of emission rates, and total OH reactivity fluxes. When comparing the measured with the calculated TOHRE, on average missing emissions of OH reactive compounds could be found. These varied seasonally between on average $0.04\,s^{-2}\,g(dw)^{-1}\,m^{-3}$ (relative missing fraction: 15 %) in spring and $0.7\,s^{-2}\,g(dw)^{-1}\,m^{-3}$ (84 %) in late summer (Figure 4.7).
During springtime measurements (24 May – 31 May 2011), the TOHRE generally followed temperature, increasing around 7:00 [local time, utc+3], reaching maximum values between 9:00 and 16:00, and afterwards decreasing again. Calculated TOHRE in total was slightly lower than the measured median profile (although within the error bars). Total O_3 loss rates showed a different median variation throughout the day. It rapidly increased starting at 7:00 (in good agreement with temperature and radiation), reached a maximum at 9:00 (coincident with isoprene emission peak, maximal transpiration rates, and ahead of sesquiterpene emission peak) and then decreased in the course of the day.

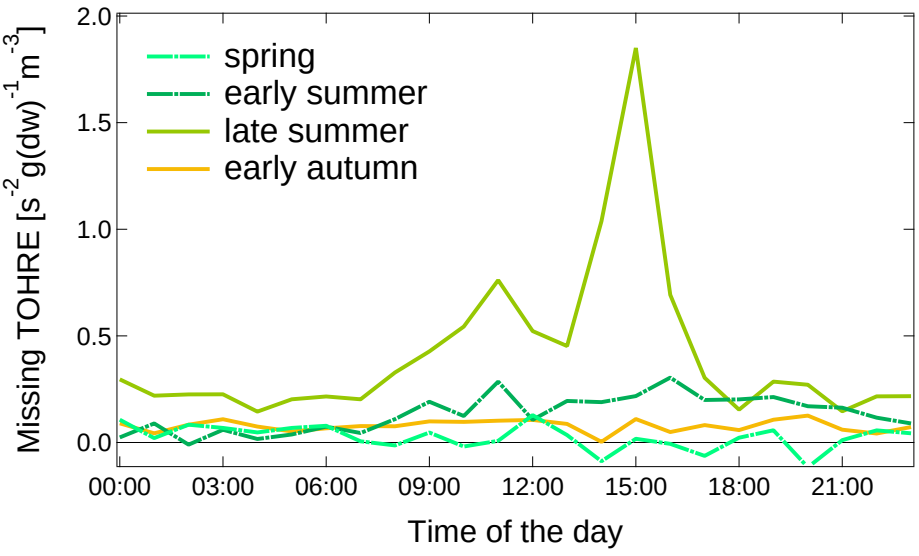

Fig. 4.7: Missing TOHRE as median diel profile for spring, early summer, late summer and early autumn. Missing total OH reactivity fluxes describe the unknown or unmeasured difference which was found by comparing calculated and measured TOHRE.

Early summertime conditions (1 June – 14 June 2011) led to elevated median measured and calculated TOHRE compared to spring. Daytime emissions started with the increase in temperature at 7:00 and returned to a stable, lower level at night. The gap between measurements and calculation (i.e. missing OH reactivity flux) was greater during daytime than at night (Figures 4.6 and 4.7). Relatively low levels of total O_3 loss rates during day were characteristic for early summertime, closely following the calculated TOHRE median diel profile.
Much higher temperatures were characteristic for the observations made during late summer (12 Aug – 26 Aug 2011). Here both, total OH reactivity emissions and the total ozone loss rates reached maximum median values (highest values during this study) in the afternoon of about 2.3 s^{-2} $g(dw)^{-1}$ m^{-3} and -111 pptV s^{-1}, respectively. Total O_3 loss rates had maximum values at 13:00, two hours before measured and calculated TOHRE peaked. Coincident with the maximum total ozone loss rate inside the cuvette, missing TOHRE had a local minimum (Figure 4.7). As observed in spring, as soon as temperature rose and radiation impinged on the cuvette, total O_3 loss rates increased rapidly. The general trend to high levels in late summer did not occur in the calculated total OH reactivity emissions. These showed even lower values than in spring and early summertime revealing high missing OH reactivity emissions.
The diel variation seen in spring and summertime for TOHRE was not as distinct in early autumn (27 Aug – 07 Sept 2011). Measurements and calculations showed a consistent stable gap throughout the entire day. In contrast to total OH reactivity emissions, total O_3 loss rates varied throughout the day as before in late summer closely following temperature and radiation. The increase at 7:00 coincided with an increase in isoprene and sesquiterpene emissions and was followed by a decrease after 16:00 in the afternoon.
Summarized in Figure 4.7 are the median profiles of spring, summer and autumn absolute missing TOHRE values. In late summer a significant fraction of the CRM measured total OH reactivity flux could not be explained when compared to the calculation based on individual PTR-MS measured species.

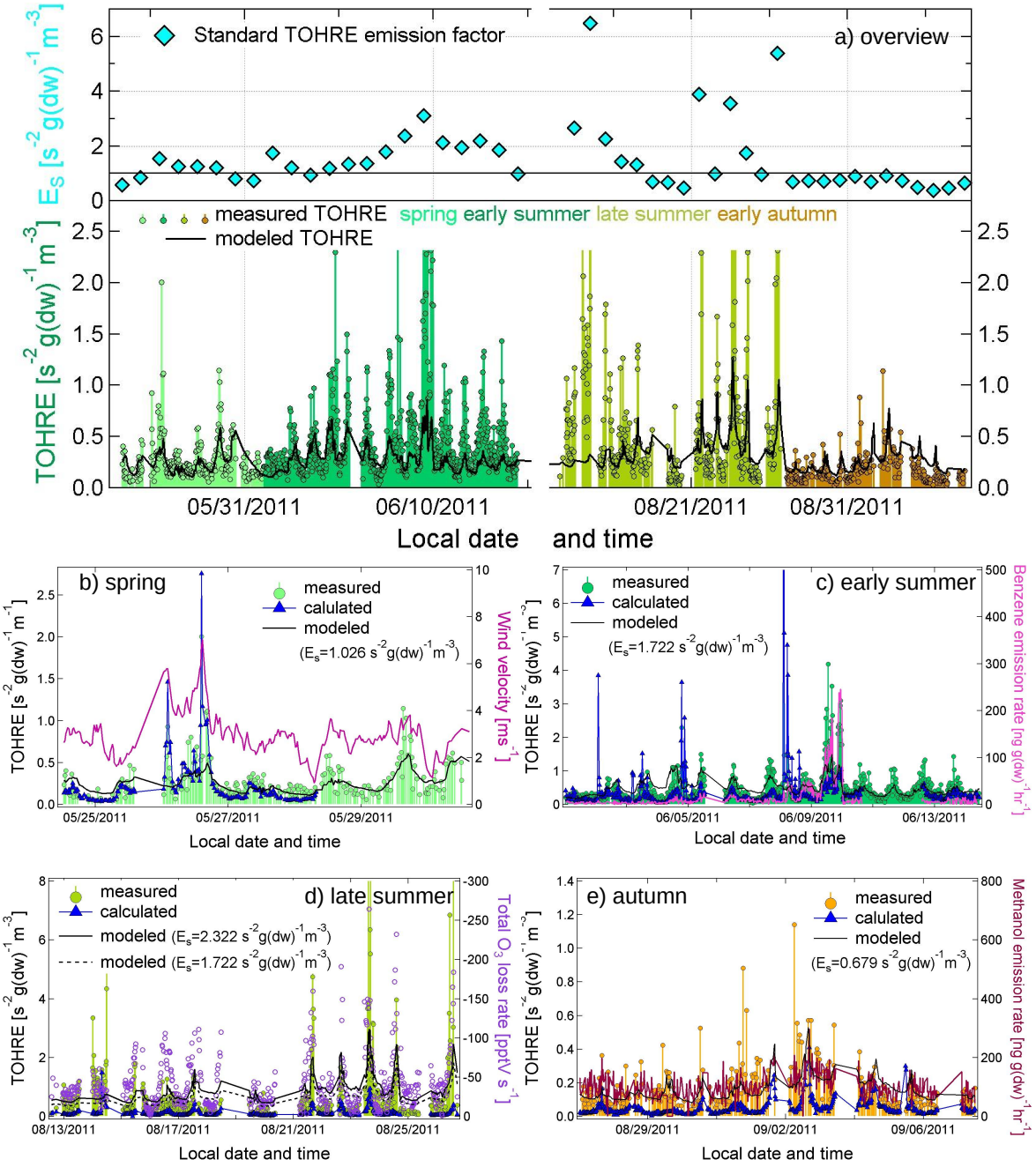

Fig. 4.8: Overview for model, calculation and measurement comparison of TOHRE: a) The entire campaign has been modeled (black line) using an unscaled temperature-only dependent algorithm to compare to measured TOHRE (markers on sticks), superimposed the daily standard total OH reactivity emission factor is pictured. Each of the other graphs (b-e) presents measured, calculated and modeled TOHRE as well as one parameter such as wind velocity, benzene emission rates, total O_3 loss rate and methanol emission rates.

4.4 Discussion

The effect of seasonal trends, day-to-day variability, and rapidly changing environmental conditions on Norway spruce total OH reactivity emission rates are summarized in Figure 4.8.

4.4.1 Comparison to a temperature dependent emission algorithm

Figure 4.8a presents an overview of the measured total OH reactivity emission rates alongside a solely temperature dependent model algorithm (Guenther et al. (1993), see Equation 4.3). In this way a temperature-only dependent response of plant emissions (E) can be described. The algorithm has been used for modeling e.g. monoterpene emission rates from coniferous needle storage pools (e.g. Taipale et al., 2011) and has also proved to be effective in representing missing OH reactivity in the Michigan forest reasonably well (Di Carlo et al., 2004).

$$E = E_S \, exp^{(\beta(T-T_S))} \tag{4.3}$$

A typical value for β=0.09 K^{-1} was chosen, the standard total OH reactivity emission rate E_S in Figure 4.8a kept equal to 1 $s^{-2}\,g(dw)^{-1}\,m^{-3}$. In this way, the general trend of a temperature-only driven emission rate could be compared qualitatively to the measured values of TOHRE. Additionally, the standard TOHRE factor E_S was calculated for each day through the linear fit between measured TOHRE and the un-scaled model values. As can be seen superimposed in Figure 4.8a, slowly increasing values during early summer and a decrease in early autumn describe a seasonal trend of E_S. The temperature related model itself reflects the measured TOHRE throughout the observed period of the year reasonably well, emphasizing the temperature dependence of the observed TOHRE. Nevertheless, on several occasions TOHRE reveals different characteristics that the model does not resolve. Due to the seasonal trend in E_S, mean standard TOHRE factors of each season (spring, early summer, late summer, autumn) were used to scale the modeled values. The results are presented in Figure 4.8 (b-e) in four separate graphs representing each season. Each graph pictures TOHRE measured by CRM, calculated from PTR-MS results and the scaled model prediction for the observed time period. On the right hand axis different parameters are added for comparison.

During springtime observations the diurnal variation of measured and calculated TOHRE were in generally good agreement to the temperature dependent model. Two peaks stand out, which were found within the measurements and the calculation but not in the model. The high total OH reactivity emissions up to 1.5 and 2.7 $s^{-2}\,g(dw)^{-1}\,m^{-3}$ could not be satisfactorily explained by the temperature-only dependent emissions. These high TOHRE events correspond to two peaks in the wind velocity. Wind speeds

higher than $5.5\,\mathrm{m\,s^{-1}}$ are termed meteorologically as "moderate breeze" and are characterized by moving branches. It is likely that wind induced mechanical stress was a driving force in VOC and total OH reactivity emission fluxes from the Norway spruce branch on these two occasions. Similarly, ambient measurements of monoterpene levels in rural New Hampshire (USA) showed a high impact from storm events. Haase et al. (2011) observed that PTR-MS measured monoterpene mixing ratios increased on average by a factor of 93 % above pre-storm levels for heavy storms including high precipitation and sometimes hail. Interestingly in this study, monoterpene emission rates and TOHRE increased significantly for the examined Norway spruce during elevated wind velocities. No missing total OH reactivity flux was observed in these cases. From selected events throughout the two measurement intensives during 2011, total OH reactivity emissions generally rose by a factor of 6 (on average for wind speeds higher than $5.5\,\mathrm{m\,s^{-1}}$).

Emission rates in June, during early summer conditions, were generally higher than in spring. Increasing temperatures over the first five days in June enhanced both measured and calculated TOHRE. During daytime the measurements typically exceeded the values for TOHRE calculations. For one outstanding day (09 June 2011) measured TOHRE was significantly elevated when compared to PTR-MS measurements. This day was characterized by high temperature and low wind speeds. Windy days prior to this had caused spikes in calculated and measured TOHRE (similarly to the characterized event in spring), and perhaps even damaged the branch. Monoterpene emission rates closely followed the temperature-dependent pattern, whereas measured total OH reactivity emissions increased up to $4.2\,\mathrm{s^{-2}\,g(dw)^{-1}\,m^{-3}}$ on that day. One compound among the PTR-MS quantified VOCs showed the same behavior as TOHRE, which was benzene (Figure 4.8c). Peak emission rates of $280\,\mathrm{ng\,g(dw)^{-1}\,hr^{-1}}$ were reached while benzene average emission rates for the other three defined periods varied between 5.2 and $9.8\,\mathrm{ng\,g(dw)^{-1}\,hr^{-1}}$. Benzenoids could be possibly emitted by plants following stress, although little is known about biochemical pathways of formation (Heiden et al., 1999, White et al., 2009, Dudareva et al., 2006). Other stress induced plant emissions e.g. methyl salicylate (MeSa), or higher mass oxygenated VOCs were not monitored and are therefore potential explanations for the high missing OH reactivity emission at that particular stress event.

While the scaled temperature driven model and total OH reactivity emissions agreed relatively well during the first measurement period, large discrepancies occurred during the second campaign. The mean emission factor during late summer was elevated by four outliers during this period. Hence, the modeled temperature dependence tends to overestimate the true emission rates. For comparison, the lower standard emission factor of the early summer is also included into the graph. For this period the comparison of measured and calculated TOHRE reveals remarkable discrepancies. The

measurements by CRM seem significantly underestimated by the calculated TOHRE from PTR-MS results. Since it was cold and wet, low emission rates were expected until 21 August 2011. Afterwards temperature increased and reached the annual maximum (23 Aug 2011). Generally, humid and windy nights were followed by days with extremely high emissions of total OH reactivity (e.g. peak value for 23 Aug 2011: TOHRE=13.6 s^{-2} g(dw)$^{-1}$ m^{-3}). The same behavior could be observed from total O_3 loss rates, which rose as well during daytime to high levels.
It seems that mechanisms that contributed to both, the production of OH reactive compounds and stimulation of ozone uptake or reactions, increased during daytime in late summer. The ratio of temperature driven pool emissions and de novo production with light and temperature seems to have changed, so that the temperature-only dependent model does not match the diel variation of TOHRE. The PTR-MS was not able to detect this increase in the emission rates of OH reactive VOCs both at night and daytime, which led to an average of 84 % missing OH reactivity emissions.
Meteorological characteristics changed markedly on 26 August 2011, but the gap between measured and calculated TOHRE remained high (on average 70 %, see also Table 4.2). Absolute values were found to be generally much lower due to cold and wet environmental conditions. Diel profiles were no longer pronounced, with less than 20 % variation between night and day which can also be noted from Figure 4.6d. The measured total OH reactivity emission rates even stayed high for some nights (e.g. 01 – 03 Sept 2011). A similar trend was found for methanol emission rates which remained relatively high during the night compared to the monoterpene signal.
From springtime and early summer to late summer and early autumn, a clear change could be observed in measured TOHRE and total O_3 loss rates. By comparing to the temperature related emission model, diurnal trends in the observations could be generally well explained for the first measurement campaign, whereas the second dataset revealed large discrepancies. The emissions of most VOCs did not change throughout the year, although the signal of total monoterpenes, acetaldehyde decreased and total sesquiterpenes increased in late summer and autumn. Despite this, total OH reactivity emissions reached maximum values during late summer. Major contributions to total OH reactivity emissions at that time of the year remained unexplained. Interestingly, also the estimated total loss of ozone increased, giving evidence for either a higher rate of stomatal-uptake or the release of highly ozone reactive compounds. Possibly, both loss mechanisms are coupled which complicates the interpretation of this study's simplified approach.

4.4.2 A climatological perspective

It should be noted that from a climatological point of view the year 2011 was unusual in comparison to long-term meteorological observations. It had a cold and

rainy summer with relatively low ozone mixing ratios (e.g. on average for July: $O_{3,ave}$(2011)=37.7 ppbV, $O_{3,ave}$(1997-2011)=48.8 ppbV). After the cold and rainy summer, for the second measurement period generally elevated soil moisture (by a factor of 2) and transpiration rates (by a factor of 1.6) have been observed when compared to the springtime measurements. In addition, during the measurement period in August 2011 sesquiterpene emission rates were significantly increased (from on average 46.7 ng g(dw)$^{-1}$ hr^{-1} to 92.6 ng g(dw)$^{-1}$ hr^{-1}), subsequently decreasing to very low levels in autumn (on average 25.5 ng g(dw)$^{-1}$ hr^{-1}). This is indicative of a high activity (in terms of both the total OH reactivity emission rates and the ozone loss rates inside the cuvette system) of the tree during late summer, the period of the high missing OH reactivity flux.
Interestingly, highest total OH reactivity fluxes as well as peak ozone loss rates inside the cuvette coincided with the climatological, seasonal maximum of ambient ozone. It also has been found, that sesquiterpene emissions were triggered not only by temperature but also by atmospheric ozone levels (Bourtsoukidis et al., 2012).

4.4.3 Variation in mono- and sesquiterpene composition

One reason for the discrepancy between measurements and calculations in late summer and autumn TOHRE might be that the composition of mono- and sesquiterpenes seasonally changed which was not considered in the calculations (Section 4.3.1). This was tested with a range of rate coefficients based on previous studies of mono- and sesquiterpenes from Norway spruce (Kempf et al., 1996, Martin et al., 2003, Yassaa et al., 2012). Additionally, an exceptional high reaction rate coefficient for monoterpenes has been applied to TOHRE calculations from PTR-MS measurements. The gap between measured and calculated TOHRE remains, being decreased by less than 2 % for Yassaa et al. (2012) (k_{MT}=1.3×10^{-10} cm^3 molecules^{-1} s^{-1}), Martin et al. (2003) (k_{SQT}=2.2×10^{-10} cm^3 molecules^{-1} s^{-1}), and Kempf et al. (1996) (k_{MT}=1.4×10^{-10} cm^3 molecules^{-1} s^{-1}). The unrealistic high rate coefficient (k_{MT}=5.0×10^{-10} cm^3 molecules^{-1} s^{-1}) resulted in a missing OH reactivity emission rate of still 53 % in summer and 20 % in autumn, compared to originally 84 % (summer) and 70 % (autumn) (see Table 4.2). Therefore, it seems unlikely that variability in the mono- and sesquiterpene composition alone causes the high unexplained TOHRE in late summer and autumn. Additionally, it has to be noted, that uncalibrated and unidentified peaks in the analysis of the GC-MS chromatograms remained which leaves the estimate of the reaction rate coefficient somewhat uncertain, and provides direct evidence of unidentified contributors to total OH reactivity emissions.

4.4.4 Brief literature review

Evidence for a temperature related missing OH reactivity has been already reported in ambient air by Di Carlo et al. (2004) and Nölscher et al. (2012b). As presented in this study, the unexplained portion of total OH reactivity emission rates was high from Norway spruce emissions especially for high temperatures. Di Carlo et al. (2004) compared direct total OH reactivity measurements in the Michigan Forest from summer 2000 to BVOC measurements that were conducted two years earlier at the same site. The resulting "missing OH reactivity" showed terpene-like temperature dependency. Having included both, mono- and sesquiterpene direct emissions into the budget for total OH reactivity emission rates, a relatively large missing OH reactivity flux remains in this study for summer and early autumn. Despite a comprehensive set of atmospheric measurements during the HUMPPA-COPEC campaign 2010, high missing OH reactivity was found in summertime boreal forest (Nölscher et al., 2012b). Comparison of in and above canopy total OH reactivity measurements have indicated a biogenic origin of the highest unexplained total OH reactivity. This missing total OH reavtivity, occurring during prolonged periods of enhanced temperatures, was likely related to heat stress induced direct emissions and also to secondary oxidation products of various biogenically released compounds.

In contrast to these findings, Kim et al. (2011) reported that, based on alternate branch enclosure measurements of total OH reactivity, isoprene and selected mono- and sesquiterpenes, no missing OH reactivity was emitted directly from four observed tree species. No oxygenated species were included in Kim et al. (2011)'s total OH reactivity calculation, nor were they required to close the OH reactivity budget. In our study acetaldehyde was found to contribute significantly through spring, summer and autumn. In Kim et al. (2011) it is not clear whether the branch was impacted by the cuvette, and which compounds and reaction rate coefficients have been used for calculations. Such a good agreement of total OH reactivity measurements and calculations might be due to mechanical stress and the release of elevated monoterpene levels, as has been shown in this study. Furthermore, for the examined Norway spruce summertime exhibited the most missing total OH reactivity flux, whereas no missing OH reactivity from the four enclosed tree branches for measurements in July was found by Kim et al. (2011). Possibly, the species investigated did only emit isoprene, mono- and sesquiterpenes as significant contributors to total OH reactivity.

These contrasting studies emphasize the importance of further measurements of total OH reactivity in the atmosphere and also in closed systems such as branch cuvettes or plant chambers. Emission strength and composition may vary between species and individual plants, so that the completion of the current view requires more investigative field studies.

4.5 Summary and conclusions

Seasonal variation, diel behavior and the feedback to environmental stress of total OH reactivity emission (TOHRE) rates and total O_3 loss rates from Norway spruce were studied intensively for the first time. Direct measurements of total OH reactivity fluxes from a branch enclosure system via CRM could be compared to VOC emission rates determined simultaneously by a PTR-MS. TOHRE showed seasonal variability, being highest in late summer and lowest in early autumn. A clear temperature dependence was found when comparing the measured TOHRE to the temperature-only dependent algorithm for needle pool emissions of vegetation. Diel median profiles showed generally higher total OH reactivity flux by day than by night. Similarly, total O_3 loss rates increased during the daytime and stayed low at night. The total loss rate of ozone increased in late summer and autumn, which was consistent with the measured TOHRE (in late summer).

The predominant VOC emission measured by PTR-MS was the sum of monoterpenes. On average this accounted for 56-69 % of the measured TOHRE in spring and early summer, and for 11-16 % in late summer and early autumn. However, tests with previously reported typical compositions of mono- and sesquiterpenes emitted by Norway spruce did not significantly improve the mismatch. Besides monoterpenes, both isoprene and acetaldehyde contributed significantly to total OH reactivity emissions.

Fluxes of oxygenated compounds such as methanol showed a similar diel pattern to the measured TOHRE in late summer and autumn, when monoterpene emission rates drastically decreased compared to the growing season in May/June. It seems that instead, reactive compounds, not detected by PTR-MS, were produced and released by the Norway spruce during daytime. These were likely linked to total ozone loss rates that correlated well with temperature and light. Whether this was due to enhanced stomatal-uptake of ozone, surface reactions or total ozone reactivity caused by the tree emissions remains to be examined in future studies. However, enhanced transpiration rates and greater fluxes of total sesquiterpenes in late summer additionally support the hypothesis of higher daytime productivity of the examined Norway spruce.

In addition to seasonal and diurnal variation, environmental feedback impacted TOHRE from Norway spruce. Mechanical stress due to moderate to strong wind events led to elevated emissions of monoterpenes. Such wind events happen regularly in forested regions and their impact on monoterpene emissions has been already noted in several studies (Haase et al., 2011, Bamberger et al., 2011). Generally, in such wind events, both the calculated and the measured TOHRE increased significantly. Another feedback mechanism is stress related to heat. Surprisingly, benzene was found to correlate very well with the measured total OH reactivity emission for a hot day, for which the calculated TOHRE could not explain the observations by CRM. During this event the total OH reactivity emissions had a large unexplained fraction, which is likely to

be caused by stress related compounds.
Although for springtime almost the entire signal of TOHRE could be explained by PTR-MS detected biogenic compounds (15 % missing total OH reactivity emissions), the fraction of unaccounted for total OH reactivity tree emissions increased in summer to 84 % and stayed high in autumn with 70 %. Light induced production and release of undetected highly reactive compounds add to the large fraction of unexplained total OH reactivity flux during the summer measurements from the Norway spruce branch enclosure. Peak total OH reactivity fluxes as well as highest estimated ozone loss rates inside the cuvette coincided with the maximum in the ten year average seasonal ozone profile. This study showed, that unmeasured and possibly unknown compounds, which are biogenically produced and released during daytime, contribute to the observed high missing fraction of OH reactivity generally reported from summertime observations in forested regions.

Acknowledgments

We are grateful for the supporting GC-MS analysis determined by W. Song, H. Hakola and H. Hellén. Many thanks for the technical support by T. Klüpfel and the entire PARADE-team. We acknowledge the use of the Taunus Observatory facilities of Goethe University, Frankfurt.

5

A total OH reactivity perspective on isoprene photooxidation via measurement and model - CHEERS 2011

A. C. Nölscher[1], T. Butler[2], J. Auld[1], P. Veres[1], A. Muñoz[3], D. Taraborrelli[1], L. Vereecken[1], and J. Williams[1]

[1]Department of Atmospheric Chemistry, Max Planck-Institute for Chemistry, Mainz, Germany
[2]Institute for Advanced Sustainability Studies, Potsdam, Germany
[3]Instituto Universitario CEAM-UMH, Paterna, Valencia, Spain

Manuscript in preparation

Summary. The tropics provide a reactive atmospheric environment with high levels of biogenic emissions, rapidly growing anthropogenic input, significant irradiation and high temperatures. The major biogenic emission is isoprene which reacts rapidly with the most important atmospheric oxidant OH, the hydroxyl radical. This key photooxidation process has recently been the focus of several experimental studies and computational calculations. In addition of the commonly used degradation scheme (MCM 3.2) a novel isoprene mechanism was developed (MIMEv4), base on the latest theoretical findings.

This study examined the photooxidation of isoprene in a low NO_x environment in the controlled conditions of the Valencia atmospheric reaction chamber, EUPHORE. Besides the detection of isoprene and its major products formaldehyde, methyl vinyl ketone (MVK) and methacrolein (MACR), total OH reactivity, the total loss rate of OH, was measured. The total OH reactivity can be used as a measure for the oxidative capacity of a mixture. When compared to individual measurements of reactants and products, it may reveal important or missing contributions in terms of the total OH sink. When compared to a modeled degradation scheme, it may be used to evaluate and test known mechanisms.

For the isoprene photooxidation during CHEERS 2011, total OH reactivity was dominated by isoprene and its major products: MVK, MACR and HCHO. Calculations made by using the individually detected compounds and the traditional degradation scheme (MCM 3.2) could account for the measured total OH reactivity throughout the reaction reasonably well. Big discrepancies between the observations and modelled values were found for the recently

developed isoprene mechanism MIMEv4. Crucially switching off a large part of the new chemistry (i.e. 1,5 and 1,6 H-shifts which efficiently recycle OH during the isoprene oxidation) resulted in excellent agreement to the measurements.

5.1 Introduction

Photooxidation processes in the troposphere impact the concentration of trace gases, ozone and aerosols, and determine the formation and destruction rates of radicals (e.g. Atkinson and Arey, 2003, Kanakidou et al., 2005, Hofzumahaus et al., 2009). The most important oxidant in the daytime is the hydroxyl radical (OH). Sources (predominantly radiation dependent) and sinks (due to all OH reactive species) are as yet poorly constrained (Di Carlo et al., 2004, Rohrer and Berresheim, 2006, Mao et al., 2012). The sum of all OH sinks, the overall loss rate of hydroxyl radicals, is termed total OH reactivity. Recently, the direct measurement of total OH reactivity became an important tool for examining the atmospheric composition, oxidative capacity and ozone formation potential (Jeanneret et al., 2001, Yoshino et al., 2011, Nölscher et al., 2012b, Sinha et al., 2012).
Globally isoprene accounts for almost half of the emitted biogenic volatile organic compounds (VOCs) (Guenther et al., 2006), regionally, i.e. in the tropics, it can be the most abundant non-methane hydrocarbon (e.g. Williams et al., 2001). First mentioned by Sanadze (1956) as an emission from vegetation, it is now known that isoprene is released through the plant's stomata, closely dependent on light and temperature (Rasmussen and Jones, 1973, Tingey et al., 1980, Lamb et al., 1987). Due to its high reactivity to OH (k=1×10^{-10} molecules^{-1}cm^{3}s^{-1}), emission rate and recycling potential especially over forests, it is a driving factor of tropospheric chemistry. It's impact on radical consumption and re-generation is highly debated, hence it has been the focus of many experimental and computational studies (Paulot et al., 2009, Peeters and Mueller, 2010, Taraborrelli et al., 2012).
Isoprene and its oxidation products have been observed in various ambient field studies (Pierotti et al., 1990, Montzka et al., 1995, Williams et al., 2001, Karl et al., 2009, Eerdekens et al., 2009a). Product studies via chamber photooxidation experiments have identified and quantified a multitude of isoprene secondary products such as formaldehyde (HCHO), methyl vinyl ketone (MVK), methacrolein (MACR), methylglyoxal, hydroxycarbonyls and peroxyacetyl nitrates (PANs)(Tuazon and Atkinson, 1990, Paulson and Seinfeld, 1992, Kwok and Atkinson, 1995, Ruppert and Becker, 2000).
Based on these studies, detailed degradation schemes of isoprene were developed (Paulson and Seinfeld, 1992, Carter et al., 1996, Jenkin et al., 1997, Geiger et al., 2003) which could be applied to atmospheric models. The Leeds Master Chemical Mechanism (MCM), constructed as a detailed protocol for atmospheric degradation processes

of various VOCs, includes a highly explicit isoprene reaction scheme (Saunders et al., 2003, Pinho et al., 2005). For the purpose of global modeling, a condensed isoprene oxidation mechanism has been developed, based on the complex MCM reaction schemes. The first version of the Mainz Isoprene Mechanism (MIM) included 16 organic species and 44 chemical reactions (Pöschl et al., 2000).
However, atmospheric field investigations in low NO_x and isoprene-rich environments revealed a significant discrepancy between predicted hydroxyl radical levels and the direct measurements of OH (Tan et al., 2001, Lelieveld et al., 2008, Hofzumahaus et al., 2009). Within the tropics, a key-region for atmospheric chemistry, coexisting high isoprene and high OH levels puzzled scientists. Reasons for this can be twofold: the measurement of the OH mixing ratio could have been impacted by interferences (e.g. Mao et al., 2012) or the applied atmospheric model could not reproduce atmospherically relevant photooxidation mechanisms correctly (e.g. Butler et al., 2008).
Based on theoretical treatments, novel isoprene photooxidation schemes were suggested and some have been included in atmospheric models (Peeters et al., 2009, Paulot et al., 2009, Wolfe et al., 2010). Taraborrelli et al. (2012) extended MIM in order to investigate this novel isoprene chemistry in detail. As a result, 900 species and 4000 reactions have been implemented into MIME (MIM Extended).
Here, the OH-initiated isoprene photooxidation was studied in the controlled environment of the EUPHORE (**E**uropean **PHO**to**RE**actor). **C**hamber **E**xperiments **E**xamining **R**eactivity and **S**pecies (CHEERS) were set up to compare the two isoprene oxidation mechanisms, MCM and MIME, with measurements of individual species and total OH reactivity.
The individually measured or modeled compounds were converted to OH reactivities, through their mixing ratios [X] and the rate coefficients with OH (k_{X+OH}), which sum up to the total calculated OH reactivity (Equation 5.1). For the reaction of isoprene and OH, an overall decreasing total OH reactivity is expected because isoprene, as the predominant contributor to the total OH sink, is converted into less reactive secondary products (Atkinson and Arey, 2003, Karl et al., 2006, Nakashima et al., 2012).

$$R_{total,calc} = \sum [X] \times k_{X+OH} \tag{5.1}$$

In this way total OH reactivity, calculated, modeled and directly measured, functioned as diagnostic tool to evaluate the traditional and novel view of isoprene degradation by OH under controlled conditions.

5.2 EUPHORE and Instrumentation

The EUPHORE chamber in Valencia (Siese et al., 2001) provided an excellent reaction vessel for studying atmospheric photooxidation processes during the CHEERS campaign in autumn 2011. All experiments (CHEERS 1-9) started in the morning with background measurements from the empty chamber, after flushing it for cleaning purposes over night. The compound of interest was injected (except for the empty-chamber-background experiment: CHEERS 4) and kept inside the closed chamber (for ca. 15 minutes) to homogeneously mix in the entire volume. The roof over the about 200 m^3 half spherical Teflon chamber opened automatically to start the experiment (Figure 5.1). Natural irradiation initiated both, OH production from HONO at the walls (Rohrer et al., 2005, Zador et al., 2006), and the photooxidation of the compound inside the chamber. Experiments were planned to last for 6 hours and were centered on local noon.

Fig. 5.1: EUHPORE chamber in Valencia while opening the roof to start the experiments.

The instrumentation provided by the EUPHORE team monitored chamber temperature, pressure and relative humidity (typically in a range of 18-34 °C, 1002–1009.4 mbar and max. 18 %), ozone (0–65 ppbV), NO_x (0–11 ppbV) and CO (896–1092 ppbV) mixing ratios. Humidity was kept low to limit the formation of aerosol during the study. A **P**roton-**T**ransfer-**R**eaction-**T**ime-**O**f-**F**light-**M**ass-**S**pectrometer (PTR-TOF-MS, IONICON) followed the development of the examined VOC and the evolution of some of the reaction products (e.g. Jordan et al., 2009). Compounds with a higher proton affinity than water can be ionized by the reaction with H_3O^+, accelerated in the drift-tube and selectively separated by mass. The high resolution separation using a TOF, configured in V-mode with a mass resolution of approximately 3700 $m/\Delta m$ allows for example to distinguish the compounds methylglyoxal (m/z 73.03) and methyl ethyl

ketone (m/z 73.07). The signal was calibrated using a standard gas mixture (Apel-Riemer Environmental) and a portable permeation source e.g. for formaldehyde (Table 5.1).

Table 5.1: PTR-TOF-MS measured mass, the corresponding compounds, overall uncertainty, detection limit (LOD = 3σ of background), calibration method and calibrated compounds. Italic highlighted compounds have been used to constrain the model to EUPHORE conditions.

mass	compound	uncertainty [%]	LOD [ppbV]	calibration method, compound
m/z 31	*formaldehyde*	6	0.4	permeation tube, formaldehyde
m/z 33	*methanol*	18	0.9	gas standard, methanol
m/z 45	*acetaldehyde*	6	0.2	gas standard, acetaldehyde
m/z 59	*acetone*	13	1.9	gas standard, acetone
m/z 61	acetic acid, glycolaldehyde	11	2.4	permeation tube, acetic acid
m/z 69	isoprene	3	0.3	gas standard, isoprene
m/z 71	methyl vinyl ketone, methacrolein	4	0.1	gas standard, MVK
m/z 73.03	methylglyoxal	8	0.08	adopted calibration factor for acetone
m/z 75	*hydroxyacetone*	16	0.5	permeation tube, hydroxyacetone
m/z 83	methylfuran	11	0.1	permeation tube, furan

The total OH reactivity was measured by the Comparative Reactivity Method (CRM), an instrument which compares the reaction of a reagent with OH alone and then in the presence of the reactive molecules from the chamber (Sinha et al., 2008). As reagent pyrrole (C_4H_5N) was used and detection was conducted using a quadrupole PTR-MS (pyrrole detection at m/z 68). The total OH reactivity method was tested by introducing known amounts of calibration gases (such as propene and isoprene). In addition, the initial closed chamber concentration of the reacting compound was used to prove good sensitivity and linearity for the CRM.
The overall uncertainty for this experiment was calculated as a propagation of errors including the uncertainty of the gas standard (5 %), the reaction rate coefficient (14 %), PTR-MS error (5 %), flow variability (2 %), and an additional uncertainty occuring in corrections which have been applied afterwards (18 %). These included the correction for dilution of the sampled air and chamber effects, that occured during the CHEERS experiments. In total, the measurement uncertainty was 24 %, and the limit of detection (2σ of the baseline noise) was $4\,s^{-1}$. Both instruments, the PTR-TOF-MS and the CRM, were located underneath the chamber floor with short inlet lines (< 4 m).

5.3 Modeling CHEERS

Simulations of the CHEERS experiments were performed using the photochemical box model MECCA (Sander et al., 2005) employing the chemical mechanisms of the MCM version 3.2, MIMEv4 and a modified MIMEv4 version (MIMEv4*) (Jenkin et al., 1997, Saunders et al., 2003, Pöschl et al., 2000, Taraborrelli et al., 2012). This modified version of MECCA has been previously described in Butler et al. (2011).
For the present study, the model was further modified to simulate EUPHORE chamber conditions according to the instructions given on the MCM website (http://mcm.leeds.ac.uk/MCM/MCMChamber.htt):

- reactions were added to account for processes occurring on the walls of the chamber;
- photolysis rates were calculated based on observed $J(NO_2)$ accounting for transmission through the chamber walls, backscatter from the chamber floor and cloud cover;
- and a dilution rate based on observations of SF_6 was applied to all model species.

Previous simulations in the EUPHORE environmental chamber with the MCM have found that the mechanism underestimates the concentration of OH in the chamber, manifesting as insufficient removal of the primary VOC (Bloss et al., 2005). Following Bloss et al. (2005), the model used in the present study is modified to optionally include an artificial source of OH radicals tuned at every model timestep so that the measured VOC decay rate is reproduced by the model.
For each experiment, the model is initialized with the observed mixing ratio of the VOC of interest as measured by PTR-TOF-MS. A constant mixing ratio of 1.8 ppmV was assumed for CH_4. Time-dependent boundary conditions representing conditions in the chamber and sources, and sinks of species on the chamber walls were applied to the model. These boundary conditions are based on measurements of temperature, pressure, humidity, $J(NO_2)$, O_3, CO, HONO, and NO_2, as well as formaldehyde, methanol, acetaldehyde, acetone, and hydroxyacetone measured by PTR-TOF-MS (Table 5.1).
Measurements of HONO were only available for the experiments CHEERS 2 (polluted toluene oxidation) and CHEERS 4 (background experiment) due to instrument malfunction. For simulations of the experiment CHEERS 7 (isoprene oxidation), a range of HONO boundary conditions was employed based on values of 80 % to 120 % of the measurements from the CHEERS 4 experiment. The chemiluminescent detector used for the NO_2 measurements is known to be affected by interferences from other nitrogen-containing compounds (e.g. Winer et al., 1974). For this reason the NO_2 boundary condition was used to constrain the modelled sum of NO_2 and all nitrate species. The identity of the nitrogen-containing molecules desorbing from the chamber walls was unknown. To account for this uncertainty, it was assumed to be the relatively unstable peroxyacetylnitrate, and a range of simulations was performed where the constraint

was varied between 0 and 100 % of the NO_2 reported by the chemiluminescent detector. Model results for each experiment are reported as a range of values based on a set of model runs done using the above-mentioned ranges of boundary conditions for HONO and NO_2.

5.4 Results

The controlled environment of the EUPHORE reaction chamber was used for investigating the photooxidation of isoprene under natural light and low NO_x conditions. The degradation of isoprene and the formation of major reaction products were monitored with time. These were compared to total OH reactivity measurements using CRM and model simulations.

5.4.1 Oxidation of isoprene

High levels of isoprene (197 ppbV) were injected into the EUPHORE chamber and photooxidation initiated in low NO_x conditions (< 3 ppbV – initially). Isoprene depletion and the formation of products such as formaldehyde (HCHO), methyl vinyl ketone and methacrolein (detected on one m/z 71 as MVK&MACR), and methylglyoxal were monitored by PTR-TOF-MS (Figure 5.2, top panel). Isoprene mixing ratios decreased over the 6 hour reaction time to 31 % of the initially introduced value. Formaldehyde and MVK&MACR, which are major products of the isoprene photooxidation, increased significantly. At the end of the experiment formaldehyde reached the same concentration level as isoprene (61 ppbV). MVK&MACR had a level of 47 ppbV after 6 hours reaction time (Table 5.2).

Table 5.2: Initial and final level and contribution to OH reactivity of individually measured compounds by PTR-TOF-MS. On the right: relative contribution of each compound to the total (calculated) OH reactivity.

	initial		final		
Compound	mixing ratio [ppbV]	OH reactivity [s^{-1}]	mixing ratio [ppbV]	OH reactivity [s^{-1}]	relative contribution [%]
formaldehyde	1	0	61	13.0	6.5
methanol	19	0	95	2.1	1.0
acetaldehyde	0	0	16	6.0	3.0
acetone	1	0	9	0.04	0.02
acetic acid	2	2	29	0.5	0.2
isoprene	197	487	61	151.0	75.4
MVK&MACR	0	0	47	23.0	11.5
methylglyoxal	0	0	1	0.4	0.2
hydroxyacetone	0	0	6	0.5	0.2
methylfuran	0	0	2.5	3.7	1.8

5.4.2 Total OH reactivity comparison and temporal trend

The total OH reactivity perspective highlights the relevance of detected components for the OH-initiated isoprene photooxidation. By converting each component's mixing ratio into individual OH reactivities, highly reactive and abundant compounds are separated from species, that contribute only minimally to the total OH sink term. Measured total OH reactivity decreased from initially $512\,s^{-1}$ to $202\,s^{-1}$ after 6 hours of reaction. Initially isoprene was the only reactive compound in the chamber, accounting for $487\,s^{-1}$ (Figure 5.2, lower panel). The initial background total OH reactivity was found to be around $4\,s^{-1}$. The empty chamber experiment (CHEERS 4) showed that this was mostly caused by CO. In Table 5.2 initial and final single compound OH reactivities (and mixing ratios) are summarized. Throughout the experiment isoprene dominated the total OH reactivity. After 6 hours reaction time, isoprene was still the greatest contributor and accounted relatively with 75.4 % to the total (calculated) OH reactivity. MVK&MACR (11.5 %), formaldehyde (6.5 %) and acetaldehyde (3 %) were the most relevant products in terms of total OH reactivity. As can be seen from Figure 5.2 (lower panel), the sum of all single compound OH reactivities, the total calculated OH reactivity, agreed well with the measurements by CRM for the whole experiment. Hence, the sum of isoprene and it's most dominant reaction products accounted for the entire total measured OH reactivity.

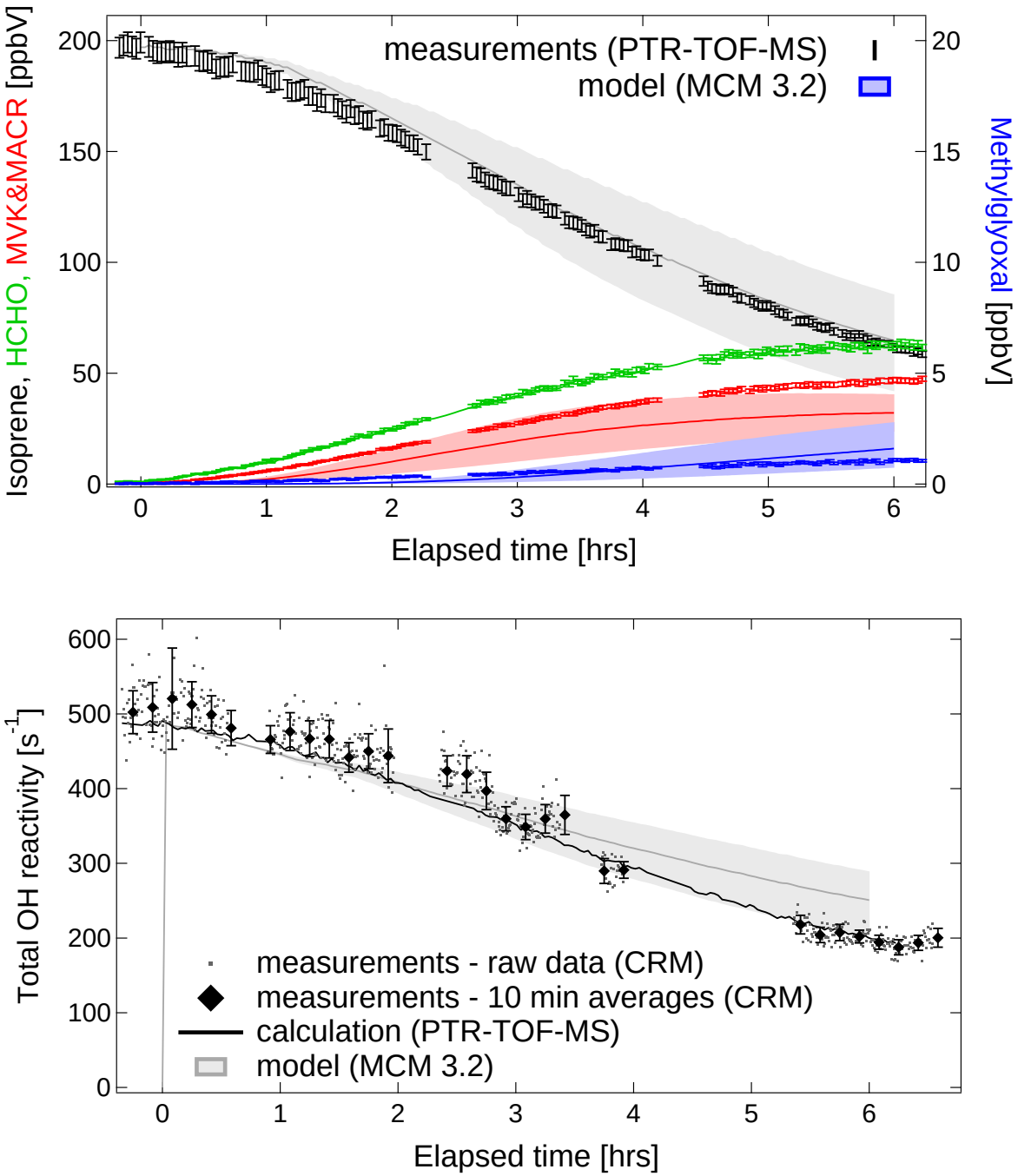

Fig. 5.2: Isoprene photooxidation in low NO_x: Mixing ratios of isoprene and oxidation products (HCHO, MVK&MACR, and methylglyoxal) were measured by PTR-TOF-MS and compared to simulated mixing ratios by the **MCM 3.2** degradation scheme (top panel). The model has been constrained to formaldehyde. Shaded areas depict the variability of the model results due to various simulations performed in the given uncertainty of HONO and NO_2 (detailed in Section 5.3). Total OH reactivity during oxidation in the chamber was measured via CRM, calculated from single compound measurements (PTR-TOF-MS) and modeled by the **MCM 3.2** (lower panel). Standard deviations of total OH reactivity mean values are given as error bars.

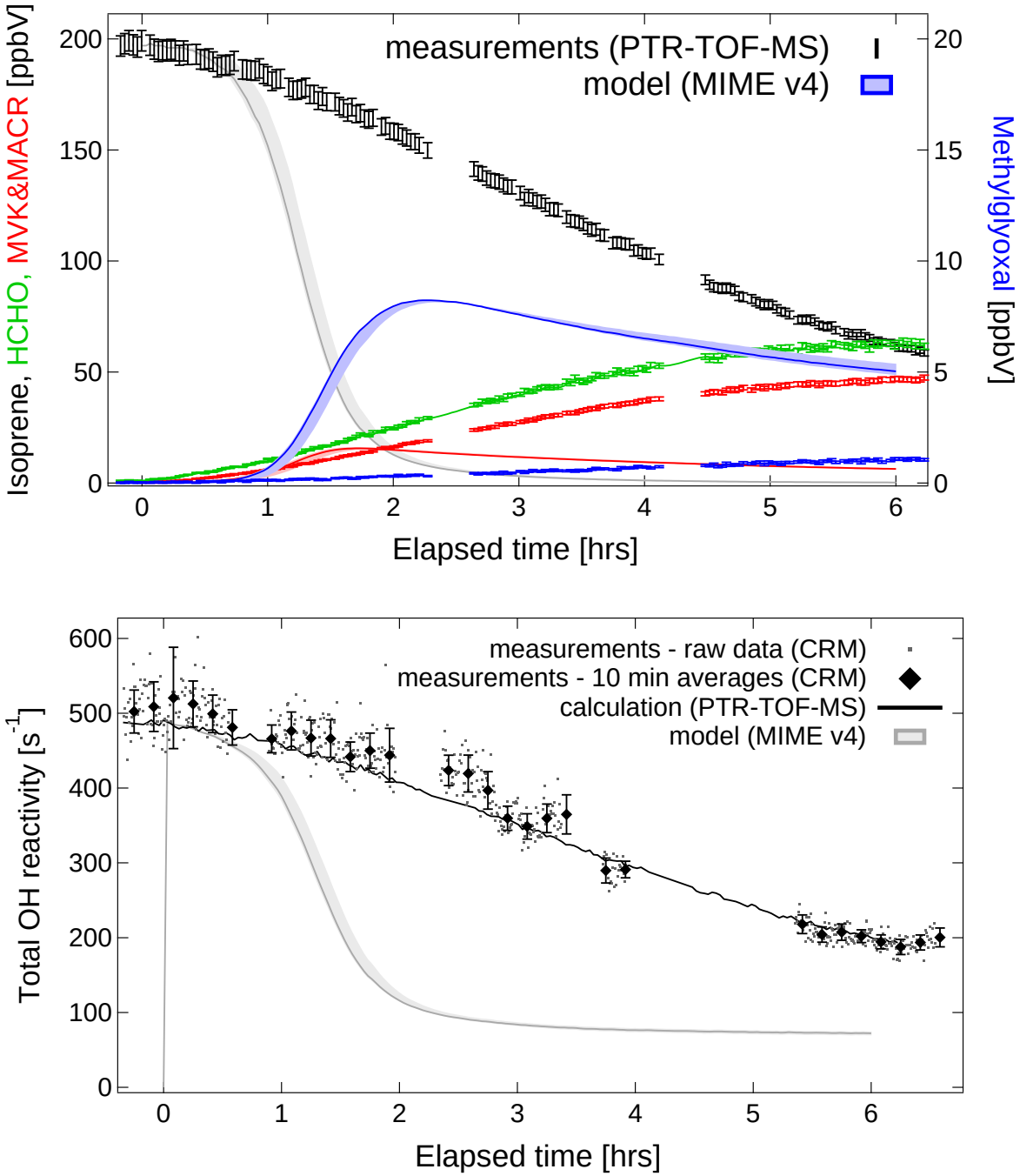

Fig. 5.3: PTR-TOF-MS (top panel) and CRM (lower panel) measurements were compared to the **MIMEv4** mechanism.

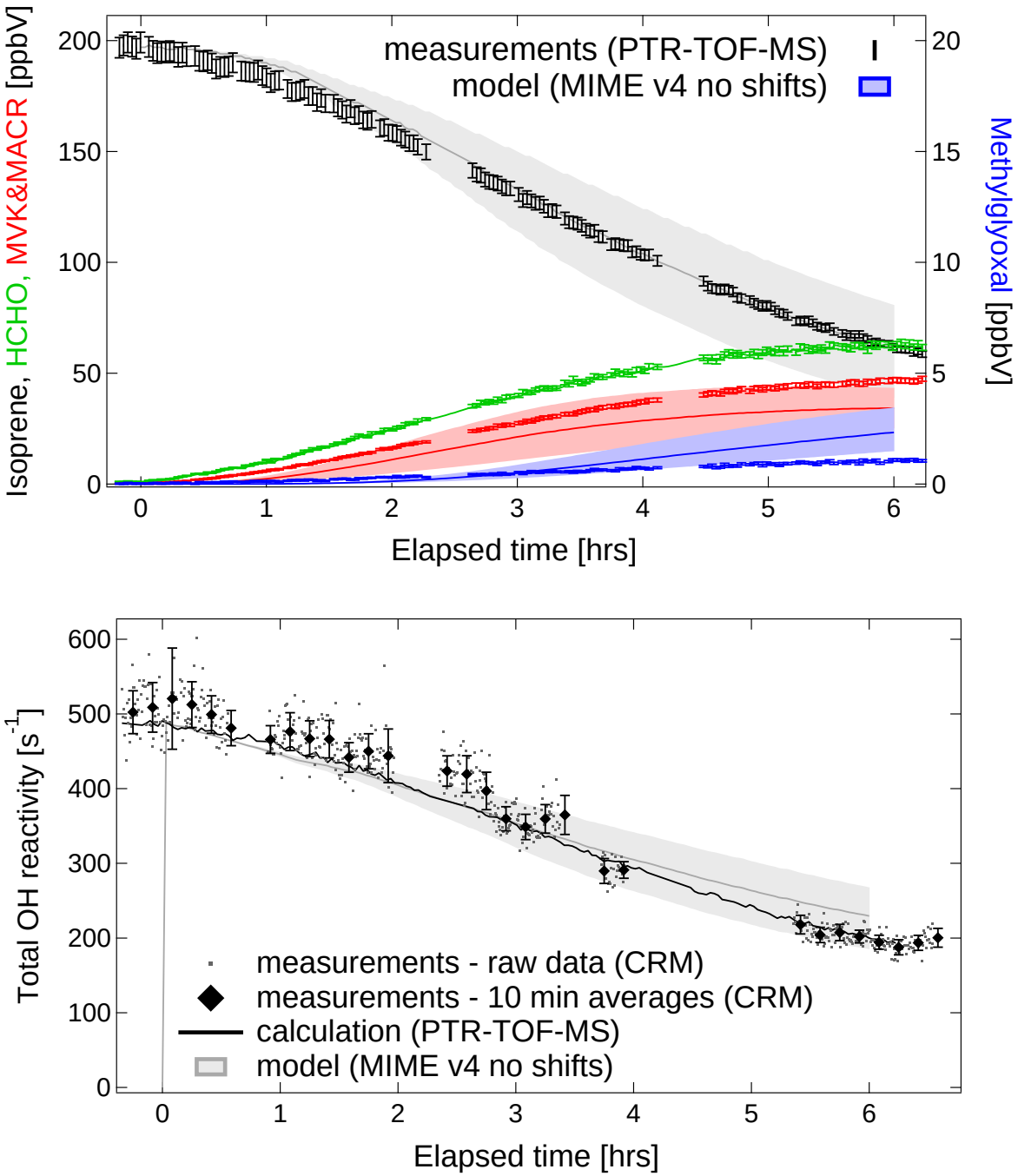

Fig. 5.4: PTR-TOF-MS (top panel) and CRM (lower panel) measurements were compared to a **modified MIMEv4*** mechanism. Parts of the novel isoprene chemistry were switched off: The 1,5 and 1,6 H-shifts were disabled in this model run.

5.4.3 Model comparison and evaluation via measurements

Figures 5.2–5.4 compare measured results with modeled predictions. Traditional isoprene chemistry (**MCM 3.2**), the recently proposed degradation scheme **MIMEv4**, and a modified version of MIMEv4 – **MIMEv4*** have been implemented in the photochemical box model MECCA.
Initialized with measured values of isoprene, the **MCM 3.2** reproduced the general trend of isoprene (Figure 5.2, top panel) and the measured total OH reactivity (Figure 5.2, lower panel). Shaded areas indicate the range of possible model results due to unavailable HONO and unspecific NO_2 measurements which have been used as "variable" input parameters for the model as was described in Section 5.3. Within this model "uncertainty", isoprene measurements and model agreed very well. About 96 % of the measured isoprene values fell into the shaded model area. When comparing the medium values of the model (solid line) with the measurements, both agreed for 43 % of all values within the error of the measured isoprene level.
MCM 3.2 and isoprene measurements had the largest discrepancies after ca. 35 min reaction time. In the first two hours isoprene was slightly overestimated by the model. This coincided with the time of products starting to build up in the chamber. While formaldehyde was forced in the model to match measurements, MVK&MACR and methylglyoxal were underestimated at the beginning of the experiment. At that time, total OH reactivity was slightly lower in the model results than measured. After 2 hours the model matched measured MVK&MACR within it's uncertainty. After 2.5 hours methylglyoxal was modeled at similar levels to those observed. Within the uncertainty of the model, this product of isoprene was predicted reasonably well. Final measured MVK&MACR could not be reached by the model and it was underestimated after 6 hours reaction time about 32 % when compared to medium model values. However, measured and calculated total OH reactivity agreed within the model "uncertainty" at the end of the experiment. After 6 hours reaction time, medium model values overestimated the measurement by about 24 %. Lowest possible model values just matched the measured total OH reactivity.
The extended isoprene degradation chemistry, implemented in **MIMEv4**, was modeled in similar fashion and compared to the measurements in Figure 5.3. Both, isoprene levels and total OH reactivity were significantly underestimated for most of the experiment (from ca. 1 hour elapsed time onwards). **MIMEv4** depleted isoprene very fast, so that after 2 hours reaction time only 6.5 % of the initial isoprene was simulated in the chamber and the model total OH reactivity was dominated by a multitude of secondary products. Modeled MVK&MACR and methylglyoxal levels could neither reproduce the observed level nor the trend. Final levels of MVK&MACR were significantly underestimated by a factor of 7.8. Final detected methylglyoxal was overestimated by **MIMEv4** (by a factor of 5).

A modified version of MIMEv4 – **MIMEv4*** (details in Section 5.5.2) was used to generate the result presented in Figure 5.4. Parts of the new isoprene chemistry have been switched off, and a better agreement between model and measurement could be noted. These parts included additional OH formation during the isoprene degradation process due to isomerization through 1,5 and 1,6 H-shifts. Following modification, excellent agreement for isoprene occurred after 3 hours reaction time. Similarly to **MCM 3.2** results, 96 % of the measured isoprene values were within the model "uncertainty", the shaded area. 93 % agreement between model medium values and measurement was found within the error of the PTR-TOF-MS, which is an improvement compared to the **MCM 3.2** results. Generally, modeled MVK&MACR levels tended to underestimate the measurements. MVK&MACR levels were slightly elevated in **MIMEv4***, compared to MCM 3.2, closing the gap to the measured values. Interestingly, **MIMEv4*** total OH reactivity results showed a better match to the observations than MCM 3.2 results. Final measured values were within the uncertainty of the model, which slightly overestimated the measured total OH reactivity by 14 % (compared to medium model values).

5.5 Discussion

5.5.1 Chamber observations of total OH reactivity

During CHEERS 2011, the measurement of isoprene and its major secondary products via PTR-TOF-MS could explain the entire measured total OH reactivity within the experimental uncertainty. The presented experiment was conducted in low NO_x and high isoprene conditions. This is in contrast to the majority of chamber experiments, in which high NO_x mixing ratios have been used. Dominant for total OH reactivity throughout the 6 hour reaction was isoprene. Less than 25 % of the final total OH reactivity was caused by oxidation products, out of which MVK&MACR were the most important compounds. This finding can be compared to recently reported total OH reactivity measurements from isoprene oxidation in high NO_x. Nakashima et al. (2012) used LIF based total OH reactivity measurements and FT-IR (Fourier Transform Infrared Spectroscopy) results, and found a fraction of almost 40 % missing OH reactivity. The gap between measurement and calculation increased in the course of the reaction at different rates. Initially, during the first hour of reaction, the reported missing total OH reactivity increased rapidly (although being within the error of the measurement) when isoprene and NO were present at very high levels. Afterwards, for the rest of the photooxidation, missing OH reactivity stayed rather constant.
The authors argue, that different products form and contribute to this missing OH reactivity in the presence of high and low NO. This is in agreement with the results presented here, which did not observe missing OH reactivity in low NO_x conditions.

It seems that the different composition of isoprene oxidation products in the presence of NO induced missing OH reactivity, since many nitrate-compounds were not measured during the experiment. Interestingly, Nakashima et al. (2012)'s total OH reactivity measurements, which were conducted with a different analytical method than the CHEERS experiments (LIF based total OH reactivity measurements, Sadanaga et al., 2004), show similar variability as CRM measurements during the presented study. In contrast to model and calculations of total OH reactivity, the direct measurement of total OH reactivity had a finer structure, indicating the high sensitivity of this observable in the course of the reaction.
These two isoprene oxidation studies, Nakashima et al. (2012) in high NO_x and CHEERS 2011 in low NO_x, are the first experiments using the total OH reactivity measurement for evaluation and comparison of known products and reaction mechanisms.

5.5.2 Details of the model isoprene photooxidation mechanisms

While measured and calculated total OH reactivity agreed well, the comparison of model and measurements revealed large discrepancies between the applied model degradation schemes. The isoprene oxidation scheme implemented in the MCM 3.2, showed good agreement to the observations. The novel chemistry in MIMEv4 failed for the presented study, whereas the modified MIMEv4* degradation mechanism was in excellent agreement with the measurements. The principle idea and a detailed schematic of both basic mechanisms (MCM 3.2 and MIMEv4) is presented in Figure 5.5.
MIMEv4 and MCM describe the initial isoprene reaction with OH similarly. The hydroxyl radical adds to the two double bonds of isoprene, in MCM on position 1 and 4, and in MIMEv4 also on position 2 and 3. Oxygen subsequently reacts with the adduct to form six peroxy radicals. According to Peeters et al. (2009) this reaction can be easily reversed, which is part of the novel isoprene chemistry and included in MIMEv4. Assuming low NO_x, further reactions of the peroxy radical involve mainly HO_2 and other peroxy radicals (RO_2). Typical products, that are present in both mechanisms are HCHO, MVK, MACR, acetaldehyde, methylglyoxal, glyoxal and other carbonyls. Major products have been measured in this study, and have been used to evaluate the model mechanism.
Additionally included in MIMEv4 is the isomerization of four of the peroxy radicals, namely the 1,5 and 1,6 H-shifts. While the 1,5 H-shift is thought to immediately generate HCHO, MVK, MACR and OH, the 1,6 H-shift should produce HO_2 and HPALDs, which are unsaturated hydroxyperoxide-aldehydes.

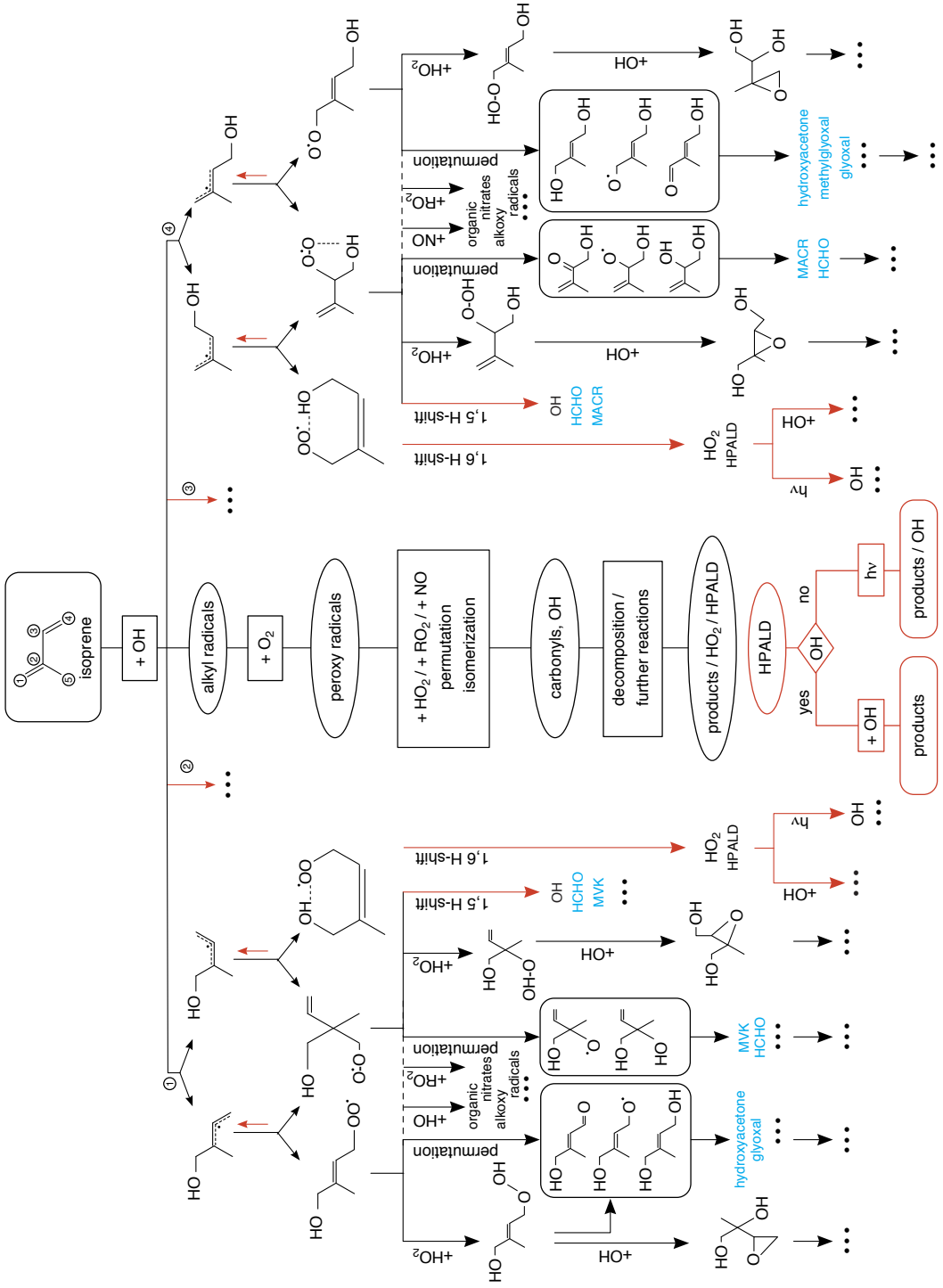

Fig. 5.5: Schematic isoprene-OH oxidation scheme as implemented in MCM 3.2 and MIMEv4. The traditional isoprene chemistry (MCM 3.2) includes the addition of OH to the two double bonds on position 1 and 4, subsequential reactions with oxygen and HO_2, RO_2, NO or permutations. This mechanism is pictured in **black**. Additional for the MIMEv4 mechanism (in **red**) OH addition to positions 2 and 3 is allowed as well as the back-reaction with O_2, and 1,5 and 1,6 H-shifts. Through these additional reaction paths, OH can be recycled. In **blue** typical measured products are highlighted. Recently also the epoxides have been detected by Paulot et al. (2009).

As presented in Taraborrelli et al. (2012), HPALDs may buffer the tropic isoprene-OH-chemistry. Therefore, implemented in the isoprene degradation scheme of MIMEv4 are two reaction paths: Depending on ambient OH levels, HPALDs either are oxidized by OH , or they form OH through photolysis (Peeters et al., 2009, Wolfe et al., 2010). MIMEv4 explicitly treats all reaction paths to undergo further reaction including 1,5 and 1,6 H-shifts. Many of the applied rate coefficients or energy barriers for H-shifts have been calculated computationally (e.g. in Kuwata et al., 2007, Peeters et al., 2009). Experimental evidence for HPALDs, recently reported by Crounse et al. (2011) found substantially slower rates for the 1,6 H-shift than assumed in the model mechanisms albeit with a high uncertainty (about 50 %) within their measurements. Chemical products have been studied in low NO_x by Paulot et al. (2009), who was able to detect isprene-epoxides.

According to these modifications MIMEv4 has additional, chemical OH sources. These additional OH sources in MIMEv4 are visible in Figure 5.3. High OH levels, build up quickly in the modeled chamber, and rapidly destroy isoprene and later the isoprene oxidation products. Compared to the MCM 3.2, MIMEv4 generated OH levels were about an order of magnitude higher and reached maximum values ahead of the peak in radiation (which typically was observed at 3 hours reaction time). However, in Figure 5.4 the result of MIMEv4* showed excellent agreement to the measured results. In this isoprene degradation scheme, the additional isomerization processes were crucially switched off. No 1,5 and 1,6 H-shifts were allowed to recycle additional OH. As a result OH levels in MIMEv4* showed similar, slightly elevated OH profiles to the MCM 3.2 output, and isoprene and total OH reactivity could be well simulated.

The novel isoprene mechanism MIMEv4 generated too high OH levels via the 1,5 and 1,6 H-shifts and subsequent chemistry. Possibly, in the absence of available rate measurements, the rates for the isomerization steps have been estimated too high. Since these isomerizations occur several times in the course of the degradation scheme, they add to each other, and form unrealistically high OH.

From the mismatch of the final MVK&MACR levels in all tested mechanisms it seems that already the initial yield and branching ratios were described incorrectly in the model. The model has been constrained to formaldehyde measurements made by PTR-TOF-MS. Since the proton affinity of formaldehyde is close to that of water, humidity may cause non-linearity which has to be taken account via accurate calibrations in humid conditions. During CHEERS 2011, measurements were well calibrated using a permeation source, and conducted in low relative humidity. Nevertheless, simultaneous FT-IR measurements showed slightly lower values (about 10 %), which could result in slightly lower OH levels, hence possibly higher final MVK&MACR mixing ratios. In contrast to this, isoprene and methylglyoxal were simulated correctly by the MCM 3.2 with the given (PTR-TOF-MS measured) HCHO level.

5.5.3 Chamber challenges

Reaction chambers are a highly valuable tool to examine atmospheric relevant processes in a controlled environment. Still, they are not a perfect facsimile of the atmosphere and several side-effects occur.

- Walls release and absorb substances that cause an undefined background which was characterized by the help of a background experiment (CHEERS 4). However, the interaction between wall-released compounds and studied species remained unknown.
- This study made use of the known release of HONO from the walls for OH generation. Due to instrumental failure, HONO was only poorly characterized within the set of available instruments which leaves the production term of OH somewhat uncertain. Also, due to the photolysis of HONO, NO increased in the course of the day, which changed the oxidation conditions gradually with time.
- Due to high isoprene and relatively low OH levels, the oxidation process examined in this study led to only a 70 % destruction of the initial isoprene. In the given time, no full degradation of isoprene and it's products was possible. In order to explore the chemistry further down the oxidation path, smaller initial concentrations should be used.
- Experimental errors, unavailable calibration compounds, and the lack of several measurements limited the achievements of this study.

Also, applying a model to atmospheric conditions is very different from using it in the chamber.

- The model was initialized with measured parameters. Therefore measurement uncertainties and detection limits had to be taken into account. The model adapted to the inaccurate and unavailable measurements, and hence showed a great spread of possible results.
- Constraining the model to measured values such as formaldehyde, should improve the modeled MVK&MACR. This major product was still poorly reproduced by the model under these conditions.
- Problems might occur due to the use of a global model in a chamber. MIME is thought to simulate atmospheric processes on a global scale, whereas the MCM has already been compared and evaluated with several chamber experiments, e.g. (Pinho et al., 2005).

The ideal chamber experiment for examining isoprene photooxidation needs to combine highly sensitive and comprehensive instrumental equipment with the needs of the model. The chamber should be well characterized, and initial concentration levels set to perform a complete degradation. Accurate measurements of key parameters such

as NO, NO_2, ozone, HONO, OH, important VOCs, known products, and total OH reactivity can complete the overall picture, and generate a data-set which might be compared extensively to the model.

5.6 Summary

Total OH reactivity measurements showed that in this study all important contributors were monitored and could account for it throughout the oxidation process. The isoprene degradation scheme MCM 3.2 was able to simulate isoprene and total OH reactivity reasonably well. Discrepancies occurred for the major products MVK and MACR under these low NO_x conditions.
A novel isoprene oxidation scheme, included in MIMEv4, was not appropriate to simulate this chamber experiment. Modeled OH levels were too high, hence the isoprene oxidation in the model was too fast compared to the measurements. When the 1,5 and 1,6 H-shifts were switched off, which are responsible for most of the additional OH formation, excellent agreement between model and measurement was found for isoprene and total OH reactivity. By disabling additional OH generation through isomerization one important mechanism in the novel isoprene-chemistry is crucially switched off. Remaining difference to the MCM 3.2 isoprene mechanism is a more detailed treatment of many reactions of isoprene and it's secondary products. For example in the MIMEv4 isoprene chemistry, initial OH addition is also allowed on position 2 and 3. Reverse reactions between alkyl and peroxy radicals involving oxygen are implemented as well as the explicit degradation of all important isoprene products. Latest knowledge about reaction rate coefficients has been used and theoretical assumptions applied if necessary. The modifications for MIMEv4 used in this study do not attempt to propose a new isoprene oxidation mechanism, e.g. without the isomerization reactions. It just has to be noted, that the original MIMEv4 could not reproduce the conducted experiment during CHEERS 2011. Possible reasons need to be elucidated in future studies.
Thus, this first CHEERS study emphasizes the need for future investigations on isoprene photooxidation. It is essential in order to understand, explain and simulate atmospheric chemical processes involving the most important oxidant OH and isoprene with low NO_x in an atmospheric hotspot, the tropics. Furthermore, this study could highlight the use of total OH reactivity as a diagnostic tool for oxidation schemes.

Acknowledgements

We are grateful for the technical and logistical support by the EUPHORE team and Thomas Klüpfel. This European project was funded by EUROCHAMP-2 Transnational Access Activities.

6

Conclusions - Total OH reactivity: an atmospheric cocktail

The puzzle of high missing OH reactivity in forests remains. Through this thesis it became obvious that total OH reactivity at the biosphere-atmosphere interface is a highly variable parameter which depends on a diversity of influences.
The measurements of total OH reactivity in the summertime boreal forest at two different heights showed this is great detail. Meteorological conditions impacted the atmospheric total OH reactivity as well as stress factors for vegetation, local emissions, transportation of long-lived pollutants, and atmospheric photooxidation processes. According to these observations, the high unexplained fraction in forested environments is a cocktail of contributing compounds of various origins. The comparison of in and above canopy total OH reactivity measurements gave evidence for both, strong impact of direct biogenic emissions (particularly during periods of elevated temperature) and the contribution of transported pollutants or secondary products.
The direct measurement of TOHRE, the total OH reactivity emission flux, from a Norway spruce branch, confirmed that especially during summer, high temperatures and stress, unexplained OH sink compounds are released into the atmosphere. In this study, the PTR-MS measured compounds, including major known biogenic emissions such as isoprene, monoterpenes and sesquiterpenes, could not account for the total OH reactivity emission flux, especially in summertime. At that time, TOHRE compared well to the estimated total ozone loss rate inside the cuvette, and differed from the temperature-only dependent emission algorithm. This gave evidence for the daytime production and emission of highly reactive, as yet undetected (via PTR-MS) compounds. The large emission of unmeasured and potentially unknown biogenic VOCs, induces an even greater amount of undetected secondary products which also likely contribute to the atmospheric total OH reactivity measurement.
For many biogenic compounds, the photooxidation products are less reactive than the primary emission itself. Isoprene products, from OH-initiated oxidation, for example do not contribute as strong to the total OH reactivity as isoprene itself. Hence, as expected during the observation of the controlled isoprene photooxidation experiment, isoprene dominated the monitored total OH reactivity and accounted in sum with

the products MVK, MACR and HCHO to the entire measured total OH reactivity throughout the oxidation process. Significant disagreement was found for the modeled total OH reactivity when implementing the novel isoprene chemistry MIMEv4, which regenerates OH during isoprene degradation. By disabling the strongest chemical OH source, the H-shifts, excellent agreement with the measurements of isoprene and total OH reactivity could be found, similar to the results of the traditional isoprene mechanism MCM 3.2. The implementation of new theoretical findings into the isoprene oxidation mechanism, such as additional OH sources, was motivated by recent field studies in the tropics. Higher OH concentrations than predicted by the model (using e.g. MCM chemistry) were observed in the isoprene-rich environment. It needs to be further investigated whether these disagreements are due to experimental problems or uncertainties in the atmospheric models.

A "perfect" chamber experiment could provide elusive results for the isoprene oxidation. Especially for low NO_x conditions studies are rare and results wanted to compare to natural environments. Therefore, accurate detection of reactants, oxidant source compounds, oxidants, background species, and products are required. Total OH reactivity measurements are a beneficial add-on to evaluate model results, the OH sink budget, and also the atmospheric relevance of individual species.

To determine the close coupling of biosphere-atmosphere interaction a huge diversity has to be taken into account. Field studies, as conducted during this thesis e.g. examining the atmosphere in forested environments or biogenic emissions using enclosing systems, are hence needed for various ecosystems, seasons and plant species. One key-region for atmospheric chemistry are the tropics. To date measurements of total OH reactivity from this ecosystem are sparse, so that a detailed study of total OH reactivity in the tropical forest is desirable.

Not only the comparison of total OH reactivity to individual compounds, also the flux of total OH reactivity e.g. above a forest can by a valuable parameter to determine in order to examine the emission strength of OH sink compounds, deposition rates and timescales of photochemical processes. With this, the boundary layer dynamics in close coupling to atmospheric chemistry between the biosphere and the atmosphere could be characterized. Practically, the total OH reactivity instrument could be installed for gradient measurements e.g. on a forest tower or on a platform such as an airplane or a zeppelin. Since, the CRM is an easily convertible and adaptable method to measure the total OH reactivity, these various applications can be possibly accomplished in the near future.

References

Altimir, N., Vesala, T., Keronen, P., Kulmala, M., and Hari, P.: Methodology for direct field measurements of ozone flux to foliage with shoot chambers, Atmos. Environ., 36, 19 – 29, doi:10.1016/S1352-2310(01)00478-2, 2002.

Atkinson, R. and Arey, J.: Atmospheric Degradation of Volatile Organic Compounds, Chem. Rev., 103, 4605–4638, doi:10.1021/cr0206420, 2003.

Bäck, J., Aalto, J., Kolari, P., Hari, P., and Kulmala, M.: Contribution of developing foliage to canopy emissions of volatile organic compounds, Atmos. Chem. Phys., in preparation, 2012.

Bamberger, I., Hörtnagl, L., Ruuskanen, T. M., Schnitzhofer, R., Müller, M., Graus, M., Karl, T., Wohlfahrt, G., and Hansel, A.: Deposition fluxes of terpenes over grassland, 116, 0148 – 0227, doi:10.1029/2010JD015457, 2011.

Blake, R. S., Monks, P. S., and Ellis, A. M.: Proton-Transfer Reaction Mass Spectrometry, Chem. Rev., 109, 861 – 896, doi:10.1021/cr800364q, 2009.

Bloss, C., Wagner, V., Bonzanini, A., Jenkin, M. E., Wirtz, K., Martin-Reviejo, M., and Pilling, M. J.: Evaluation of detailed aromatic mechanisms (MCMv3 and MCMv3.1) against environmental chamber data, Atmos. Chem. Phys., 5, 623–639, doi:10.5194/acp-5-623-2005, URL http://www.atmos-chem-phys.net/5/623/2005/, 2005.

Bonan, G. B.: Forests and Climate Change: Forcings, Feedbacks, and the Climate Benefits of Forests, Science, 320, 1444–1449, doi:10.1126/science.1155121, 2008.

Bourtsoukidis, E., Bonn, B., Dittmann, A., Hakola, H., Hellén, H., and Jacobi, S.: Ozone stress as a driving force of sesquiterpene emissions: a suggested parameterization, Biogeosciences Discussions, 9, 7661–7700, doi:10.5194/bgd-9-7661-2012, 2012.

Butler, T., Lawrence, M., Taraborrelli, D., and Lelieveld, J.: Multi-day ozone pro-

duction potential of volatile organic compounds calculated with a tagging approach, Atmos. Environ., 45, 4082 – 4090, doi:DOI:10.1016/j.atmosenv.2011.03.040, URL http://www.sciencedirect.com/science/article/pii/S1352231011003001, 2011.

Butler, T. M., Taraborrelli, D., Brühl, C., Fischer, H., Harder, H., Martinez, M., Williams, J., Lawrence, M. G., and Lelieveld, J.: Improved simulation of isoprene oxidation chemistry with the ECHAM5/MESSy chemistry-climate model: lessons from the GABRIEL airborne field campaign, Atmospheric Chemistry and Physics, 8, 4529–4546, doi:10.5194/acp-8-4529-2008, 2008.

Calogirou, A., Jensen, N. R., Nielsen, C. J., Kotzias, D., and Hjorth, J.: Gas-Phase Reactions of Nopinone, 3-Isopropenyl-6-oxo-heptanal, and 5-Methyl-5-vinyltetrahydrofuran-2-ol with OH, NO3, and Ozone, Environ. Scien. Techn., 33, 453–460, doi:10.1021/es980530j, 1999.

Calpini, B., Jeanneret, F., Bourqui, M., Clappier, A., Vajtai, R., and van den Bergh, H.: Direct measurement of the total reaction rate of OH in the atmosphere, Analusis, 27, 328, doi:10.1051/analusis:1999270328, 1999.

Carter, W., , Carter, N. W. P. L., and Atkinson, R.: Development and Evaluation of a Detailed Mechanism for the Atmospheric Reactions of Isoprene and NO, 1996.

Cazorla, M., Brune, W. H., Ren, X., and Lefer, B.: Direct measurement of ozone production rates in Houston in 2009 and comparison with two estimation methods, Atmos. Chem. Phys., 12, 1203–1212, doi:10.5194/acp-12-1203-2012, 2012.

Cojocariu, C., Kreuzwieser, J., and Rennenberg, H.: Correlation of short-chained carbonyls emitted from Picea abies with physiological and environmental parameters, New Phytologist, 162, 717–727, doi:10.1111/j.1469-8137.2004.01061.x, 2004.

Crounse, J. D., Paulot, F., Kjaergaard, H. G., and Wennberg, P. O.: Peroxy radical isomerization in the oxidation of isoprene, Phys. Chem. Chem. Phys., 13, 13 607–13 613, doi:10.1039/C1CP21330J, 2011.

Cruz, G., Morales, J., and Olayo, R.: Films obtained by plasma polymerization of pyrrole, Thin Solid Films, 342, 119 – 126, doi:10.1016/S0040-6090(98)01450-3, 1999.

Davis, M. E., Talukdar, R. K., Notte, G., Ellison, G. B., and Burkholder, J. B.: Rate Coefficients for the OH + Pinonaldehyde (C10H16O2) Reaction between 297 and 374 K, Environ. Scien. Techn., 41, 3959–3965, doi:10.1021/es070048d, 2007.

de Gouw, J., Warneke, C., Holzinger, R., Kluepfel, T., and Williams, J.: Intercomparison between airborne measurements of methanol, acetonitrile and acetone using two differently configured PTR-MS instruments, Int. J. of Mass Spectrom.,

239, 129 – 137, doi:10.1016/j.ijms.2004.07.025, 2004.

Derwent, R., Jenkin, M., and Saunders, S.: Photochemical ozone creation potentials for a large number of reactive hydrocarbons under European conditions, Atmospheric Environment, 30, 181 – 199, doi:10.1016/1352-2310(95)00303-G, 1996.

Di Carlo, P., Brune, W. H., Martinez, M., Harder, H., Lesher, R., Ren, X., Thornberry, T., Carroll, M. A., Young, V., Shepson, P. B., Riemer, D., Apel, E., and Campbell, C.: Missing OH Reactivity in a Forest: Evidence for Unknown Reactive Biogenic VOCs, Science, 304, 722 – 725, doi:10.1126/science.1094392, 2004.

Dillon, T., Tucceri, M., Dulitz, K., Horowitz, A., Vereecken, L., and Crowley, J.: Reaction of Hydroxyl Radicals with C4H5N (Pyrrole): Temperature and Pressure Dependent Rate Coefficients, doi:10.1021/jp211241x, 2012.

Dolgorouky, C., Gros, V., Sarda-Esteve, R., Sinha, V., Williams, J., Marchand, N., Sauvage, S., Poulain, L., Sciare, J., and Bonsang, B.: Total OH reactivity measurements in Paris during the 2010 MEGAPOLI winter campaign, Atmospheric Chemistry and Physics Discussions, 12, 10 937 – 10 994, doi:10.5194/acpd-12-10937-2012, URL http://www.atmos-chem-phys-discuss.net/12/10937/2012/, 2012.

Dudareva, N., Pichersky, E., and Gershenzon, J.: Biochemistry of Plant Volatiles, Plant Physiology, 135, 1893–1902, doi:http:/âĂŃ/âĂŃdx.âĂŃdoi.âĂŃorg/âĂŃ10.âĂŃ1104/âĂŃpp.âĂŃ104.âĂŃ049981, 2004.

Dudareva, N., Negre, F., Nagegowda, D. A., and Orlova, I.: Plant Volatiles: Recent Advances and Future Perspectives, Critical Reviews in Plant Sciences, 25, 417–440, doi:10.1080/07352680600899973, 2006.

Eerdekens, G., Ganzeveld, L., Vilà-Guerau de Arellano, J., Klüpfel, T., Sinha, V., Yassaa, N., Williams, J., Harder, H., Kubistin, D., Martinez, M., and Lelieveld, J.: Flux estimates of isoprene, methanol and acetone from airborne PTR-MS measurements over the tropical rainforest during the GABRIEL 2005 campaign, Atmospheric Chemistry and Physics, 9, 4207–4227, doi:10.5194/acp-9-4207-2009, 2009a.

Eerdekens, G., Yassaa, N., Sinha, V., Aalto, P. P., Aufmhoff, H., Arnold, F., Fiedler, V., Kulmala, M., and Williams, J.: VOC measurements within a boreal forest during spring 2005: on the occurrence of elevated monoterpene concentrations during night time intense particle concentration events, Atmos. Chem. Phys., 9, 8331–8350, doi:10.5194/acp-9-8331-2009, 2009b.

FAO: Global forest resources assessment, Food and Agriculture Organisation, Forestry paper, 163, 2010.

Fehsenfeld, F., Calvert, J., Fall, R., Goldan, P., Guenther, A., Hewitt, C., Lamb, B., Liu, S., Trainer, M., Westberg, H., and Zimmerman, P.: Emissions of volatile organic compounds from vegetation and the implications for atmospheric chemistry, Global Biogeochem. Cycles, 6, 389–430, doi:10.1029/92GB02125, 1992.

Filella, I., Wilkinson, M. J., Llusia, J., Hewitt, C. N., and Penuelas, J.: Volatile organic compounds emissions in Norway spruce (Picea abies) in response to temperature changes, Physiologia Plantarum, 130, 58–66, doi:10.1111/j.1399-3054.2007.00881.x, 2007.

Finlayson-Pitts, B. and Pitts, J.: Atmospheric Chemistry: Fundamental and experimental techniques, John Wiley & Sons, 1986.

Fortner, E. C., Zheng, J., Zhang, R., Berk Knighton, W., Volkamer, R. M., Sheehy, P., Molina, L., and André, M.: Measurements of Volatile Organic Compounds Using Proton Transfer Reaction-Mass Spectrometry during the MILAGRO 2006 Campaign, Atmos. Chem. Phys., 9, 467–481, doi:10.5194/acp-9-467-2009, 2009.

Geiger, H., Barnes, I., Bejan, I., Benter, T., and Spittler, M.: The tropospheric degradation of isoprene: an updated module for the regional atmospheric chemistry mechanism, Atmospheric Environment, 37, 1503–1519, doi:10.1016/S1352-2310(02)01047-6, 2003.

Ghirardo, A., Koch, K., Taipale, R., Zimmer, I., Schnitzler, J.-P., and Rinne, J.: Determination of de novo and pool emissions of terpenes from four common boreal/alpine trees by 13CO2 labelling and PTR-MS analysis, Plant Cell Environ., 33, 781–792, doi:10.1111/j.1365-3040.2009.02104.x, 2010.

Goldstein, A. H. and Galbally, I. E.: Known and Unexplored Organic Constituents in the Earth's Atmosphere, Environ. Scien. Techn., 41, 1514–1521, doi:10.1021/es072476p, 2007.

Grabmer, W., Kreuzwieser, J., Wisthaler, A., Cojocariu, C., Graus, M., Rennenberg, H., Steigner, D., Steinbrecher, R., and Hansel, A.: VOC emissions from Norway spruce (Picea abies L. [Karst]) twigs in the field – Results of a dynamic enclosure study, Atmos. Environ., 40, Supplement 1, 128–137, doi:10.1016/j.atmosenv.2006.03.043, 2006.

Guenther, A., Zimmermann, P., Harley, P., Monson, R., and Fall, R.: Isoprene and Monoterpene Emission Rate Variability: Model Evaluations and Sensitivity Analyses, J. Geophys. Res., 98, 12,609–12,617, 1993.

Guenther, A., Hewitt, C., Erickson, D., Fall, R., Geron, C., Graedel, T., Harley, P., Klinger, L., Lerdau, M., Mckay, W., Pierce, T., Scholes, B., Steinbrecher, R., Tal-

lamraju, R., Taylor, J., and Zimmermann, P.: A global model of natural volatile organic compound emissions, J. Geophys. Res., 100, 8873–8892, 1995.

Guenther, A., Karl, T., Harley, P., Wiedinmyer, C., Palmer, P., and Geron, C.: Estimates of global terrestrial isoprene emissions using MEGAN (Model of Emissions of Gases and Aerosols from Nature), Atmos. Chem. Phys., 6, 3181–3210, 2006.

Guenther, A. B., Jiang, X., Heald, C. L., Sakulyanontvittaya, T., Duhl, T., Emmons, L. K., and Wang, X.: The Model of Emissions of Gases and Aerosols from Nature version 2.1 (MEGAN2.1): an extended and updated framework for modeling biogenic emissions, Geoscientific Model Development Discussions, 5, 1503–1560, doi:10.5194/gmdd-5-1503-2012, URL http://www.geosci-model-dev-discuss.net/5/1503/2012/, 2012.

Haagen-Smit, A.: Chemistry and Physiology of Los Angeles Smog, Ind. Eng. Chem., 44, 13 425–1346, 1953.

Haase, K. B., Jordan, C., Mentis, E., Cottrell, L., Mayne, H. R., Talbot, R., and Sive, B. C.: Changes in monoterpene mixing ratios during summer storms in rural New Hampshire (USA), Atm. Chem. Phys., 11, 11 465–11 476, doi:10.5194/acp-11-11465-2011, 2011.

Heard, D. E. and Pilling, M. J.: Measurement of OH and HO2 in the Troposphere, Chemical Reviews, 103, 5163–5198, doi:10.1021/cr020522s, 2003.

Heiden, A. C., Kobel, K., Komenda, M., Koppmann, R., Shao, M., and Wildt, J.: Toluene emissions from plants, Geophys. Res. Lett., 26, 1283–1286, doi:10.1029/1999GL900220, 1999.

Hewitt, C., Langford, B., Possell, M., Karl, T., and Owen, S.: Quantification of VOC emission rates from the biosphere, Trends Anal. Chem., 30, 937 – 944, doi:10.1016/j.trac.2011.03.008, 2011.

Hites, R. A. and Turner, A. M.: Rate constants for the gas-phase β-myrcene + OH and isoprene + OH reactions as a function of temperature, Int. J. Chem. Kinet., 41, 407–413, doi:10.1002/kin.20413, 2009.

Hoffmann, T., Odum, J., Bowman, F., Collins, D., Klockow, D., Flagan, R., and Seinfeld, J. H.: Formation of Organic Aerosols from the Oxidation of Biogenic Hydrocarbons, Journal of Atmospheric Chemistry, 26, 189–222, 10.1023/A:1005734301837, 1997.

Hofzumahaus, A., Rohrer, F., Lu, K., Bohn, B., Brauers, T., Chang, C.-C., Fuchs, H., Holland, F., Kita, K., Kondo, Y., Li, X., Lou, S., Shao, M., Zeng, L., Wahner,

A., and Zhang, Y.: Amplified Trace Gas Removal in the Troposphere, Science, 324, 1702–1704, doi:10.1126/science.1164566, 2009.

Ingham, T., Goddard, A., Whalley, L. K., Furneaux, K. L., Edwards, P. M., Seal, C. P., Self, D. E., Johnson, G. P., Read, K. A., Lee, J. D., and Heard, D. E.: A flow-tube based laser-induced fluorescence instrument to measure OH reactivity in the troposphere, Atmos. Meas. Tech., 2, 465–477, doi:10.5194/amt-2-465-2009, 2009.

Jardine, K. J., Monson, R. K., Abrell, L., Saleska, S. R., Arneth, A., Jardine, A., Ishida, F. Y., Serrano, A. M. Y., Artaxo, P., Karl, T., Fares, S., Goldstein, A., Loreto, F., and Huxman, T.: Within-plant isoprene oxidation confirmed by direct emissions of oxidation products methyl vinyl ketone and methacrolein, Global Change Biology, 18, doi:10.1111/j.1365-2486.2011.02610.x, 2012.

Jeanneret, F., Kirchner, F., Clappier, A., von den Bergh, H., and Calpini, B.: Total VOC reactivity in the planetary boundary layer 1. Estimation by a pump and probe OH experiment, J. Geophys. Res., 106, 3083–3093, 2001.

Jenkin, M. E., Saunders, S., and Pilling, M.: The tropospheric degradation of volatile organic compounds: a protocol for mechanism development, Atmos. Env., 31, 81 – 104, doi:10.1016/S1352-2310(96)00105-7, 1997.

Jordan, A., Haidacher, S., Hanel, G., Hartungen, E., Maerk, L., Seehauser, H., Schottkowsky, R., Sulzer, P., and Maerk, T.: A high resolution and high sensitivity proton-transfer-reaction time-of-flight mass spectrometer (PTR-TOF-MS), International Journal of Mass Spectrometry, 286, 122–128, doi:10.1016/j.ijms.2009.07.005, 2009.

Juuti, S., Arey, J., and Atkinson, R.: Monoterpene Emission Rate Measurements From a Monterey Pine, J. Geophys. Res., 7, 5883–5897, doi:10.5194/acp-7-5883-2007, 1990.

Kanakidou, M., Seinfeld, J. H., Pandis, S. N., Barnes, I., Dentener, F. J., Facchini, M. C., Van Dingenen, R., Ervens, B., Nenes, A., Nielsen, C. J., Swietlicki, E., Putaud, J. P., Balkanski, Y., Fuzzi, S., Horth, J., Moortgat, G. K., Winterhalter, R., Myhre, C. E. L., Tsigaridis, K., Vignati, E., Stephanou, E. G., and Wilson, J.: Organic aerosol and global climate modelling: a review, Atmos. Chem. Phys., 5, 1053–1123, doi:10.5194/acp-5-1053-2005, 2005.

Kang, E., Root, M. J., Toohey, D. W., and Brune, W. H.: Introducing the concept of Potential Aerosol Mass (PAM), Atmos. Chem. Phys., 7, 5727–5744, doi:10.5194/acp-7-5727-2007, 2007.

Karl, M., Dorn, H.-P., Holland, F., Koppmann, R., Poppe, D., Rupp, L., Schaub, A.,

and Wahner, A.: Product study of the reaction of OH radicals with isoprene in the atmosphere simulation chamber SAPHIR, Journal of Atmospheric Chemistry, 55, 167–187, 10.1007/s10874-006-9034-x, 2006.

Karl, T., Guenther, A., Turnipseed, A., Tyndall, G., Artaxo, P., and Martin, S.: Rapid formation of isoprene photo-oxidation products observed in Amazonia, Atmos. Chem. Phys., 9, 7753–7767, doi:10.5194/acp-9-7753-2009, 2009.

Karl, T. G., Christian, T. J., Yokelson, R. J., Artaxo, P., Hao, W. M., and Guenther, A.: The Tropical Forest and Fire Emissions Experiment: method evaluation of volatile organic compound emissions measured by PTR-MS, FTIR, and GC from tropical biomass burning, Atmos. Chem. Phys., 7, 5883–5897, doi: 10.5194/acp-7-5883-2007, 2007.

Kato, S., Sato, T., and Kajii, Y.: A method to estimate the contribution of unidentified VOCs to OH reactivity, Atmos. Env., 45, 5531–5539, doi:10.1016/j.atmosenv.2011.05.074, 2011.

Kempf, K., Allwine, E., Westberg, H., Claiborn, C., and Lamb, B.: Hydrocarbon emissions from spruce species using environmental chamber and branch enclosure methods, Atmospheric Environment, 30, 1381–1389, doi:10.1016/1352-2310(95)00462-9, 1996.

Kesselmeier, J.: Exchange of Short-Chain Oxygenated Volatile Organic Compounds (VOCs) between Plants and the Atmosphere: A Compilation of Field and Laboratory Studies, Journal of Atmospheric Chemistry, 39, 219–233, 2001.

Kesselmeier, J. and Staudt, M.: Biogenic Volatile Organic Compounds (VOC): An Overview on Emission, Physiology and Ecology, J. Atmos. Chem., 33, 23–88, 10.1023/A:1006127516791, 1999.

Kesselmeier, J., Bode, K., Hofmann, U., Mueller, H., Schaefer, L., Wolf, A., Ciccioli, P., Brancaleoni, E., Cecinato, A., Frattoni, M., Foster, P., Ferrari, C., Jacob, V., Fugit, J., Dutaur, L., Simon, V., and Torres, L.: Emission of short chained organic acids, aldehydes and monoterpenes from Quercus ilex L. and Pinus pinea L. in relation to physiological activities, carbon budget and emission algorithms, Atmospheric Environment, 31, Supplement 1, 119 – 133, doi:10.1016/S1352-2310(97)00079-4, 1997.

Kim, S., Guenther, A., Karl, T., and Greenberg, J.: Contributions of primary and secondary biogenic VOC tototal OH reactivity during the CABINEX (Community Atmosphere-Biosphere INteractions Experiments)-09 field campaign, Atmos. Chem. Phys., 11, 8613–8623, doi:10.5194/acp-11-8613-2011, 2011.

Kleffmann, J., Gavriloaiei, T., Hofzumahaus, A., Holland, F., Koppmann, R., Rupp,

L., Schlosser, E., Siese, M., and Wahner, A.: Daytime formation of nitrous acid: A major source of OH radicals in a forest, Geophys. Res. Lett., 32, L05 818, doi: 10.1029/2005GL022524, 2005.

Kovacs, T. A. and Brune, W.: Total OH Loss Rate Measurement, J. Atmos. Chem., 39, 105–122, 2001.

Kulmala, M., Hienola, J., Pirjola, L., Vesala, T., Shimmo, M., Altimir, N., and Hari, P.: A model for NOx-O3-terpene chemistry in chamber measurements of plant gas exchange, Atmos. Environ., 33, 2145–2156, doi:10.1016/S1352-2310(99)00069-2, 1999.

Kurpius, M. and Goldstein, A.: Gas-phase chemistry dominates O3 loss to a forest, implying a source of aerosols and hydroxyl radicals to the atmosphere, Geophys. Res. Lett., 30, 0094–8276, doi:10.1029/2002GL016785, 2003.

Kuwata, K. T., Dibble, T. S., Sliz, E., and Petersen, E. B.: Computational Studies of Intramolecular Hydrogen Atom Transfers in the β-Hydroxyethylperoxy and β-Hydroxyethoxy Radicals, The Journal of Physical Chemistry A, 111, 5032–5042, doi:10.1021/jp0704113, 2007.

Kwok, E. S. and Atkinson, R.: Estimation of hydroxyl radical reaction rate constants for gas-phase organic compounds using a structure-reactivity relationship: An update, Atmospheric Environment, 29, 1685–1695, doi:10.1016/1352-2310(95)00069-B, 1995.

Lamb, B., Guenther, A., Gay, D., and Westberg, H.: A national inventory of biogenic hydrocarbon emissions, Atmospheric Environment (1967), 21, 1695–1705, doi:10.1016/0004-6981(87)90108-9, 1987.

Laothawornkitkul, J., Taylor, J., Paul, N., and Hewitt, C. N.: Biogenic volatile organic compounds in the Earth system, New Phytologist, 183, 27–51, doi:10.1111/j.1469-8137.2009.02859.x, 2009.

Lelieveld, J., Dentener, F. J., Peters, W., and Krol, M. C.: On the role of hydroxyl radicals in the self-cleansing capacity of the troposphere, Atmospheric Chemistry and Physics, 4, 2337–2344, doi:10.5194/acp-4-2337-2004, URL http://www.atmos-chem-phys.net/4/2337/2004/, 2004.

Lelieveld, J., Butler, T. M., Crowley, J. N., Dillon, T. J., Fischer, H., Ganzeveld, L., Harder, H., Lawrence, M. G., Martinez, M., Taraborrelli, D., and Williams, J.: Atmospheric oxidation capacity sustained by a tropical forest, Nature, 452, 737–740, 2008.

Lewis, A. C., Carslaw, N., Marriott, P. J., Kinghorn, R. M., Morrison, P., Lee, A. L.,

Bartle, K. D., and Pilling, M. J.: A larger pool of ozone-forming carbon compounds in urban atmospheres, Nature, 405, 778–781, doi:10.1038/35015540, 2000.

Lindinger, W., Hansel, A., and Jordan, A.: On-line monitoring of volatile organic compounds at pptv levels by means of Proton-Transfer-Reaction Mass Spectrometry (PTR-MS): Medical applications, food control and environmental research, Int. J. Mass Spect. and Ion Processes, 173, 191–241, doi:10.1016/S0168-1176(97)00281-4, 1998.

Logan, J., Prather, M., Wofsy, S., and McElroy, M.: Tropospheric chemistry: A global perspective, J. Geophys. Res, 86, 7210 – 7255, 1981.

Loreto, F. and Schnitzler, J.-P.: Abiotic stresses and induced BVOCs, Trends Plant Sci., 15, 154–166, doi:10.1016/j.tplants.2009.12.006, 2010.

Loreto, F., Mannozzi, M., Maris, C., Nascetti, P., Ferranti, F., and Pasqualini, S.: Ozone Quenching Properties of Isoprene and Its Antioxidant Role in Leaves, Plant Physiology, 126, 993–1000, doi:10.1104/pp.126.3.993, 2001.

Lou, S., Holland, F., Rohrer, F., Lu, K., Bohn, B., Brauers, T., Chang, C., Fuchs, H., Häseler, R., Kita, K., Kondo, Y., Li, X., Shao, M., Zeng, L., Wahner, A., Zhang, Y., Wang, W., and Hofzumahaus, A.: Atmospheric OH reactivities in the Pearl River Delta-China in summer 2006: measurement and model results, Atmos. Chem. Phys., 10, 11 243–11 260, doi:10.5194/acp-10-11243-2010, 2010.

Mahajan, a., Whalley, L., Kozlova, E., Oetjen, H., Mendez, L., Furneaux, K., Goddard, A., Heard, D., Plane, J., and Saiz-Lopez, A.: DOAS observations of formaldehyde and its impact on the HOx balance in the tropical Atlantic marine boundary layer, J. Atmos. Chem., 66, 167–178, doi:10.1007/s10874-011-9200-7, 2011.

Mao, J., Ren, X., Chen, S., Brune, W., Chen, Z., Martinez, M., Harder, H., Lefer, B., Rappenglück, B., Flynn, J., and Leuchner, M.: Atmospheric oxidation capacity in the summer of Houston 2006: Comparison with summer measurements in other metropolitan studies, Atm. Environ., pp. 1–9, doi:10.1016/j.atmosenv.2009.01.013, 2009.

Mao, J., Ren, X., Zhang, L., Van Duin, D. M., Cohen, R. C., Park, J.-H., Goldstein, A. H., Paulot, F., Beaver, M. R., Crounse, J. D., Wennberg, P. O., DiGangi, J. P., Henry, S. B., Keutsch, F. N., Park, C., Schade, G. W., Wolfe, G. M., Thornton, J. A., and Brune, W. H.: Insights into hydroxyl measurements and atmospheric oxidation in a California forest, Atmos. Chem. Phys., 12, 8009–8020, doi:10.5194/acp-12-8009-2012, 2012.

Martin, D. M., Gershenzon, J., and Bohlmann, J.: Induction of Volatile Terpene

Biosynthesis and Diurnal Emission by Methyl Jasmonate in Foliage of Norway Spruce, Plant Physiology, 132, 1586–1599, doi:10.1104/pp.103.021196, 2003.

Martinez, M., Harder, H., Kovacs, T., Simpas, J., Bassis, J., Lesher, R., Brune, W., Frost, G., Williams, E., Stroud, C., Jobson, B., Roberts, J., Hall, S., Shetter, R., Wert, B., Fired, A., Alicke, B., Stutz, J., Young, V., White, A., and Zamora, R.: OH and HO2 concentrations, sources, and loss rates during the Southern Oxidants Study in Nashville, Tennessee, summer 1999, J. Geophys. Res., 108, 4617, doi:10.1029/2003JD003551, 2003.

Mogensen, D., Smolander, S., Sogachev, A., Zhou, L., Sinha, V., Guenther, A., Williams, J., Nieminen, T., Kajos, M., Rinne, J., Kulmala, M., and Boy, M.: Modelling atmospheric OH-reactivity in a boreal forest ecosystem, Atmos. Chem. Phys., 11, 9133–9163, doi:10.5194/acpd-11-9133-2011, 2011.

Mollner, A. K., Valluvadasan, S., Feng, L., Sprague, M. K., Okumura, M., Milligan, D. B., Bloss, W. J., Sander, S. P., Martien, P. T., Harley, R. A., McCoy, A. B., and Carter, W. P. L.: Rate of Gas Phase Association of Hydroxyl Radical and Nitrogen Dioxide, Science, 330, 646–649, doi:10.1126/science.1193030, 2010.

Monson, R. K., Grote, R., Niinemets, l., and Schnitzler, J.-P.: Modeling the isoprene emission rate from leaves, New Phytologist, 195, 541–559, doi:10.1111/j.1469-8137.2012.04204.x, 2012.

Montzka, S. A., Trainer, M., Angevine, W. M., and Fehsenfeld, F. C.: Measurements of 3-methyl furan, methyl vinyl ketone, and methacrolein at a rural forested site in the southeastern United States, J. Geophys. Res., 100, 11 393–11 401, doi:10.1029/95JD01132, 1995.

Nakashima, Y., Tsurumaru, H., Imamura, T., Bejan, I., Wenger, J. C., and Kajii, Y.: Total OH reactivity measurements in laboratory studies of the photooxidation of isoprene, Atmospheric Environment, pp. –, doi:10.1016/j.atmosenv.2012.08.033, 2012.

Niinemets, U.: Mild versus severe stress and BVOCs: thresholds, priming and consequences, Trends Plant Sci., 15, 145–153, doi:10.1016/j.tplants.2009.11.008, 2010.

Niinemets, U., Loreto, F., and Reichstein, M.: Physiological and physicochemical controls on foliar volatile organic compound emissions, Trends Plant Sci., 9, 180–186, 2004.

Niinemets, U., Kuhn, U., Harley, P. C., Staudt, M., Arneth, A., Cescatti, A., Ciccioli, P., Copolovici, L., Geron, C., Guenther, A., Kesselmeier, J., Lerdau, M. T., Monson, R. K., and Peñuelas, J.: Estimations of isoprenoid emission capacity from enclosure

studies: measurements, data processing, quality and standardized measurement protocols, Biogeosciences, 8, 2209–2246, doi:10.5194/bg-8-2209-2011, 2011.

Nilsson, E., Rannik, U., Kulmala, M., Buzorius, G., and O'Dowd, C.: Effects of continental boundary layer evolution, convection, turbulence and entrainment, on aerosol formation, Tellus., 53B, 441–461, 2001.

Nölscher, A., Sinha, V., Bockisch, S., Klüpfel, T., and Williams, J.: A new method for direct total OH reactivity measurements using a fast Gas Chromatographic Photo-Ionization Detector (GC-PID), Atmos. Meas. Tech. Discuss., 5, 3575–3609, doi:doi:10.5194/amtd-5-3575-2012, 2012a.

Nölscher, A. C., Williams, J., Sinha, V., Custer, T., Song, W., Johnson, A. M., Axinte, R., Bozem, H., Fischer, H., Pouvesle, N., Phillips, G., Crowley, J. N., Rantala, P., Rinne, J., Kulmala, M., Gonzales, D., Valverde-Canossa, J., Vogel, A., Hoffmann, T., Ouwersloot, H. G., Vilà-Guerau de Arellano, J., and Lelieveld, J.: Summertime total OH reactivity measurements from boreal forest during HUMPPA-COPEC 2010, Atmos. Chem. Phys., 12, 8257–8270, doi:10.5194/acp-12-8257-2012, 2012b.

Ouwersloot, H. G., Vilà-Guerau de Arellano, J., Nölscher, A. C., Krol, M. C., Ganzeveld, L. N., Breitenberger, C., Mammarella, I., Williams, J., and Lelieveld, J.: Characterization of a boreal convective boundary layer and its impact on atmospheric chemistry during HUMPPA-COPEC-2010, Atmos. Chem. Phys. Discuss., 12, 13 619–13 665, doi:10.5194/acpd-12-13619-2012, 2012.

Ozanne, C. M. P., Anhuf, D., Boulter, S. L., Keller, M., Kitching, R. L., KÃ¶rner, C., Meinzer, F. C., Mitchell, A. W., Nakashizuka, T., Dias, P. L. S., Stork, N. E., Wright, S. J., and Yoshimura, M.: Biodiversity Meets the Atmosphere: A Global View of Forest Canopies, Science, 301, 183–186, doi:10.1126/science.1084507, 2003.

Paulot, F., Crounse, J. D., Kjaergaard, H. G., Kürten, A., St. Clair, J. M., Seinfeld, J. H., and Wennberg, P. O.: Unexpected Epoxide Formation in the Gas-Phase Photooxidation of Isoprene, Science, 325, 730–733, doi:10.1126/science.1172910, 2009.

Paulson, S. and Seinfeld, J.: Development and Evaluation of a Photooxidation Mechanism for Isoprene, J. Geophys. Res., 97, 20,703–20,715, doi:10.1029/92JD01914, 1992.

Peeters, J. and Mueller, J.-F.: HOx radical regeneration in isoprene oxidation via peroxy radical isomerisations. II: experimental evidence and global impact, Phys. Chem. Chem. Phys., 12, 14 227–14 235, doi:10.1039/C0CP00811G, 2010.

Peeters, J., Nguyen, T. L., and Vereecken, L.: HOx radical regeneration in the oxidation of isoprene, Phys. Chem. Chem. Phys., 11, 5935–5939, doi:10.1039/B908511D, 2009.

Pierotti, D., Wofsy, S. C., Jacob, D., and Rasmussen, R. A.: Isoprene and Its Oxidation Products: Methacrolein and Methyl Vinyl Ketone, J. Geophys. Res., 95, 1990.

Pinho, P., Pio, C., and Jenkin, M.: Evaluation of isoprene degradation in the detailed tropospheric chemical mechanism, MCM v3, using environmental chamber data, Atmospheric Environment, 39, 1303 – 1322, doi:10.1016/j.atmosenv.2004.11.014, 2005.

Pöschl, U., von Kuhlmann, R., Poisson, N., and Crutzen, P. J.: Development and Intercomparison of Condensed Isoprene Oxidation Mechanisms for Global Atmospheric Modeling, Journal of Atmospheric Chemistry, 37, 29–52, 10.1023/A:1006391009798, 2000.

Pöschl, U., Martin, S. T., Sinha, B., Chen, Q., Gunthe, S. S., Huffman, J. A., Borrmann, S., Farmer, D. K., Garland, R. M., Helas, G., Jimenez, J. L., King, S. M., Manzi, A., Mikhailov, E., Pauliquevis, T., Petters, M. D., Prenni, A. J., Roldin, P., Rose, D., Schneider, J., Su, H., Zorn, S. R., Artaxo, P., and Andreae, M. O.: Rainforest Aerosols as Biogenic Nuclei of Clouds and Precipitation in the Amazon, Science, 329, 1513–1516, doi:10.1126/science.1191056, 2010.

Rasmussen, R. and Jones, C.: Emission isoprene from leaf discs of hamamelis, Phytochemistry, 12, 15–19, doi:10.1016/S0031-9422(00)84618-X, 1973.

Ren, X., Brune, W. H., Oliger, A., Metcalf, A. R., Simpas, J. B., Shirley, T., Schwab, J. J., Bai, C., Roychowdhury, U., Li, Y., Cai, C., Demerjian, K. L., He, Y., Zhou, X., Gao, H., and Hou, J.: OH, HO2, and OH reactivity during the PMTACS-NY Whiteface Mountain 2002 campaign: Observations and model comparison, J. Geophys. Res., 111, doi:10.1029/2005JD006126, 2006.

Rennenberg, H., Loreto, F., Polle, A., Brilli, F., Fares, S., Beniwal, R. S., and Gessler, A.: Physiological Responses of Forest Trees to Heat and Drought, Plant Biology, 8, 556–571, doi:10.1055/s-2006-924084, 2006.

Rinne, J., Taipale, R., Markkanen, T., Ruuskanen, T. M., Hellén, H., Kajos, M. K., Vesala, T., and Kulmala, M.: Hydrocarbon fluxes above a Scots pine forest canopy: measurements and modeling, Atmos. Chem. Phys., 7, 3361–3372, doi:10.5194/acp-7-3361-2007, 2007.

Rinne, J., Bäck, J., and Hakola, H.: Biogenic volatile organic compound emissions from the Eurasian taiga:current knowledge and future directions, Boreal Environ. Res., 14, 807–826, 2009.

Rohrer, F. and Berresheim, H.: Strong correlation between levels of tropospheric hydroxyl radicals and solar ultraviolet radiation, Nature, 442, 184–187, doi:http://dx.doi.org/10.1038/nature04924, 2006.

Rohrer, F., Bohn, B., Brauers, T., Brüning, D., Johnen, F.-J., Wahner, A., and Kleffmann, J.: Characterisation of the photolytic HONO-source in the atmosphere simulation chamber SAPHIR, Atmospheric Chemistry and Physics, 5, 2189–2201, doi:10.5194/acp-5-2189-2005, 2005.

Ruppert, L. and Becker, K. H.: A product study of the OH radical-initiated oxidation of isoprene: formation of C5-unsaturated diols, Atmospheric Environment, 34, 1529–1542, doi:10.1016/S1352-2310(99)00408-2, 2000.

Ruuskanen, T., Kolari, P., Bäck, J., Kulmala, M., Rinne, J., Hakola, H., Taipale, R., Raivonen, M., Altimir, N., and Hari, P.: On-line field measurements of monoterpene emissions from Scots pine by proton-transfer-reaction mass spectrometry, Boreal Environ. Res., 10, 553–567, 2005.

Sadanaga, Y., Yoshino, A., Watanabe, K., Yoshioka, A., Wakazono, Y., Kanaya, Y., and Kajii, Y.: Development of a measurement system of OH reactivity in the atmosphere by using a laser-induced pump and probe technique, Rev. Sci. Instrum., 75, 8, doi:10.1063/1.1775311, 2004.

Sanadze, G.: Emission of Gaseous Organic Substances from Plants, Rep. Akad.Nauk GruzSSR, 17, 1956.

Sander, R., Kerkweg, A., Jöckel, P., and Lelieveld, J.: Technical note: The new comprehensive atmospheric chemistry module MECCA, Atmos. Chem. Phys., 5, 445–450, 2005.

Saunders, S. M., Jenkin, M. E., Derwent, R. G., and Pilling, M. J.: Protocol for the development of the Master Chemical Mechanism MCMv3 Part A: tropospheric degradation of non-aromatic volatile organic compounds, Atmos. Chem. Phys., 3, 161–180, 2003.

Schlosser, E., Brauers, T., Dorn, H.-P., Fuchs, H., Häseler, R., Hofzumahaus, A., Holland, F., Wahner, A., Kanaya, Y., Kajii, Y., Miyamoto, K., Nishida, S., Watanabe, K., Yoshino, A., Kubistin, D., Martinez, M., Rudolf, M., Harder, H., Berresheim, H., Elste, T., Plass-Dülmer, C., Stange, G., and Schurath, U.: Technical Note: Formal blind intercomparison of OH measurements: results from the international campaign HOxComp, Atm. Chem. Phys., 9, 7923–7948, doi:10.5194/acp-9-7923-2009, 2009.

Schürmann, W., Ziegler, H., Kotzias, D., Schönwitz, R., and Steinbrecher, R.: Emission of biosynthesized monoterpenes from needles of Norway Spruce, Naturwissenschaften, 80, 276–278, doi:10.1007/BF01135913, 1993.

Shao, M., Czapiewski, K., Heiden, A., Kobel, K., Komenda, M., Koppman, R., and Wildt, J.: Volatile organic compound emissions from Scots pine: Mecha-

nisms and description by algorithms, J. Geophys. Res., 16, 20,483–20,491, doi: 10.1029/2000JD000248, 2001.

Shirley, T., Brune, W., Ren, X., Mao, J., Lesher, R., Cardenas, B., Volkamer, R., Molina, L., Molina, M., Lamb, B., Velasco, E., Jobson, T., and Alexander, M.: Atmospheric oxidation in the Mexico City Metropolitan Area (MCMA) during April 2003, Atmos. Chem. Phys., 6, 2753–2765, doi:10.5194/acp-6-2753-2006, 2006.

Siese, M., Becker, K. H., Brockmann, K. J., Geiger, H., Hofzumahaus, A., Holland, F., Mihelcic, D., and Wirtz, K.: Direct Measurement of OH Radicals from Ozonolysis of Selected Alkenes: A EUPHORE Simulation Chamber Study, Environ. Scien. Technol., 35, 4660–4667, doi:10.1021/es010150p, 2001.

Sinha, V., Williams, J., Crowley, J. N., and Lelieveld, J.: The Comparative Reactivity Method - a new tool to measure total OH Reactivity in ambient air, Atmos. Chem. Phys., 8, 2213–2227, doi:10.5194/acp-8-2213-2008, 2008.

Sinha, V., Custer, T., Kluepfel, T., and Williams, J.: The effect of relative humidity on the detection of pyrrole by PTR-MS for OH reactivity measurements, Int. J. Mass Spectrom., 282, 108 – 111, doi:10.1016/j.ijms.2009.02.019, 2009.

Sinha, V., Williams, J., Lelieveld, J., Ruuskanen, T., Kajos, M., Patokoski, J., Hellen, H., Hakola, H., Mogensen, D., Boy, M., Rinne, J., and Kulmala, M.: OH Reactivity Measurements within a Boreal Forest: Evidence for Unknown Reactive Emissions, Environ. Sci. Technology, 44, 6614–6620, doi:10.1021/es101780b, 2010.

Sinha, V., Williams, J., Diesch, J. M., Drewnick, F., Martinez, M., Harder, H., Regelin, E., Kubistin, D., Bozem, H., Hosaynali-Beygi, Z., Fischer, H., Andrés-Hernández, M. D., Kartal, D., Adame, J. A., and Lelieveld, J.: OH reactivity measurements in a coastal location in Southwestern Spain during DOMINO, Atmos. Chem. Phys. Discuss., 12, 4979–5014, doi:10.5194/acpd-12-4979-2012, 2012.

Taipale, R., Kajos, M. K., Patokoski, J., Rantala, P., Ruuskanen, T. M., and Rinne, J.: Role of de novo biosynthesis in ecosystem scale monoterpene emissions from a boreal Scots pine forest, Biogeosciences, 8, 2247–2255, doi:10.5194/bg-8-2247-2011, 2011.

Tan, D., Faloona, I., Simpas, J., Brune, W., Shepson, P., Couch, T., Sumner, A., Carroll, M., Thornberry, T., Apel, E., Riemer, D., and Stockwell, W.: HOx budgets in a deciduous forest: Results from the PROPHET summer 1998 campaign, Journal of Geophysical Research-Atmospheres, 106, 24,407–24,427, doi:10.1029/2001JD900016, 2001.

Taraborrelli, D., Lawrence, M. G., Crowley, J. N., Dillon, T. J., Gromov, S., Grosz,

C. B. M., Vereecken, L., and Lelieveld, J.: Hydroxyl radical buffered by isoprene oxidation over tropical forests, Nature Geosci., doi:10.1038/ngeo1405, 2012.

Tingey, D. T., Manning, M., Grothaus, L. C., and Burns, W. F.: Influence of Light and Temperature on Monoterpene Emission Rates from Slash Pine, Plant Physiology, 65, 797–801, 1980.

Tuazon, E. C. and Atkinson, R.: A product study of the gas-phase reaction of Isoprene with the OH radical in the presence of NOx, International Journal of Chemical Kinetics, 22, 1221–1236, doi:10.1002/kin.550221202, 1990.

Tunved, P., Hansson, H.-C., Kerminen, V.-M., Ström, J., Maso, M. D., Lihavainen, H., Viisanen, Y., Aalto, P. P., Komppula, M., and Kulmala, M.: High Natural Aerosol Loading over Boreal Forests, Science, 312, 261–263, doi:10.1126/science.1123052, 2006.

Vereecken, L. and Peeters, J.: Enhanced H-atom abstraction from pinonaldehyde, pinonic acid, pinic acid, and related compounds: theoretical study of C-H bond strengths, Phys. Chem., 4, 467–472, doi:10.1039/B109370C, 2002.

Vickers, C. E., Gershenzon, J., Lerdau, M. T., and Loreto, F.: A unified mechanism of action for volatile isoprenoids in plant abiotic stress, Nat Chem Biol, 2009.

Warneck, P. and Williams, J.: The Atmospheric Chemist's Companion - Numerical Data for the Use in the Atmospheric Sciences, Springer, 2012.

Warneke, C., Roberts, J., Veres, P., Gilman, J., Kuster, W., Burling, I., Yokelson, R., and de Gouw, J.: VOC identification and inter-comparison from laboratory biomass burning using PTR-MS and PIT-MS, Int. J. Mass Spectrom., 303, 6 – 14, doi:10.1016/j.ijms.2010.12.002, 2011.

Went, F.: Blue hazes in the atmosphere, Nature, pp. 641–643, 1960.

White, M., Russo, R., Zhou, Y., Ambrose, J., Haase, K., Frinak, E., Varner, R., Wingenter, O., Mao, H., Talbot, R., and Sive, B.: Are biogenic emissions a significant source of summertime atmospheric toluene in the rural Northeastern United States?, Atmos. Chem. Phys., 9, 81–92, 2009.

Wieser, G., Matyssek, R., Götz, B., and Grünhage, L.: Branch cuvettes as means of ozone risk assessment in adult forest tree crowns: combining experimental and modelling capacities, Trees - Structure and Function, pp. 1–10, 2012.

Williams, J.: Provoking the air, Environmental Chemistry, 5, 317–319, doi:10.1071/EN08048, 2008.

Williams, J., Pöschl, U., Crutzen, P. J., Hansel, A., Holzinger, R., Warneke, C., Lindinger, W., and Lelieveld, J.: An Atmospheric Chemistry Interpretation of Mass Scans Obtained from a Proton Transfer Mass Spectrometer Flown over the Tropical Rainforest of Surinam, J. Atmos. Chem., 38, 133–166, doi:10.1023/A:1006322701523, 2001.

Williams, J., Yassaa, N., Bartenbach, S., and Lelieveld, J.: Mirror image hydrocarbons from Tropical and Boreal forests, Atm. Chem. Phys., 7, 973–980, 2007.

Williams, J., Crowley, J., Fischer, H., Harder, H., Martinez, M., Petäjä, T., Rinne, J., Bäck, J., Boy, M., Dal Maso, M., Hakala, J., Kajos, M., Keronen, P., Rantala, P., Aalto, J., Aaltonen, H., Paatero, J., Vesala, T., Hakola, H., Levula, J., Pohja, T., Herrmann, F., Auld, J., Mesarchaki, E., Song, W., Yassaa, N., Nölscher, A., Johnson, A. M., Custer, T., Sinha, V., Thieser, J., Pouvesle, N., Taraborrelli, D., Tang, M. J., Bozem, H., Hosaynali-Beygi, Z., Axinte, R., Oswald, R., Novelli, A., Kubistin, D., Hens, K., Javed, U., Trawny, K., Breitenberger, C., Hidalgo, P. J., Ebben, C. J., Geiger, F. M., Corrigan, A. L., Russell, L. M., Ouwersloot, H. G., Vilà-Guerau de Arellano, J., Ganzeveld, L., Vogel, A., Beck, M., Bayerle, A., Kampf, C. J., Bertelmann, M., Köllner, F., Hoffmann, T., Valverde, J., González, D., Riekkola, M.-L., Kulmala, M., and Lelieveld, J.: The summertime Boreal forest field measurement intensive (HUMPPA-COPEC-2010): an overview of meteorological and chemical influences, Atmos. Chem. Phys., 11, 10 599–10 618, doi:10.5194/acp-11-10599-2011, 2011.

Winer, A. M., Peters, J. W., Smith, J. P., and Pitts, Jr., J. N.: Response of commercial chemiluminescent NO-NO_2 analyzers to other nitrogen-containing compounds, Environ. Sci. Technol., 8, 1118–1121, 1974.

Wolfe, G., Crounse, J., Parrish, J., Clair, J., Beaver, M., Paulot, F., Yoon, T., Wennberg, P., and Keutsch, F.: Photolysis, OH reactivity and ozone reactivity of a proxy for isoprene-derived hydroperoxynals (HPALDs), Annu. Rev. Genet., 44, 1–24, doi:10.1146/annurev-genet-102209-163500, 2010.

Wu, J. and Baldwin, I. T.: New Insights into Plant Responses to the Attack from Insect Herbivores, Annu. Rev. Genet., 44, 1–24, doi:10.1146/annurev-genet-102209-163500, 2010.

Xu, X., Stee, L. L. P., Williams, J., Beens, J., Adahchour, M., Vreuls, R. J. J., Brinkman, U. A., and Lelieveld, J.: Comprehensive two-dimensional gas chromatography (GCxGC) measurements of volatile organic compounds in the atmosphere, Atmos. Chem. Phys., 3, 665–682, doi:10.5194/acp-3-665-2003, 2003.

Yang, X. and Lu, Y.: Preparation of polypyrrole-coated silver nanoparticles by one-

step UV-induced polymerization, Materials Letters, 59, 2484 – 2487, doi:10.1016/j.matlet.2005.03.033, 2005.

Yassaa, N. and Williams, J.: Enantiomeric monoterpene emissions from natural and damaged Scots pine in a boreal coniferous forest measured using solid-phase microextraction and gas chromatography/mass-spectrometry., J. Chromatogr., 1141, 138–144, doi:10.1016/j.chroma.2006.12.006, 2007.

Yassaa, N., Song, W., Lelieveld, J., Vanhatalo, A., Bäck, J., and Williams, J.: Diel cycles of isoprenoids in the emissions of Norway spruce, four Scots pine chemotypes, and in Boreal forest ambient air during HUMPPA-COPEC-2010, Atmos. Chem. Phys., 12, 7215–7229, doi:10.5194/acp-12-7215-2012, 2012.

Yokelson, R. J., Karl, T., Artaxo, P., Blake, D. R., Christian, T. J., Griffith, D. W. T., Guenther, A., and Hao, W. M.: The Tropical Forest and Fire Emissions Experiment: overview and airborne fire emission factor measurements, Atmos. Chem. and Phys., 7, 5175–5196, doi:10.5194/acp-7-5175-2007, 2007.

Yoshino, A., Nakashima, Y., Miyazaki, K., Kato, S., Suthawaree, J., Shimo, N., Matsunaga, S., Chatani, S., Apel, E., Greenberg, J., Guenther, A., Ueno, H., Sasaki, H., ya Hoshi, J., Yokota, H., Ishii, K., and Kajii, Y.: Air quality diagnosis from comprehensive observations of total OH reactivity and reactive trace species in urban central Tokyo, Atmos. Env., 49, 51 – 59, doi:10.1016/j.atmosenv.2011.12.029, 2011.

Zador, J., Turanyi, T., Wirtz, K., and Pilling, M.: Measurement and investigation of chamber radical sources in the European Photoreactor (EUPHORE), J. Atmos. Chem., 55, 147–166, 2006.